Shallow laccolithic emplacement of the Land's End and Tregonning granites, Cornwall, UK: Evidence from aureole field relations and P-T modeling of cordierite-anthophyllite hornfels

Jonathan M. Pownall[1,*], David J. Waters[1], Michael P. Searle[1], Robin K. Shail[2], and Laurence J. Robb[1]
[1]*Department of Earth Sciences, University of Oxford, South Parks Road, Oxford OX1 3AN, UK*
[2]*Camborne School of Mines, College of Engineering, Mathematics and Physical Sciences, University of Exeter, Cornwall Campus, Penryn TR10 9EZ, UK*

ABSTRACT

The Land's End and Tregonning-Godolphin granites of the >250 km-long Permian Cornubian Batholith are heterogeneous medium- to coarse-grained peraluminous biotite-, tourmaline-, and lithium-mica granites traditionally thought to be emplaced as massive magmatic diapirs. Although S-type characteristics are dominant (quartz + biotite + muscovite + tourmaline ± topaz ± lithium-micas in the melt, numerous greisen and pegmatite veins, Sn-W mineralization), some characteristics of evolved I-type granites are also exhibited (hornblende-bearing enclaves, elevated ε_{Nd}, Cu mineralization, batholithic dimensions). Here, we present an investigation focusing on the contact metamorphism and deformation of the aureole rocks adjacent to the Land's End and Tregonning granites as an approach to better determine the method of granite emplacement and the depth at which it occurred. New 1:5000-scale geological maps are presented for ~15 km of coastal exposure of the granites and their aureoles. We propose that the granites were emplaced non-diapirically by intrusion of sills that amalgamated to form a sheeted laccolith-type body. Granite contacts cleanly truncate all faults, folds, and cleavages generated during both Variscan convergence and subsequent latest Carboniferous–Early Permian (end-Variscan) extension, and it is likely that granite was emplaced during continuation of this extensional episode. There is evidence for stoping of the country rocks by an outward-migrated sill and dyke network, and uplift and doming of the host rocks can be partially attributed to laccolith inflation. Host meta-siltstones of the Devonian Mylor Slate Formation formed a contact aureole of cordierite + biotite + chlorite ± andalusite "spotted slates." Several interspersed pillow basalts and dolerites, previously affected by hydrothermal alteration, underwent isochemical contact metamorphism to form cordierite- and orthoamphibole-bearing hornfels, including cordierite-anthophyllite rocks that are present in Kenidjack cliff, NW Land's End aureole. THERMOCALC P-T modeling and pseudosection construction for these rocks in the large Na_2O-CaO-K_2O-FeO-MgO-Al_2O_3-SiO_2-H_2O-TiO_2-Fe_2O_3 (NCKFMASHTO) chemical system indicates contact metamorphism occurred at 1.5 ± 1.0 kbar and 615 ± 50 °C. This ultra-low pressure metamorphism equates to a likely emplacement depth of 5–6 km for the adjacent granite sheets. The Cornubian Batholith is highly composite and likely comprises an amalgamation of discrete shallow-seated sheeted laccoliths that are dyke-fed from a common lower-crustal/upper-mantle melt region to result in the batholith's mixed S-type/I-type character.

INTRODUCTION

Hypotheses for the emplacement of granitoids have been frequently led by the two extreme end-member concepts for granite genesis: (1) the diapiric emplacement of igneous-derived "I-type" granites typified by the Andean batholiths (e.g., Pitcher, 1979; Petford and Atherton, 1996); and (2) the emplacement of sheeted complexes of crustal-melt- (or sedimentary-) derived "S-type" granites typified by the Himalayan leucogranites (e.g., Harris and Massey, 1994; Harris et al., 1995; Searle, 1999; Searle et al., 2009). The I- and S-type distinction was initially proposed by Chappell and White (1974) and is still widely utilized. Andean-type granites are characterized by long, linear granites of batholitic proportions, intrusive hornblende- and biotite-bearing gabbro-granodiorite-granite-tonalite fractionation sequences with extrusive andesite-rhyolite-dacite volcanics, and abundant Cu-Mo(-Pb-Zn-Au) mineralization. Crustal-derived Himalayan-type leucogranites are less voluminous, tend to be peraluminous (containing garnet, muscovite, biotite, and tourmaline), are associated with regional high-grade metamorphic-migmatite belts, have no extrusive volcanic component, and are in many cases associated with Sn-W mineralization. However, there are increasing numbers of granitoid bodies that have been found, compositionally, to fit neither of these examples or that represent a hybrid between the two types. Examples include the Baltoro Batholith in the Pakistani Karakoram, which comprises subduction-related I-type diorites, granodiorites and granites intruded by large-scale post-collision S-type two-mica ± garnet leucogranites (Searle et al., 2010), and the Main Range Tin granites of the Malay

*Present address: Southeast Asia Research Group, Department of Earth Sciences, Royal Holloway University of London, Egham, Surrey TW20 0EX, UK; Email: j.pownall@es.rhul.ac.uk.

Geosphere; December 2012; v. 8; no. 6; p. 1467–1504; doi:10.1130/GES00802.1; 29 figures; 4 tables; 1 plate.
Received 8 March 2012 ♦ Revision received 10 August 2012 ♦ Accepted 12 August 2012 ♦ Published online 16 November 2012

Peninsula, which include both I-type granodiorites and S-type biotite granites (Searle et al., 2012). Furthermore, the concept of granite diapirism has, in recent years, faced increasing scrutiny (Petford, 1996; Clemens, 1998; Petford and Clemens, 2000; Petford et al., 2000), and several plutons traditionally viewed as diapiric—including both S-type bodies such as the Monte Capanne granite on Elba, Italy (Farina et al., 2010; Rocchi et al., 2010) and I-type bodies such as the Mount Kinabalu granite in Borneo (Cottam et al., 2010)—have been re-interpreted, often as incrementally emplaced laccoliths or lopoliths (cf. Pollard and Johnson, 1973; Jackson and Pollard, 1988; Cruden, 1998).

Most approaches in determining emplacement style have been concerned with mapping internal granite fabrics as defined by phenocryst alignment, anisotropy of magnetic susceptibility (AMS), or geochemical trends, and the systematic dating of different granite facies. These methods have proved very successful in unraveling the emplacement history for many sheeted, composite or laccolith-type bodies (e.g., Morgan et al., 1998; de Saint-Blanquat et al., 2001; Michel et al., 2008; Clemens and Benn, 2010; Cottam et al., 2010; Farina et al., 2010; Rocchi et al., 2010; Leuthold et al., 2012). However, the effect of pluton emplacement on host rocks—specifically contact metamorphism and deformation (or lack thereof)—has sometimes received less attention. The study of aureole rocks can provide great insight into the details of pluton emplacement that cannot easily be discerned from focusing exclusively on the granite itself (as demonstrated by Paterson et al., 1991; Pattison and Harte, 1997; Ciavarella and Wyld, 2008). In particular, the depth of granite emplacement can be determined by calculating the pressure of peak aureole metamorphism. Also, the timing of emplacement relative to host-rock deformation can be inferred so that, for instance, it can be determined whether granite emplacement was a cause, an effect, or of no consequence to a specific tectonic episode.

Here, we present an investigation of the metamorphic aureoles of the Land's End and Tregonning granites of the Cornubian Batholith, Southwest England (Fig. 1). Despite the Cornubian granites being a prominent component of Britain's geological history, relatively little has been published on the field relations with their aureole rocks (Rattey and Sanderson, 1984; Hughes et al., 2009), and the majority of recent studies have instead focused on the granites' mineralogical and geochemical characteristics and ore genesis (e.g., Floyd et al., 1993; Chappell and Hine, 2006; Müller et al., 2006). Some of the older interpretations for the formation of the Cornubian Batholith, as summarized in Floyd et al. (1993), have essentially assumed "large-tank" magmatism and the forceful emplacement of individual plutons as massive "hot Stokes" diapirs (e.g., Pitcher, 1979; Marsh, 1982; Bateman, 1984; Mahon et al., 1988; England, 1990; Paterson and Vernon, 1995). However, as previously mentioned, a paradigm shift (summarized by Petford et al., 2000) from diapiric ascent processes (c.f. Ramberg, 1981; Weinberg and Podladchikov, 1994) to dyke-controlled ascent and emplacement mechanisms has largely taken place, and the more recent interpretations for Cornubian Batholith emplacement do not invoke granite diapirism as the primary process (Salmon and Powell, 1998; Powell et al., 1999; Kratinová et al., 2003, 2010; Bouchez et al., 2006; Taylor, 2007; Hughes et al., 2009).

We firstly describe field relations observed during detailed (1:5000) mapping along coastal sections of the margins of the Land's End and Tregonning granites and their aureole; secondly, we discuss a petrological and structural study of the aureole rocks; and thirdly we present P-T estimates of three cordierite-anthophyllite hornfelses from Kenidjack, NW Land's End aureole. We use the field relationships and P-T estimates of the aureole rocks to determine the style of granite emplacement and the depth at which it occurred. P-T pseudosections are calculated using the computer program THERMOCALC (Powell and Holland, 1988, 2008) in the recently enhanced Na_2O-CaO-K_2O-FeO-MgO-Al_2O_3-SiO_2-H_2O-TiO_2-Fe_2O_3 (NCKFMASHTO) system for cordierite-orthoamphibole assemblages (Diener et al., 2007, 2008). An additional aim of this study is therefore to contribute to the understanding of cordierite-anthophyllite rock petrogenesis by determining the peak P-T conditions of their formation in this classic locality (Tilley and Flett, 1929; Tilley, 1935; Chinner and Fox, 1974).

Although this study is primarily concerned with the Land's End and Tregonning granites, the ideas and approach detailed herein could be applied to all granites of the Cornubian Batholith. We hope to further clarify the petrogenesis and emplacement of the Land's End and Tregonning Granites in relation to Variscan orogenesis. In a wider sense, we hope to (1) illustrate the use of aureole geobarometry in deciphering granite emplacement depth, and (2) further demonstrate some of the insights that can be drawn from the study of metamorphic aureole deformation and aureole-granite contact relations.

GEOLOGICAL SETTING: THE VARISCAN OROGEN

The European Variscides formed through the collision of Laurussian and Gondwanan continental fragments after closure of the Rheic Ocean (Late Devonian to Early Carboniferous) and are represented in several large massifs stretching from Iberia to Bohemia (Fig. 1A). Remnants of Rheic oceanic crust and mantle, or that of associated marginal ocean basins to the north, are only sporadically preserved (e.g., the Mid-Devonian Lizard complex in Cornwall; Kirby, 1979; Shail and Leveridge, 2009). The orogen comprises distinct E–W trending tectonostratigraphic terranes of the Rhenohercynian, Saxothuringian, and Moldanubian rift-oceanic basins separated by Palaeozoic and Precambrian basement (Kossmat, 1927; Matte, 1986; Franke, 1989; Nance et al., 2010). Early Devonian to Early Carboniferous passive margin sedimentary rocks were affected by Carboniferous inversion and crustal shortening and thickening involving folding and NNW-vergent thrusting (Shackleton et al., 1982; Coward and McClay, 1983; Leveridge et al., 1984). In the Early Permian, widespread lower crustal anatexis led to ascent and emplacement of granites into the upper crust. Published emplacement depths for granitoids along the orogen are far from uniform (Table 1), although Vigneresse (1999), using gravity surveys conducted across the whole Variscan belt, estimated that a consistent 6–8 km of erosion has occurred since their emplacement.

Southwest England represents part of the western Rhenohercynian passive margin of the Variscan Orogen (Warr, 2000; Shail and Leveridge, 2009) and comprises a series of rift-generated basins (Culm, North Devon, Tavy, South Devon, Looe, and Gramscatho basins) infilled with deep-marine argillaceous sedimentary and rift-related igneous rocks (Fig. 1B). The southernmost of these basins, the Gramscatho Basin, includes the Mylor Slate Formation; this is composed of Famennian (375–359 Ma; Turner et al., 1979) deep marine mud/siltstones with occasional pillow-basalt horizons and dolerite sills that underwent Variscan sub-greenschist facies regional metamorphism (Warr et al., 1991) and later contact metamorphism by Permian granite intrusions (Goode et al., 1984; Goode and Taylor, 1988).

Variscan orogenesis subjected the region to an overall NNW–SSE shortening accompanied by modest crustal thickening and largely sub-greenschist facies regional metamorphism (Warr et al., 1991). The major deformational events have been categorized in the literature as follows (also, see Fig. 2): D_1 recumbent folding and slaty cleavage development, possibly associated with northwestward emplacement of Lizard Complex mantle peridotites and underlying thrust sheets; D_2 NNW-verging folding (F_2) with prominent S_2 axial planar cleavage development;

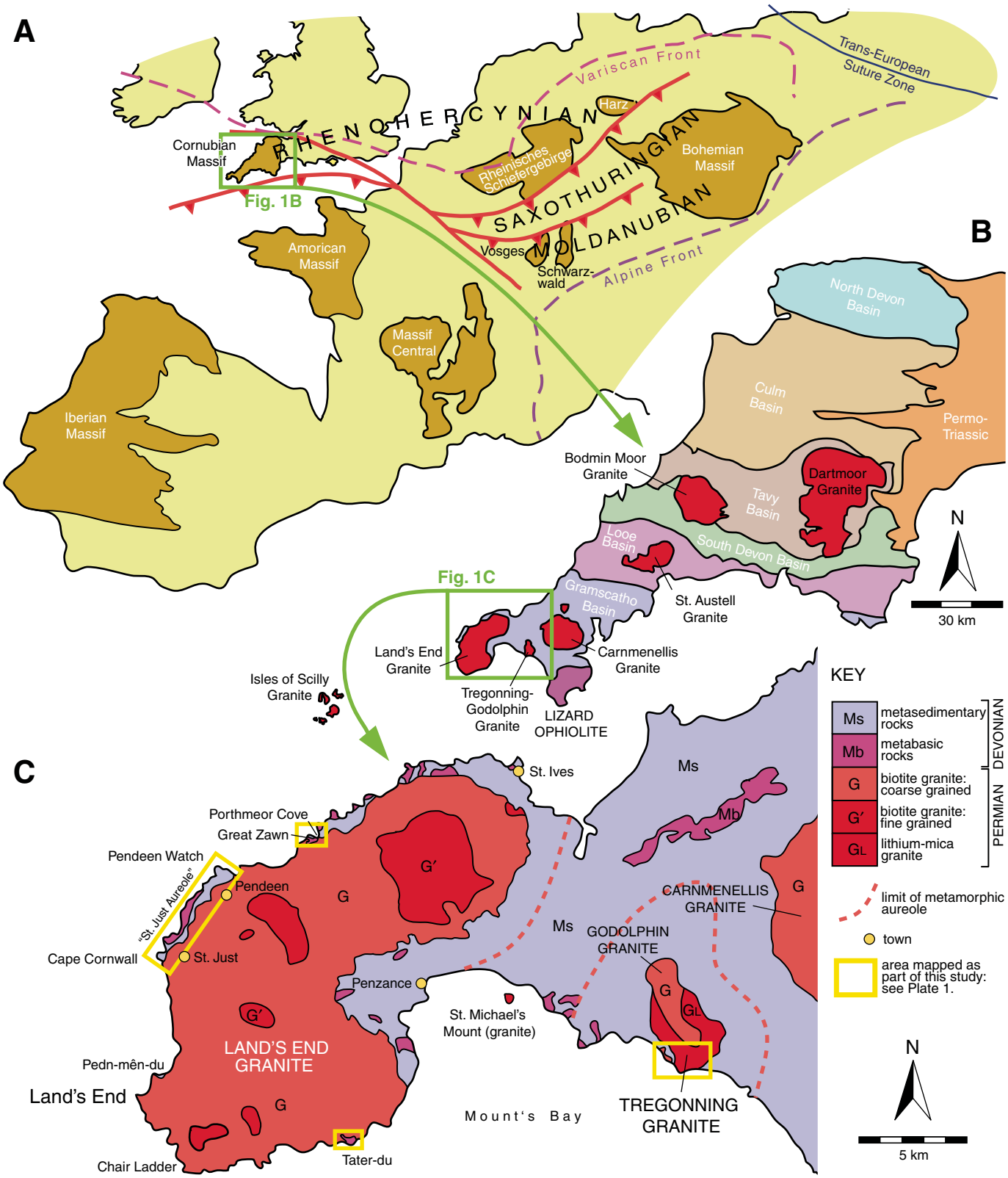

Figure 1. Geological setting of the Cornubian granites within the European Variscides. (A) The Variscan belt of Europe during the Early Carboniferous, modified from Matte (1986) and Franke (1989). (B) The Western Rhenohercynian of SW England, after Shail and Leveridge (2009). (C) Geological map of SW Cornwall, simplified from Goode et al. (1984) (British Geological Survey; 1:50,000). Yellow boxes indicate areas mapped—see Plate 1.

TABLE 1. PUBLISHED P-T CONDITIONS FOR VARISCAN GRANITES DURING THEIR EMPLACEMENT

Author(s)	Pluton	Massif	T (°C)	P (kbar)	Depth (km)	Method
Bradshaw and Stoyel (1968)	(whole batholith)	Cornubian	n.d.*	1	3	Fluid inclusion studies of quartz and fluorite veins in granites.
Floyd (1971)	(whole batholith)	Cornubian	580	1	3	"Tentative estimate" of thickness (3–4 km) and density (2800 kg m^{-3}) of eroded sedimentary cover. Temp. of 350°C calculated at 5 km dist.
Charoy (1986)	Carnmenellis Granite	Cornubian	650	2.0–2.5	6.0–7.5	Calculation of phase equilibria during crystallisation
Shail and Wilkinson (1994)	Tregonning Granite	Cornubian	n.d.*	0.5–1.0	1.5–3.0	Conditions of fluid equilibration in aureole
Chappell and Hine (2006)	(whole batholith)	Cornubian	770	0.5	1.75	Temperature from zircon saturation. Pressure is assumed.
Klein et al. (2008)	Hauzenberg Granite	Bohemian	n.d.*	4.3–4.9	16–18	Si-in-phengite geobarometry of white mica from granite
Scheuvens and Zulauf (2000)	Klatovy Granite	Bohemian	500–770	0.8–5.2	2.5–17.5	Blundy and Holland (1990) geothermometry and Schmidt (1992) Al-in-hornblende thermobarometry of granite
Pitra et al. (1999)	Central Bohemian Complex	Bohemian	620–670	3.8–4.2	12–13	THERMOCALC P-T pseudosections of *regional* metamorphism assumed synchronous to granite emplacement
Žák et al. (2011)	Mrákotía granite	Bohemian	n.d.*	< 2.5	< 9	Indicated by presence of magmatic andalusite
Tartèse and Boulvais (2010)	Lizio Granite	Amorican	n.d.*	3–4	9–12	P-T range indicated by stability of aureole mineral assemblages
Tartèse and Boulvais (2010)	Questembert Granite	Amorican	n.d.*	1–2	3–6	P-T range indicated by stability of aureole mineral assemblages

*n.d. = No data reported.

and D_3 SSE-verging folding (F_3) and axial planar cleavage development (S_3), which are variably associated with low-angle detachments, that developed during post-convergence extensional reactivation of Variscan thrusts (Alexander and Shail, 1995; Shail and Leveridge, 2009; Fig. 2).

A SYNOPSIS OF PREVIOUS WORK

Cornubian Batholith Morphology

The Cornubian Batholith is exposed in southwest England over a distance of ~200 km in seven large unroofed plutons (from west to east, the Isles of Scilly, Land's End, Tregonning-Godolphin, Carnmenellis, St. Austell, Bodmin Moor, and Dartmoor granites) that are hosted by Devonian and Carboniferous sedimentary and igneous rocks of the Rhenohercynian passive margin. Granite magmatism was a protracted event spanning some 20 m.y. during the Early Permian (from 294 to 274 Ma) with assembly times for individual plutons lasting up to 4.5 m.y. (Chen et al., 1993; Chesley et al., 1993). The Land's End granite (Fig. 3) is the youngest of the major plutons, emplaced between 277 ± 2 and 274.5 ± 2 Ma (Chen et al., 1993; Clark et al., 1993, 1994).

The Cornubian Batholith was originally modeled as a flat-bottomed body that occupies the upper 12 km of a 27-km-thick crustal section based on interpretation of a –50 mGal Bouguer anomaly and seismic refraction data (Bott et al., 1958, 1970). The batholith was also interpreted to widen with depth (e.g., Willis-Richards and Jackson, 1989), whereupon its base is possibly bound by a major late-Variscan thrust at 10–15 km depth (Brooks et al., 1984). High-resolution gravity modeling by Taylor (2007) recently showed that the individual plutons

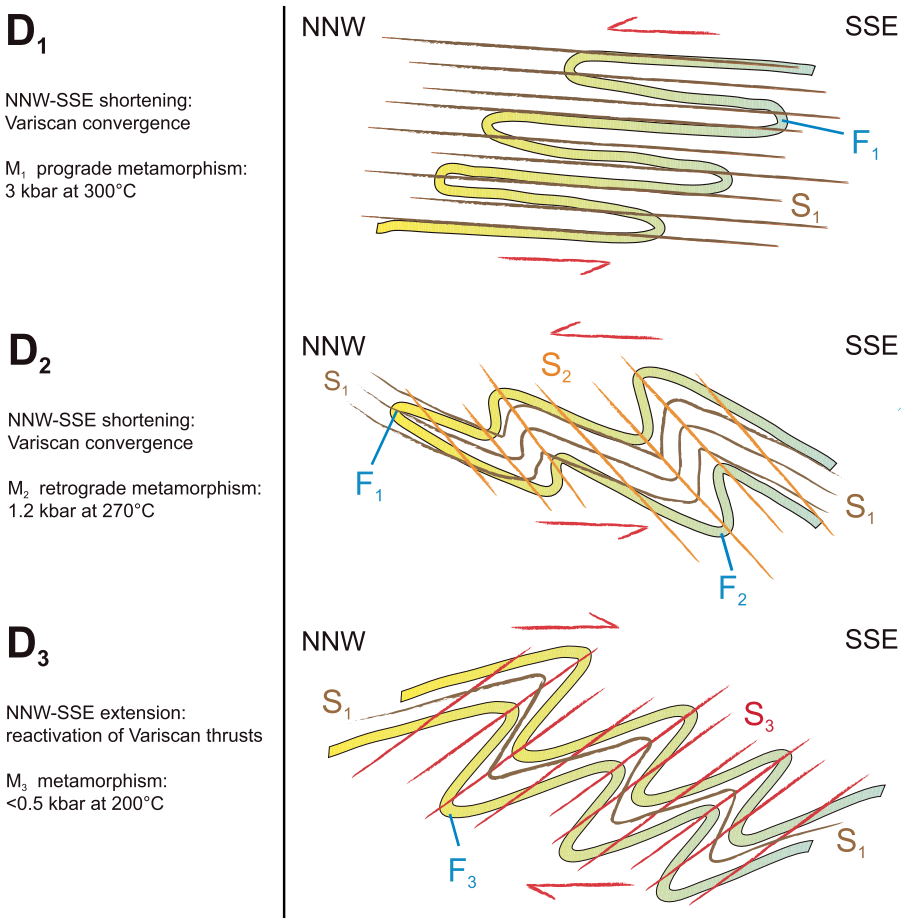

Figure 2. Summary of deformational episodes (D_1 to D_3) for the rocks of the SW Gramscatho Basin. Schematic diagrams illustrate the field relations between different fold generations (F_1 to F_3) and associated cleavages (S_1 to S_3). S_2 and S_3 are axial-planar to F_2 and F_3, respectively. S_1 has developed parallel to original bedding. The limbs of the isoclinal F_1 folds are roughly parallel to S_1 and thus difficult to identify in the field. Modified after Rattey and Sanderson (1984) and Hughes et al. (2009).

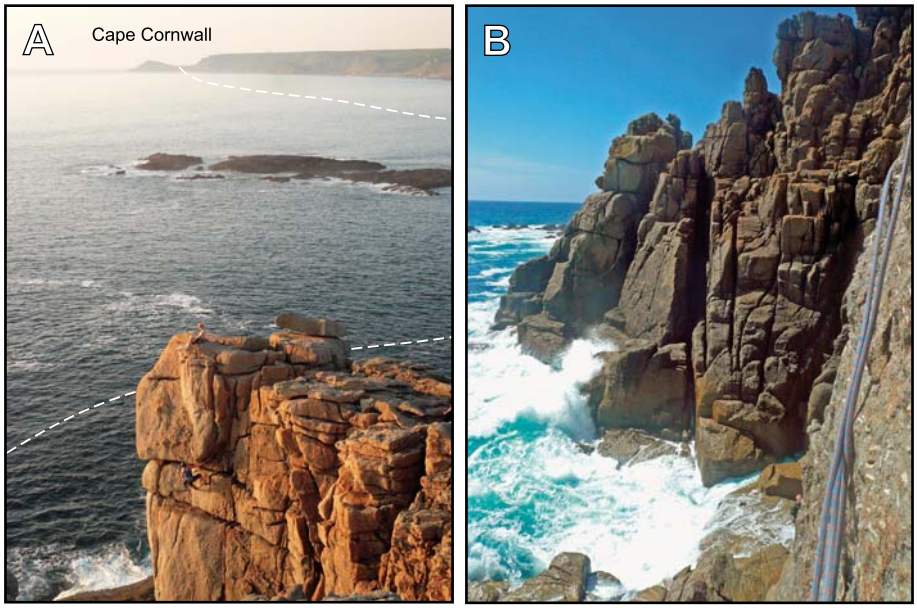

Figure 3. The Land's End granite at (A) Pedn-mên-du, Sennen Cove, looking north across Whitesands Bay to Cape Cornwall (6 km in the distance). The approximate trace of the granite–aureole contact is marked; the rocks in the sea are metapelites. Climbers for scale. (B) Chair Ladder crag, Gwennap Head, showing vertical and horizontal jointing, and alignment of orthoclase megacrysts in the foreground. See Fig. 1C for locations.

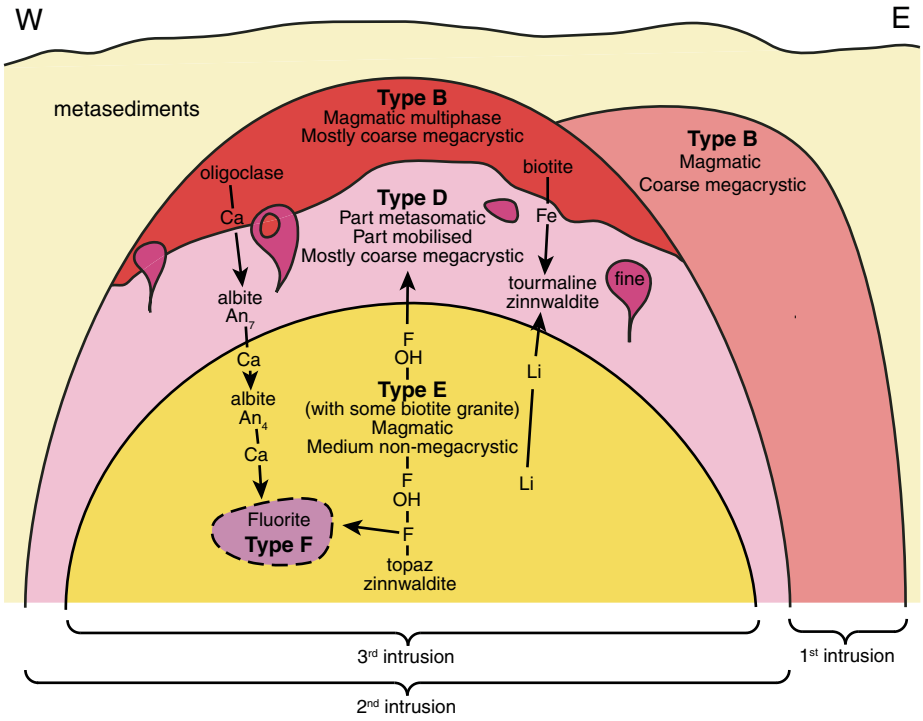

Figure 4. The "St. Austell model" of granite petrogenesis, redrawn from Floyd et al. (1993).

have pronounced tabular forms in cross section, but that they are far thinner than originally envisaged, in some cases just 3–4 km top to bottom (one-third that previously predicted). Furthermore, these smaller estimates for Cornubian pluton thicknesses would make their aspect-ratio closely comparable to several well-documented sheeted (laccolithic or lopolithic) granitoid bodies (McCaffrey and Petford, 1997; Cruden and McCaffrey, 2001). Vertical or steep conduits have also been identified, which would feed such laccolith-type plutons (Taylor, 2007).

Cornubian Batholith Petrogenesis

The Cornubian biotite granite suites have a typical S-type geochemical signature indicating derivation from a (meta-)sedimentary protolith (cf. Chappell and White, 1974, 2001; Chappell and Hine, 2006). However, there is also a mantle (I-type) component, notably prevalent in the Dartmoor granite, as inferred from whole rock geochemistry (Stone, 1997, 2000a, 2000b), Sm-Nd isotopes (elevated ε_{Nd}; Darbyshire and Shepherd, 1994), and the presence of hornblende-bearing microgranite enclaves (Stimac et al., 1995). Alongside peraluminous coarse-grained porphyritic biotite granites and two-mica granites, there is a cogenetic suite of lithium mica granites (Stone, 1992) and tourmaline granites (Lister, 1978a, 1978b) that shows B enrichment, and late stage, chemically distinct topaz and fluorite granites that show enrichment in F, Li, and P_2O_5 (Floyd et al., 1993; Manning, 1981; Manning et al., 1996; Williamson et al., 2010). The Cornubian Batholith is remarkably heterogeneous, and even within individual plutons there is a great deal of chemical and textural variation resulting from successive intrusive phases and magma mingling (e.g., Knox and Jackson, 1990; Salmon, 1994; Manning et al., 1996; Salmon and Powell, 1998). Exley et al. (1983) and Floyd et al. (1993) set out a granite classification scheme, types A to F, of which "Type-B"—coarse-grained megacrystic biotite granite—comprises over 90% of the suite. "Type-E" granite—equigranular lithium-mica (zinnwaldite and lepidolite) granite—represents the second most voluminous granite and is largely confined to the Tregonning and St. Austell plutons and the Meldon aplite dyke along the northwestern margin of the Dartmoor granite (Stone, 1984). To explain the petrogenesis of these different granite facies, Floyd et al. (1993) proposed what is now known as the "St. Austell Model," which shows the internal composition and zonation of a typical Cornish granite (Fig. 4). In this model, the early Type-B coarse megacrystic granite was intruded first by biotite granite and then by Type-E equigranular

Li-mica granite with a metasomatic halo forming "Type-D" megacrystic Li-mica and tourmaline granite. Alternatively, the so-called "1980s model" (Floyd et al., 1993; Fig. 5) considered that granitic magma was generated in the lower crust by heat derived from the mantle and later evolved by assimilation of upper-crustal components and differentiation of Li-mica granites, becoming increasingly more hydrated during the late stages until mineralized veins intrude through the carapace.

The Metamorphic Aureole

Emplacement of the Cornubian granites caused contact metamorphism of the enveloping Mylor Slate Formation. Early work by de la Beche (1839), Allport (1876), Phillips (1876), and Reid and Flett (1907) described the metasedimentary rocks ("killas") and concordant metabasic igneous rocks ("greenstones") that form the aureole, and outlined the respective increases in metamorphic grade toward the granite contact, thus identifying the effect of contact metamorphism. A certain group of greenstones, the cordierite-anthophyllite hornfelses of Kenidjack, just north of Cape Cornwall, have long been discussed (Tilley and Flett, 1929; Tilley, 1935; Vallance, 1967; Floyd, 1968; Chinner and Fox, 1974), as they are considered some of the best examples of this assemblage, aside from the classic cordierite-anthophyllite gneisses (COGs) of Orijärvi, Finland (Eskola, 1914; Schneiderman and Tracy, 1991). We targeted these rocks for P-T determination of peak aureole metamorphism (owing to their useful low-variance multiphase mineral assemblages, and to the unsuitability, commonly through late hydrothermal alteration, of pelitic hornfelses) as a way to quantify granite emplacement depth. Therefore, it is important to better understand how the petrogenesis of the Land's End cordierite-anthophyllite rocks relates to granite emplacement.

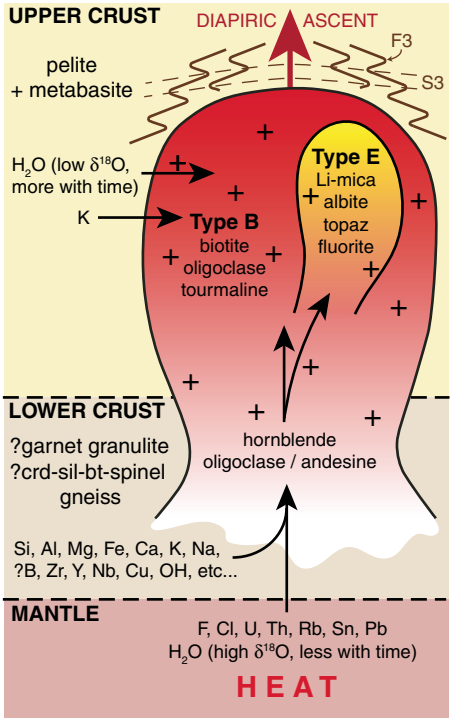

Figure 5. The "1980s model" of granite petrogenesis and emplacement, modified from Floyd et al. (1993) and Rattey and Sanderson (1984).

Tilley and Flett (1929) first proposed that the Kenidjack cordierite-anthophyllite rocks formed by weathering of parental basalts; however, Tilley (1935) later revised this theory in order to account for Fe and Mg enrichment by invoking metasomatism. However, both these interpretations were later dismissed by Vallance (1967) and Chinner and Fox (1974), who argued for formation by isochemical thermal metamorphism of pre-altered basalts. Floyd (1975) described Ca^{2+} mobility as being a key control on formation of the more "exotic" hornfelses from variably altered parental basalts, with chlorite-rich basalts metamorphosing to anthophyllite-bearing hornfelses, calcite-rich basalts forming hornblende-plagioclase hornfelses, and mobilised Ca later forming calc-silicate skarns through metasomatism.

Previous Theories Linking Cornubian Granite Emplacement to Host-Rock Deformation and Metamorphism

There has likewise been debate over the emplacement mechanisms and emplacement depths of the granites and the relationship between emplacement and host-rock deformation. Several early emplacement models assumed forceful diapiric intrusion of massive granitoid plutons (e.g., Booth, 1966; Rattey, 1980; Rattey and Sanderson, 1984; Goode and Taylor, 1988; Floyd et al., 1993), leading some to argue that S_3 and F_3 structures "are attributed to the same deformation event associated with the diapiric rise of the batholith" (Rattey and Sanderson, 1984, p. 91). Following this hypothesis, Rattey and Sanderson (1984) argued that ductile host-rock deformation, occurring in response to forceful en masse intrusion of hot buoyant granite, caused an S_3 cleavage development parallel to the diapir roof, and F_3 folds that verge away from the granite margins with a "Christmas tree" profile (Fig. 5). However, more recent work concludes that the regional D_3 event *predated* granite emplacement and is instead related to the latest Carboniferous-Early Permian extensional reactivation of Variscan thrusts (Shail and Wilkinson, 1994; Alexander and Shail, 1995, 1996; Shail and Alexander, 1997; LeBoutillier, 2003; Hughes et al., 2009; Shail and Leveridge, 2009). Such an extensional episode may have been the cause, rather than an effect, of granite generation and emplacement (Shail et al., 2003). The concept of diapiric emplacement may also be negated by more recent field studies of relationships between different granite types, which suggest the granites are largely composite bodies comprising discrete sheetlike intrusions often with sharp planar contacts (Salmon, 1994; Salmon and Powell, 1998; Powell et al., 1999; Müller et al., 2006). Nevertheless, examples of small-scale diapiric structures have been reported (Powell et al., 1999), and attributed to instances when a fluid magma has been injected into a similarly fluid granite host.

Previous P-T estimates of the Cornubian granites upon emplacement are wide ranging and often poorly constrained (see Table 1). Here, we present the first THERMOCALC P-T estimate for Cornubian granite aureole rocks in order to determine the depth of granite emplacement to better evaluate the emplacement mechanism. First, we present the field relationships of each region mapped in detail.

FIELD RELATIONSHIPS AND AUREOLE PETROGRAPHY

Four coastal sections were selected for mapping on the basis that they clearly display granite contact relations and aureole lithologies. Mapping was conducted at 1:5000 during June–August 2009 by JMP. As shown in Figure 1C, they are the: (1) 7-km-long "St. Just aureole," from Cape Cornwall to Portheras Cove, encompassing both metapelites and metabasites, including pillow basalts, calc-silicates, and the cordierite-anthophyllite hornfelses of Kenidjack and Botallack; (2) areas around the Porthmeor granite cupolas and Land's End granite contact in the vicinity of Great Zawn; (3) Tater-du peninsula, south Land's End granite; and (4) Tregonning granite coastal exposure from Praa Sands to the granite sheets at Megiliggar Rocks.

In this section, we present an account of the key field relations for both the Land's End and Tregonning aureoles. In addition to this, a more comprehensive area-by-area report on the mapped regions can be found in Appendix 1. For our new geological map, see Plate 1, which is available at its full size (1:5000) online. A schematic vertical section summarizing aureole stratigraphy, which can be used as

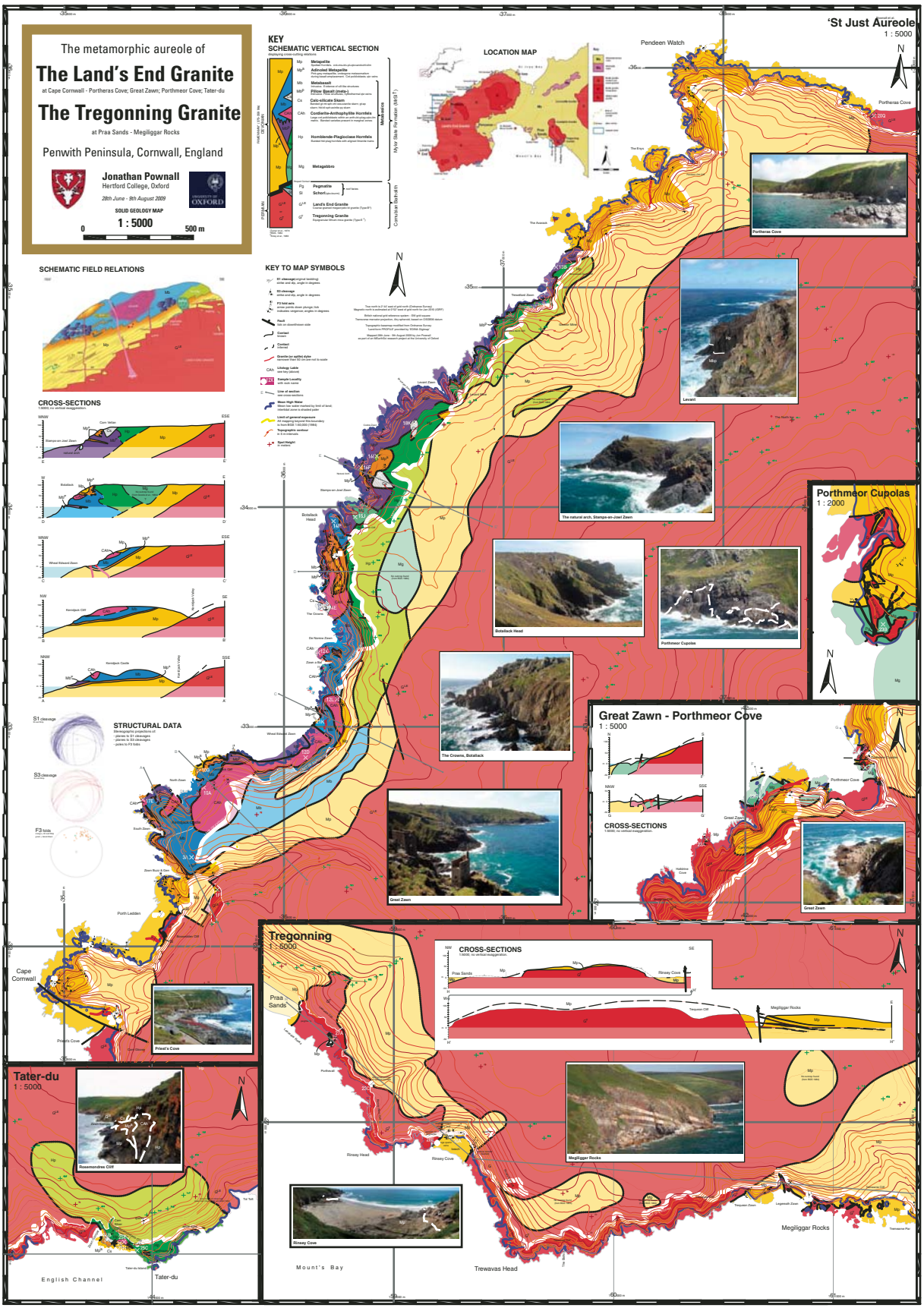

Plate 1. Geological map (1:5000) of the Land's End and Tregonning granite aureoles. If you are viewing the PDF of this paper or reading it offline, please visit http://dx.doi.org/10.1130/GES00802.S1 or the full-text article on www.gsapubs .org to view the full-sized PDF file of Plate 1.

a key to maps presented later in the paper, is shown in Figure 6.

Land's End Granite Aureole

All aureole rocks mapped as part of this study are assigned to the Devonian Mylor Slate Formation, which comprises both metapelites and concordant basic sills and lavas (Goode et al., 1984; Goode and Taylor, 1988). Metapelites are best exposed at the north (Pendeen Watch) and south (Cape Cornwall; Fig. 7) of the St. Just aureole, with only small isolated bodies occurring near Botallack and Levant. The entire Tregonning granite coastal aureole is also metasedimentary. Basalts were extruded through the sediments and are mostly exposed in the center of the St. Just aureole with some having later developed cordierite-anthophyllite and hornblende-plagioclase assemblages.

Aureole Rock Petrography and Contact Relations

Metapelites. The metapelites are typically dark gray, fine-grained, strongly foliated (S_1), remarkably hard, and can be described as "spotted hornfelses" (or "spotted slates" if poorly indurated) due to the abundance of small (<3 mm) dark patches of cordierite and/or andalusite visible in hand samples (Fig. 8B). The peak assemblage comprises Crd+Bt+Ms+Chl+Pl+Qtz ± And ± Ilm with occasional apatite, pyrite, and corundum. The cordierite is markedly poikiloblastic, and incorporates fine-grained quartz and feldspar of the siltstone protolith. The hornfelses are micaceous; biotite is abundant and aligned to cleavage although muscovite is scarcer. Cordierite spots often have pinitised rims (retrogression to muscovite and clays). Andalusite poikiloblasts were found to be rarer than cordierite; chiastolite was never observed. Abundant quartz veins and vugs result from hydrothermal fluids generated late during Variscan convergence; elsewhere they postdate regional D_2 structures but are deformed by D_3 (Hughes et al., 2009).

Metabasic rocks. Metamorphosed pillow basalts (Fig. 9A) and dolerite sills (Fig. 9B) are interbedded with metapelites as members of the Mylor Slate Formation. An excellent demonstration of the field relationship between these two lithologies is provided by the small lone dolerite sill within the folded metapelites of Priest's Cove (Fig. 8C). However, in most instances where basalt and (altered) metasedimentary beds are intricately interbanded, the exact contact plane is difficult to pinpoint (Fig. 10). The clearest indicator of such contact zones is the atypical pink-gray appearance of the metapelites at close proximity to basalt (Fig. 9B and 9C). In many localities, these altered metapelites contain large (up to 10 mm diameter) euhedral cordierite poikiloblasts, rather than amorphous spots, with biotite and ilmenite inclusions (Fig. 9C), and are often host to thin planar crosscutting quartz veins related to those in the pillow basalts. These rocks have undoubtedly been altered by basalt and dolerite emplacement and subsequent metasomatism, and thereby represent a minor basalt "aureole" that has later been overprinted by subsequent thermal metamorphism during granite emplacement (also noted by Flett, 1903; Mitropoulos, 1984). At the contact at The Avarack (Fig. 9D), where sediment was deposited onto cooled basalt with an extinct hydrothermal system, no alteration is seen and the contact is of very different character. The (meta-)basalts and dolerites display gradational contacts with cordierite-anthophyllite rocks (described separately next), strongly suggesting they are the protolith for such later-developed assemblages. Similarly, these basalts (and/or associated gabbros) are very probably the parent rock for banded hornblende-plagioclase hornfelses, described by Tilley (1935, p. 186) as "characteristic contact rocks," which crop out closer to the granite contact. Both the hornblende-plagioclase and cordierite-anthophyllite hornfelses contain early-formed ilmenite trains, suggesting that both lithologies may share similar metamorphic histories.

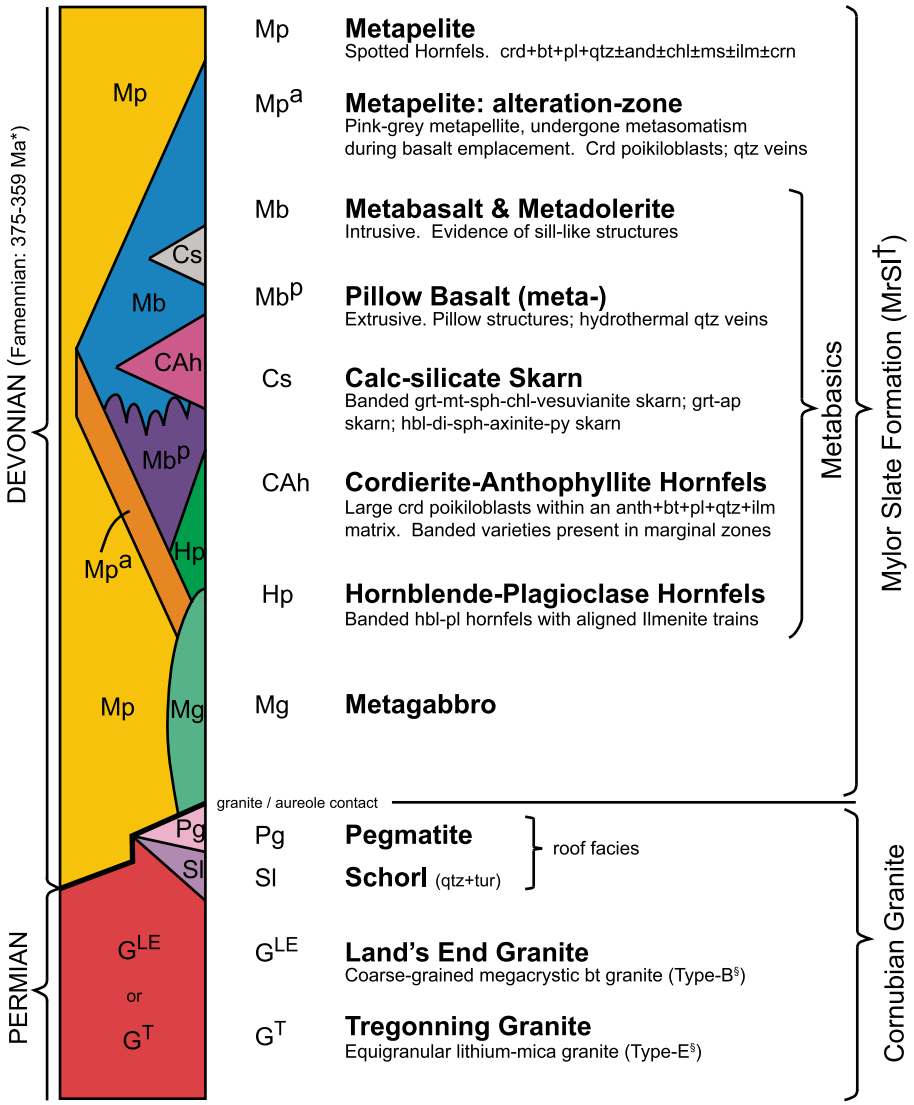

Figure 6. Schematic vertical section of lithologies mapped, displaying crosscutting field relations. Please use this diagram as a key to the maps included throughout the paper. *—Turner et al. (1979); †—abbreviation by Goode and Taylor (1988); §—granite classification of Exley et al. (1983).

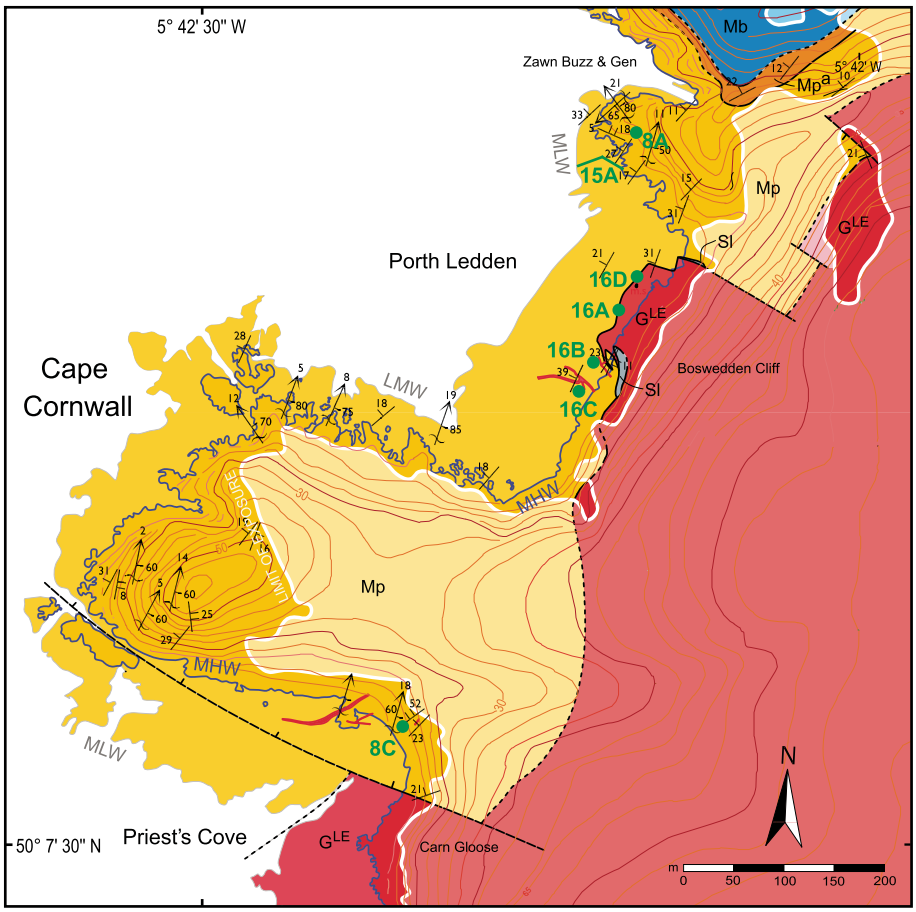

Figure 7. Geological map of Cape Cornwall taken from Plate 1**. See** Fig. 6 **for key to lithologies. Locations of photographs in other figures are marked in green. MHW and MLW indicate the mean high and low water marks, respectively, and the intertidal zone is shaded in a paler color. The limit of exposure is indicated with the white line.**

Cordierite-Anthophyllite hornfelses. Following Tilley and Flett (1929), a band of cordierite-anthophyllite facies rocks from Kenidjack Castle to The Crowns, Botallack has been remapped (Figs. 11 and 12). These rocks are derived from metamorphosed basalts with which they share a gradational contact. They are best displayed at the quarries at Kenidjack Cliff and at the small promontory between De Narrow Zawn and Zawn a Bal. At these localities, the cordierite forms large (typically 1 cm but up to 8 cm) spherical poikiloblasts that have weathered out from the matrix, forming the characteristic nodular texture termed "ball-rock" by Tilley (1935) (Fig. 13A). In more marginal localities, such as above Wheal Edward Zawn (Fig. 11B, sample 12D; Fig. 12B, sample 12L), the rock has a banded appearance comprising blue-gray cordierite-rich and brown-gray anthophyllite-bearing horizons. More homogeneous varieties also exist at closer proximity to metabasalts. These hornfelses have a pronounced foliation, concordant with the surrounding S_1 fabric, which is defined by aligned trains of biotite and ilmenite. At Tater-du (Fig. 14), cordierite-cummingtonite assemblages were observed.

Calc-silicate rocks. Calc-silicate assemblages mapped on the St. Just aureole include a sheeted garnet-magnetite-sphene-chlorite-vesuvianite skarn at The Crowns, a garnet-apatite skarn at Carn Vellan, and a massive hornblende-diopside-sphene-axinite(-pyrite) skarn on Trewellard South Cliff. Similar to the cordierite-anthophyllite rocks, these calc-silicate skarn deposits occur discordantly within metabasalts and associated assemblages and were suggested by Alderton and Jackson (1978) to have formed by metasomatic introduction of basalt-sourced Ca by granite-derived fluids during late stages of emplacement.

Granite-Aureole Field Relations

The Land's End granite and its contact relations with aureole rocks were studied at Priest's Cove, Porth Ledden, and Portheras Cove (Figs. 7 and 15). The typical facies present is a buff-pink, medium to coarse grained, two-mica granite characterized by large, often-aligned euhedral orthoclase megacrystic phenocrysts (e.g., Vernon, 1986; Vernon and Paterson, 2008), which also contains minor tourmaline, cordierite, apatite, zircon and monazite (Müller et al., 2006)—an Exley et al. (1983) Type-B granite. Splays of black tourmaline needles are especially abundant along marginal zones of the granite, including sills and dykes.

In all instances, the fabric of the aureole rocks (D_1 to D_3) is cleanly truncated by the contact with the Land's End granite and radiating aplite dykes (Figs. 16 and 18). At several localities such as Carn Veslan (Fig. 17), intense D_3 chevron folding is clearly crosscut by granite intrusions (Fig. 18A), and the deformation is therefore shown to predate granite emplacement.

At Portheras Cove (Fig. 15B) and Great Zawn (Fig. 18), the granite-aureole contact is unfaulted and forms a stepped profile revealing sheetlike granite geometries. Granites often display both horizontal jointing, which is aligned with the S_1 fabric of the adjoining hornfelses, and vertical jointing, which runs parallel to the steps in the contact, suggesting the granite was in part accommodated by the stoping of roughly cuboid blocks of country rock that broke off along and perpendicular to the S_1 plane of weakness. Sills and dykes extending from the leading edge of the granite sheets, as seen at Portheras Cove, Great Zawn, and Megiliggar Rocks (see section on the Tregonning granite) can therefore be considered precursors for pluton growth. Granite dykes also crosscut D_3-deformed quartz-veined metapelites at several localities between Porth Ledden and Portheras Cove (Fig. 16E). Wide, heavily tourmalinized quartz veins have often developed along vertical joints in the granite that have likely arisen through late-stage fluid migration. Prime examples of stoped blocks can be found at Porth Ledden (Fig. 15A), where a number of small hornfels xenoliths and a large hornfels block (> 10 m long) border the pluton margin.

At Porthmeor Cove are two small granite cupolas whose emplacement has been independent of the main Land's End granite (Figs. 17 and 19); see Appendix 1 for details.

Structure of the St. Just Aureole

It can be concluded that the structure of the aureole rocks is broadly consistent over the region mapped. F_3 folds dominate, with only a few recognized F_1 structures. F_2 folds were not knowingly observed but have been described by Hughes et al. (2009). F_3 fold axes are roughly

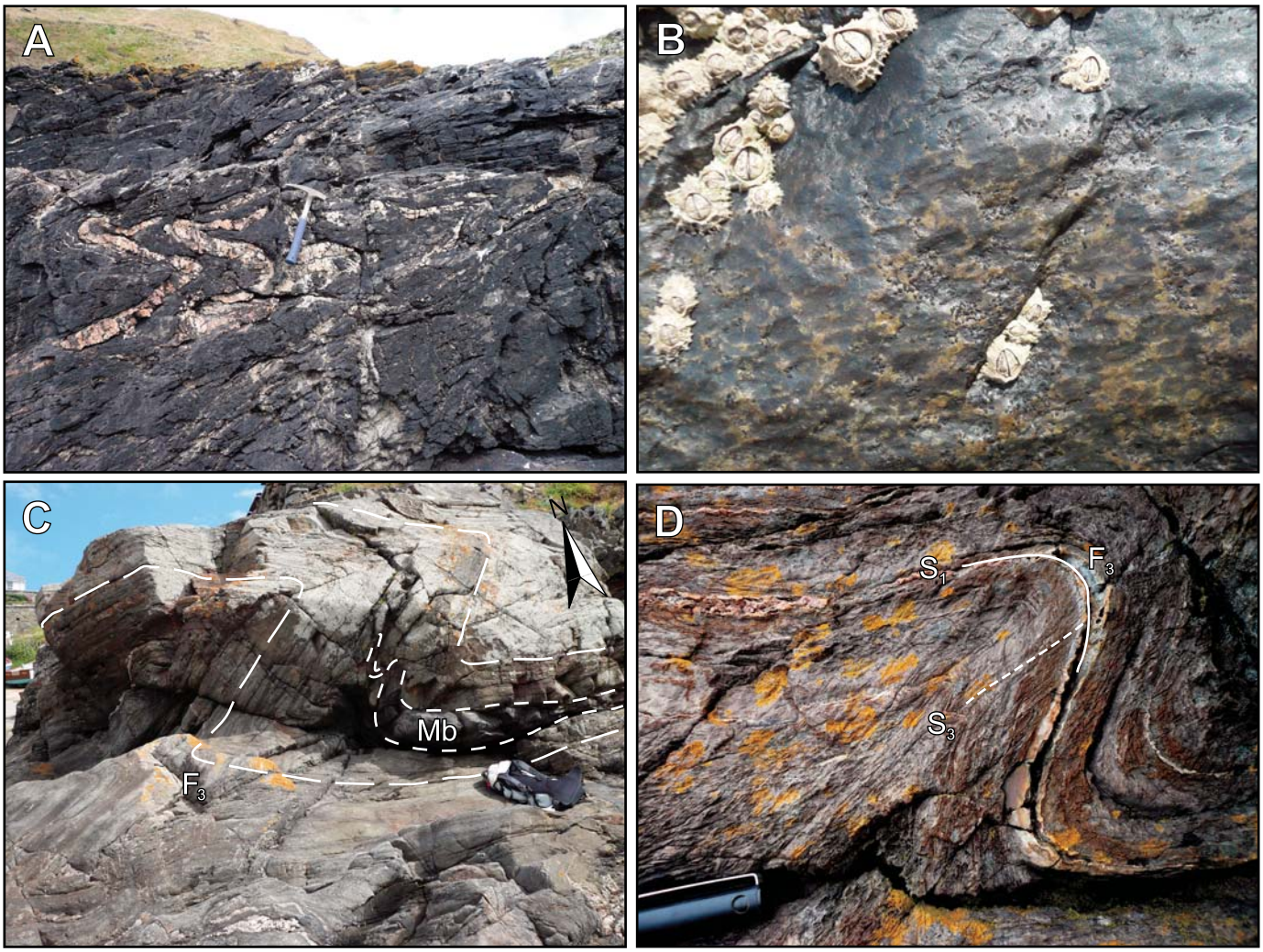

Figure 8. Metapelites of the St. Just aureole. (A) Quartz-veined hornfels displaying F_3 folds, north of Porth Ledden. (B) Typical spotted hornfels showing abundant cordierite with altered (pinitised) rims. Barnacles (~3 mm) for scale. (C) Zigzag F_3 fold at Priest's Cove, incorporating a thin metadolerite sill (Mb). Rucksack for scale. (D) Small F_3 fold with prominent S_3 axial-planar cleavage, Pendeen Watch.

parallel to the line of intersection of S_1 and S_3 planes. A dominant primary cleavage (S_1) is usually bedding-parallel as a consequence of isoclinal F_1 folding; it is often intersected by a strong secondary cleavage (S_3), axial-planar to the F_3 folds. It should be noted that F_3 fold axis azimuths at Cape Cornwall (~015°) progressively become more eastward-directed moving northward to Pendeen Watch (to ~045°); this has been ascribed to post-folding rotation across NW–SE strike-slip faults by Hughes et al. (2009).

The regional structure is revealed by compilation of S_1 and S_3 orientations (Fig. 20C), and can be generalized as a broad anticlinal structure with fold axis aligned roughly parallel to the granite/aureole contact plane of the NW pluton margin (with slight northward plunge). Although the data show relatively poor correlation, it can still be argued that the aureole shows signs of doming uplift around the margin of the granite, which could have been caused by inflative emplacement. Other studies (Alexander and Shail, 1995, 1996) show that D_3 structures have similar orientations to the east of the pluton. Therefore, D_3 deformation seems very unlikely to have been driven by a diapir-induced radial strain field as would be expected if the Rattey and Sanderson (1984) model of forceful diapiric intrusion were correct.

The nature of the contact between metabasic and metapelitic rocks is roughly parallel to original bedding. However there is a discrepancy between S_1 (35° dip) and the average dip of the contact plane (10°). This may be accounted for by two factors: (1) that the basalt was partly intruded as a sequence of parallel sills with an upwards-stepping leading edge; and (2) extensive simple shearing of the whole region by D_3, manifested as the observed downward-stepping of the ESE-verging F_3 folds, has widened the angle between measured S_1 and the actual original depositional surface (maximum strain ~70%). Cross-sections are presented in Figure 21.

Tregonning Granite Aureole

The entire Tregonning coastline was mapped at 1:5000 (see Plate 1); however, there are only three regions where the aureole rocks are exposed: east Praa Sands, Rinsey Cove, and Megiliggar Rocks. In all instances, the aureole comprises exclusively metapelites.

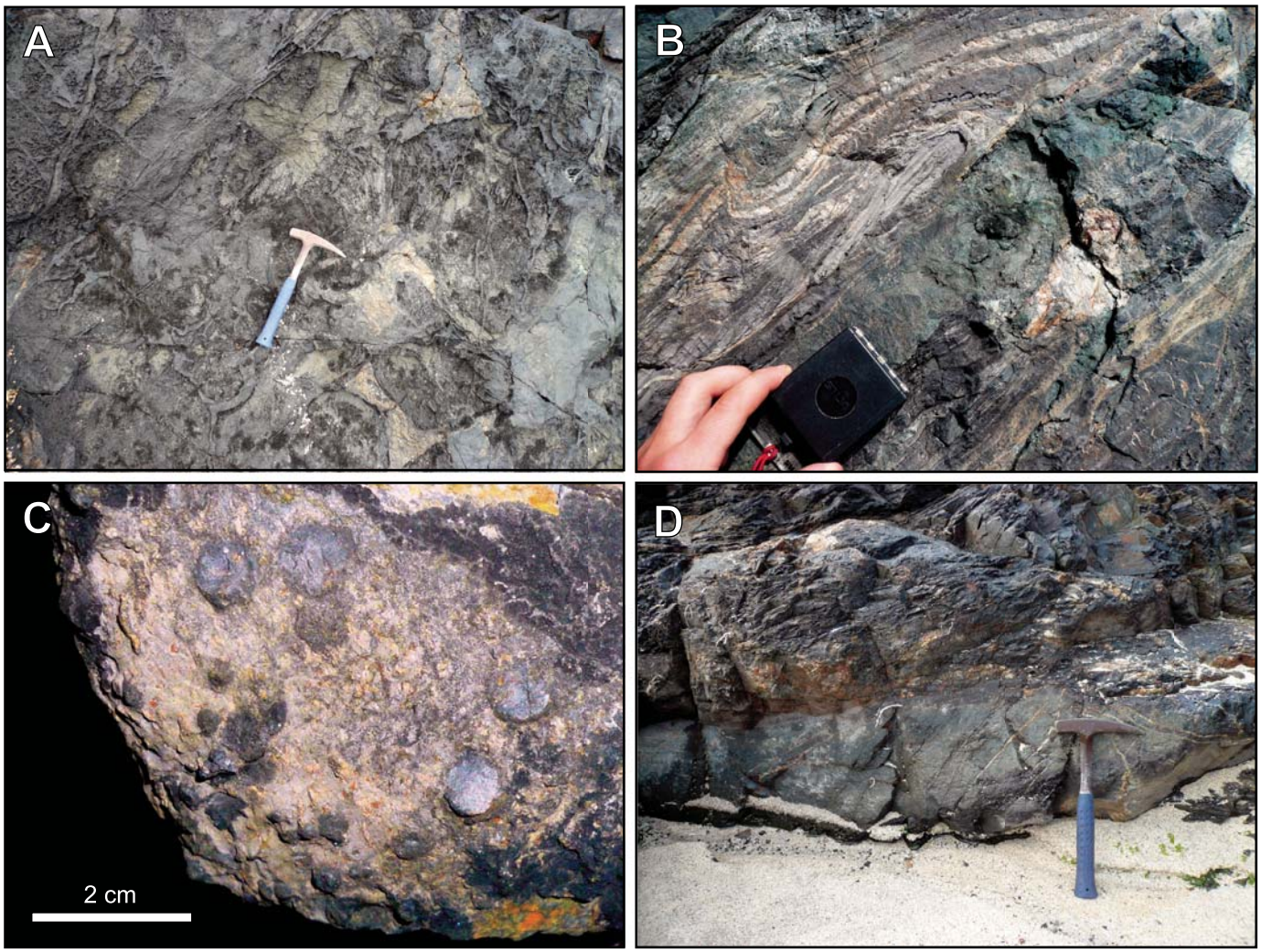

Figure 9. Metabasalts and metabasalt–metapelite contact relations, St. Just aureole. (A) Typical pillow basalts, Kenidjack. (B) Thin basalt sill intruding deformed pink-gray alteration-zone metapelites at the metabasalt–metapelite contact east of Wheal Edward Zawn. (C) Basalt-altered pink-gray metapelite containing large euhedral cordierites, Kenidjack Cliff (see Fig. 10). (D) Metapelites atop metabasalt with no alteration zone, near The Avarack.

At Megiliggar Rocks (Figs. 22 and 23; previously described by Stone, 1975, 1992), several thick granite sheets intrude the metapelites, thinning away from the Tregonning granite with a dip of ~20° (Fig. 23A). The formation is upthrown by a major fault to the west, and so provides insight into granite–country-rock relations at depth. One major sheet branches, then remerges further east entrapping a slice of hornfels, demonstrating mechanisms of country-rock isolation and sill amalgamation. Stepped contacts in association with xenoliths demonstrate that a stoping mechanism operated within individual sheets (Fig. 23B); xenoliths may result from failed bridge structures due to growth of adjacent *en echelon* intrusions. The interior of the sheets, best exposed on intersection with the wave-cut platform, display massive, homogeneous fabrics and angular jointing, and are indistinguishable from the granites of the main plutons. This suggests it is plausible for the plutons to have formed from amalgamation of granite sheets. Megiliggar Rocks may therefore represent an arrested stage of pluton construction, exhibiting mechanisms of sill-intrusion and amalgamation, accommodated by isolation and stoping of the country-rock, plus roof uplift.

DEPOSITION AND DEFORMATION OF THE MYLOR SLATE FORMATION

Deep-marine sedimentation within the Devonian Gramscatho basin was punctuated by episodes of basaltic volcanism resulting in intrusion of basic sills and extrusion of pillow basalts. Gabbros were emplaced prior to D_1 deformation and are likely associated with the basalts. Dolerite sills within the sedimentary rocks (Figs. 8C, 9B, 14B), and likewise bodies of sedimentary rock encapsulated within the basalts, demonstrate that basalt horizons are not laterally extensive. These field relationships partially account for the discrepancy between the average basalt-metapelite contact angle and the S_1 dip to which both were originally orientated, assuming a stepped leading-edge of successive basalt sheets that have since been sheared by D_3.

A hydrothermal system associated with this seafloor volcanism has evidently caused

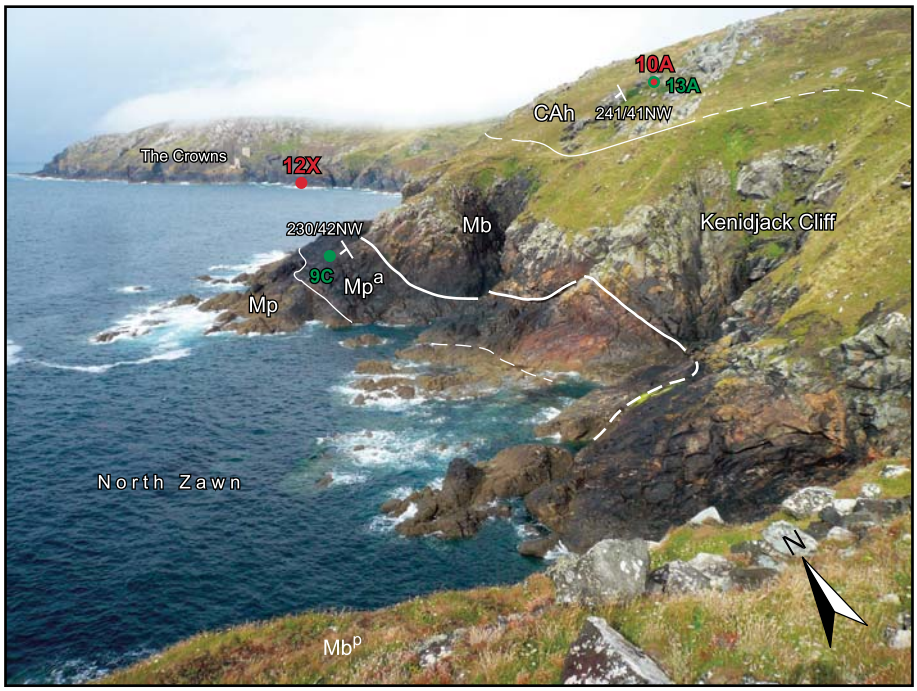

Figure 10. Photograph of Kenidjack Cliff showing the nature of the Metabasalt (Mb)—Metapelite (Mp) contact with the narrow alteration zone (Mp^a). The transitional boundary with cordierite-anthophyllite rocks (CAh) is marked approximately. Red dots indicate sampling locations of two cordierite-anthophyllite rocks. Green dots indicate locations of photographs in other figures.

fluid transport through surrounding sediments forming alteration zones characterized by soft, pink cordierite-rich metasedimentary rocks and extensive quartz-veining. This zone represents a minor basalt aureole (strictly a metasomatic adinole) that has subsequently been overprinted by granite-related contact metamorphism and incorporated into the main Land's End aureole. Widespread quartz veining present throughout the metasedimentary rocks may be related to this hydrothermal event, to granite emplacement, or to regional metamorphism predating granite emplacement. Quartz veins are affected by D_3 deformation and therefore cannot be sourced from a granite intrusion that postdates F_3 folding; a significant portion likely originated during early-Variscan regional metamorphism. These extensive F_3-defining quartz veins (plus associated S_3 axial-planar cleavage) are cleanly truncated at all observed granite contacts, and there are no perceivable effects of granite emplacement on aureole fabrics at outcrop scale (e.g., Fig. 18A).

It is concluded that D_3 deformation predates granite emplacement and must instead be caused by post-convergence extension as summarized by Shail and Leveridge (2009) and Hughes et al. (2009). We therefore reject the hypotheses of Rattey (1980) and Rattey and Sanderson (1984) that D_3 was caused by granite emplacement. Nevertheless, the structural data presented earlier indicate a broad anticlinal structure for hornfels overlying the granite roof, and we therefore acknowledge that granite emplacement has caused host-rock deformation, albeit overprinting D_3, in the form of regional (long-wavelength) uplift and doming (D_4).

THERMOBAROMETRY OF THE KENIDJACK CORDIERITE-ANTHOPHYLLITE ROCKS

Cordierite-orthoamphibole rocks, as previously mentioned, comprise an unusual metamorphic assemblage characterized by Ca-poor amphiboles and bulk compositions rich in Fe+Mg+Al. Such assemblages may be derived from either an igneous or sedimentary protolith and thus are often regarded simply as "allochemical metamorphic products" (Vallance, 1967, p. 84). The classic cordierite-orthoamphibole gneisses (COGs) of the Orijärvi region, Finland (Eskola, 1914), have in recent years been restudied in light of new analytical techniques (e.g., Schneiderman and Tracy, 1991; Smith et al., 1992); however, the cordierite-anthophyllite hornfelses of Kenidjack have only once been re-analyzed (Chinner and Fox, 1974) since the original studies by Tilley and Flett (1929) and Tilley (1935).

Five cordierite-anthophyllite rocks were collected from Kenidjack, St. Just aureole (samples 10A, 12D, 12L, 12X, and 17E; Fig. 24); three (10A, 12D, and 12L) of these were selected for thermobarometry in order to constrain the emplacement depth of the adjacent Land's End Granite.

Cordierite-Anthophyllite Hornfels Mineral Chemistry

Polished thin sections of the three samples were analyzed at the University of Oxford using a JEOL JSM-840A Scanning Electron Microscope (SEM) fitted with a Link ISIS energy-dispersive microprobe system (EDS) for quantitative analysis. Operating conditions were a 20.0 kV accelerating voltage, 5.00 nA beam current (with 2 μm beam diameter for spot analysis), 15 mm working distance, and a 100 second live counting time. Calibration was by natural and synthetic standards, and a ZAF correction procedure was applied. Spot analyses were always performed at >250 × magnification to ensure high-resolution control of beam location and minimal deviation from perpendicular beam incidence. Averaged microprobe analyses are presented in Table 2, and bulk compositions (mol% in NCKFMASHTO) are presented in Table 3.

Orthoamphibole is present throughout (at ~15 vol% abundance) as radiating sprays of acicular crystals (Figs. 13C and 13D), whose compositions (Fig. 25) plot close to the anthophyllite endmember (low Al; low Fe; low Na). Cordierites are large (~1 cm in 10A), spherical, and extremely poikiloblastic containing biotite, plagioclase, quartz, and ilmenite, and account for ~25 vol%. In 12X, cordierite is pseudomorphed by bytownite. Fine-grained biotite is present throughout but mainly confined to the matrix and has medium-high X(Mg) (~0.7 average) and fairly high Ti. The rest of the matrix comprises plagioclase and quartz. Plagioclase compositions vary widely between oligoclase and labradorite. Ilmenite trains are present through both cordierite poikiloblasts and the matrix and account for around 3 vol% of the rock (Fig. 13B). Accessory minerals include pyrite (fairly abundant in 10A) and apatite.

Ti-in-Biotite Geothermometry

The biotite Ti-saturation geothermometer of Henry et al. (2005) has been applied to

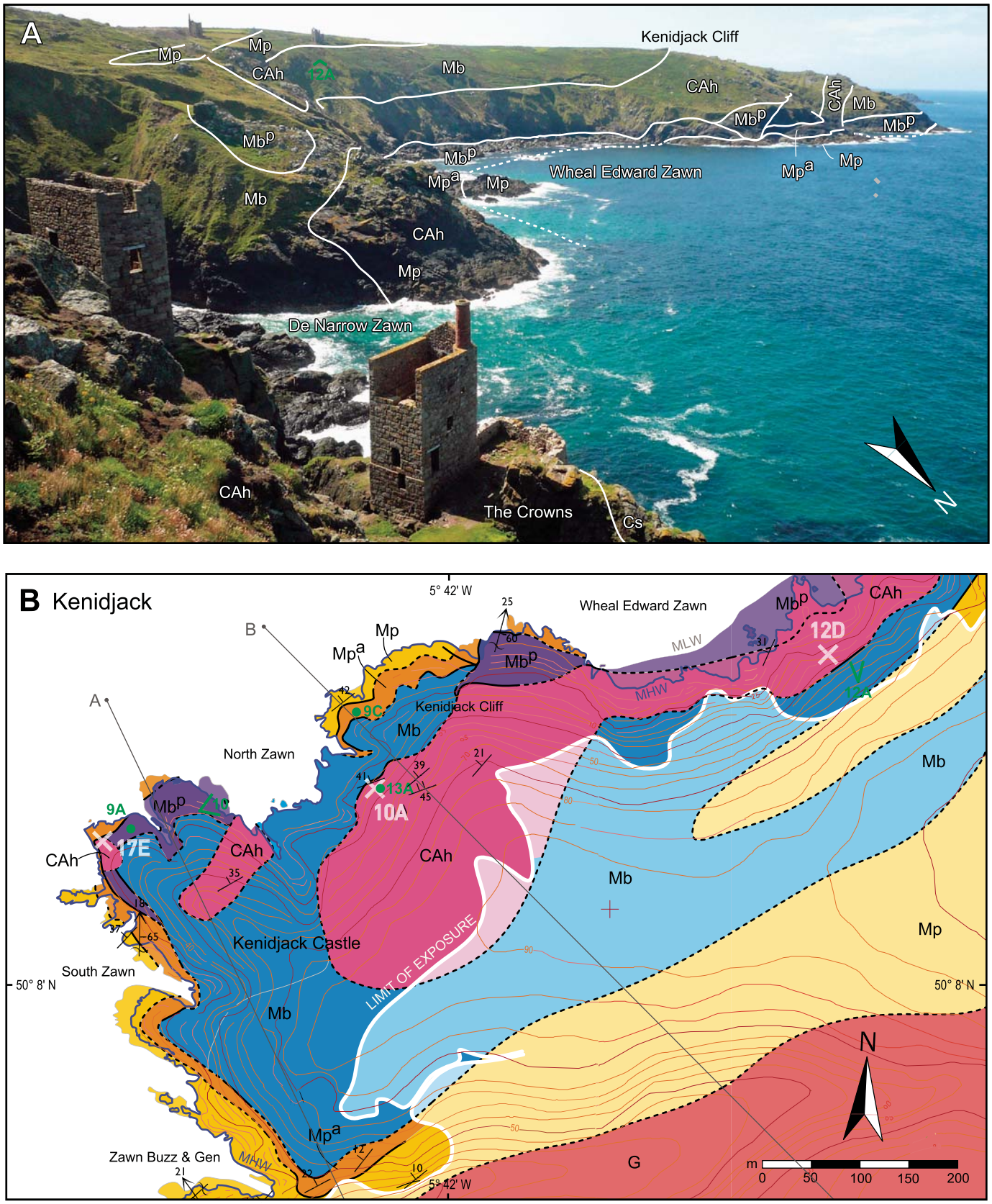

Figure 11. (A) Photograph of Kenidjack Cliff taken from The Crowns overlaid with geological boundaries. (B) Geological map of Kenidjack taken from Plate 1. See Fig. 21 for cross-sections A and B; see Fig. 6 for key to lithologies. Locations of photographs in other figures are marked in green. MHW and MLW indicate the mean high and low water marks, respectively, and the intertidal zone is shaded in a paler color. The limit of exposure is indicated with the white line.

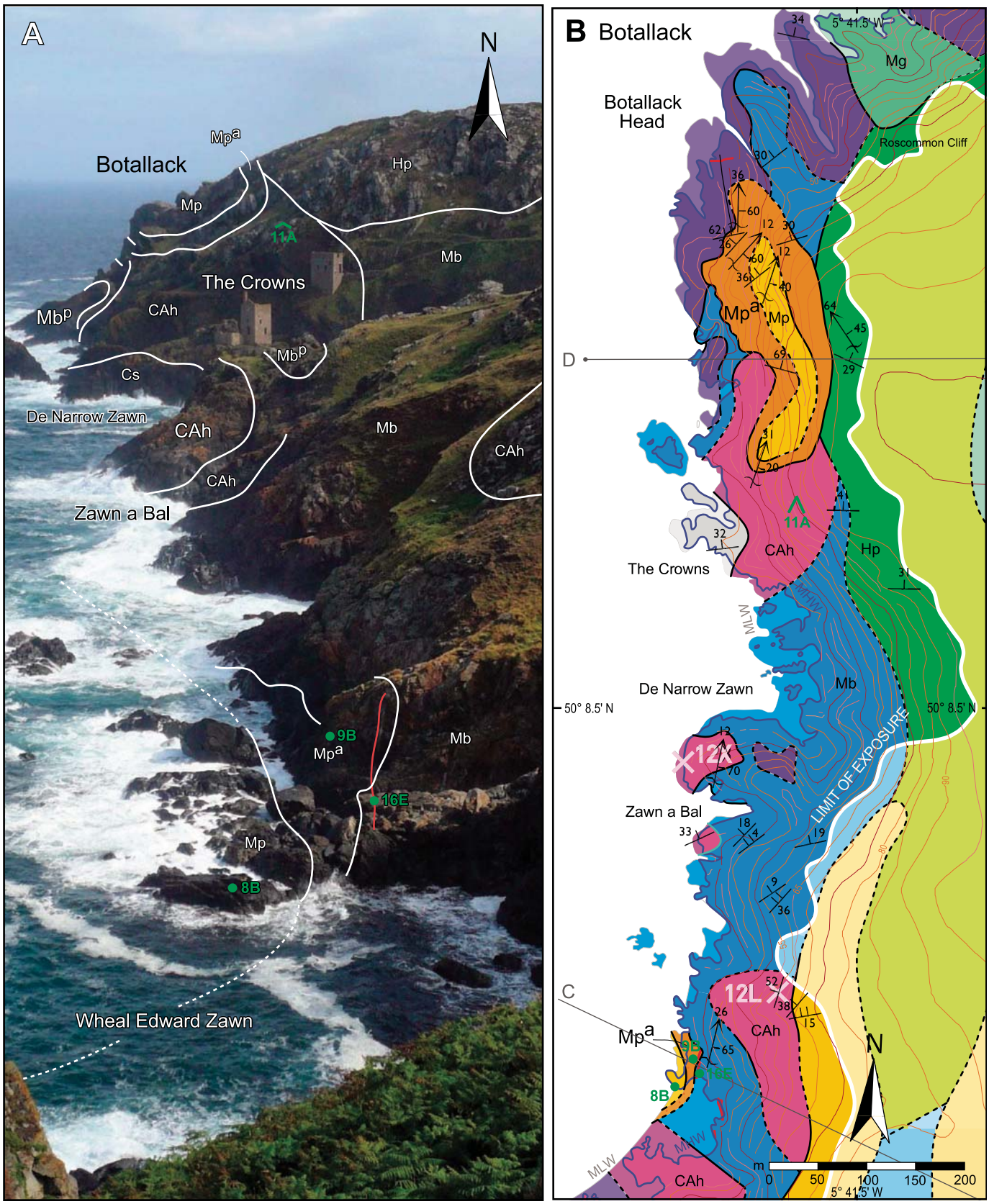

Figure 12. (A) Photograph of Botallack Cliff taken from above Wheal Edward Zawn overlaid with geological boundaries. (B) Geological map of Botallack taken from Plate 1. See Fig. 21 for cross-sections C and D; see Fig. 6 for key to lithologies. Locations of photographs in other figures are marked in green. MHW and MLW indicate the mean high and low water marks, respectively, and the intertidal zone is shaded in a paler color. The limit of exposure is indicated with the white line.

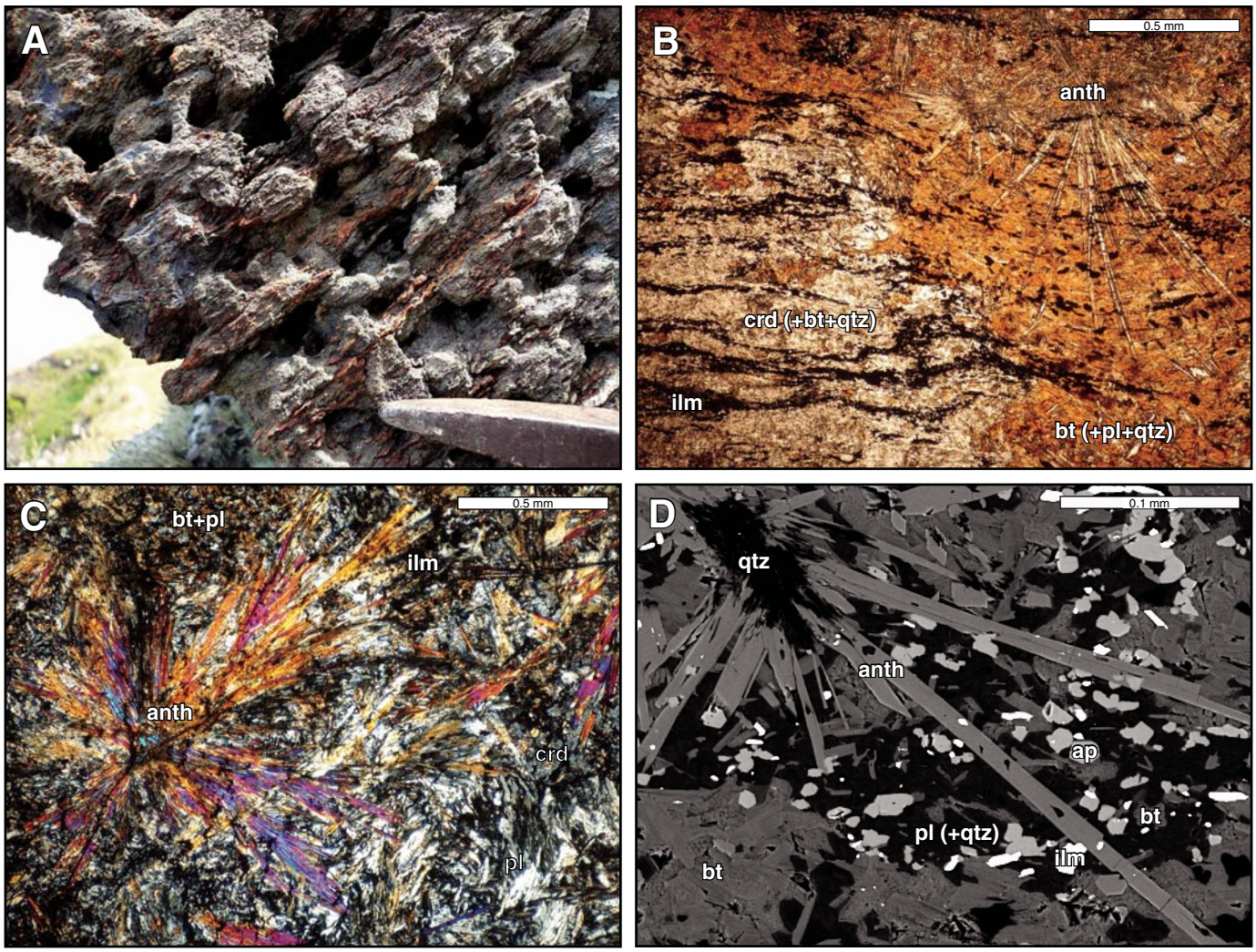

Figure 13. Cordierite-anthophyllite hornfelses. (A) Photograph of outcrop at Kenidjack exhibiting large weathered-out cordierite "knots" aligned to strong ilmenite-defined S_1 foliation (250/41°NW). Length of visible hammer is ~9 cm. (B) Photomicrograph (PPL) of sample 10A (from same locality as A) sectioned through a large cordierite poikiloblast (left). (C) Photomicrograph (XPL) of sample 12L from South Botallack displaying large anthophyllite burst. (D) Back-scattered electron (BSE) image of sample 10A displaying anthophyllite needles within bt+pl+qtz matrix.

all five cordierite-anthophyllite hornfelses and three metapelites (for comparison) and yielded temperature estimates as shown in Figure 26. It must be noted, however, that the Henry et al. (2005) geothermometer is calibrated for graphitic, peraluminous metapelites that contain ilmenite or rutile and have equilibrated at ~4–6 kbar, for which an error of ± 24 °C is quoted. This pressure is higher than calculated for the rocks in this instance, nevertheless the geothermometer is still the most suitable available, and produces a useful (although poorly constrained) temperature estimate of 615 ± ~50 °C of the cordierite-anthophyllite hornfelses, complementary to the P-T pseudosections. For comparison, the three analyzed metapelites yield notably higher (arguably implausibly high?) temperature estimates of 680 ± 50 °C.

Construction of THERMOCALC P-T Pseudosections

We used the computer program THERMOCALC (Powell and Holland, 1988, 2008) to produce P-T pseudosections for three cordierite-anthophyllite rocks in the NCKFMASHTO system, as presented in Figure 27. The recent compilation of activity composition (a-X) codings for cummingtonite-grunerite, anthophyllite, and gedrite (Dale et al., 2005; Diener et al., 2007) now allow geologically realistic modeling of cordierite-orthoamphibole rocks in large chemical systems such as NCKFMASHTO (Diener et al., 2008).

Calculations were performed with THERMOCALC 3.33 (tc333.exe; Powell and Holland, 1988, updated October 2009), using the Holland and Powell (1998) internally consistent thermodynamic data set (tc-ds55.txt) and the NCKFMASHTO system a-X codings (tc-NCKFMASHTOi.txt) for garnet, biotite and silicate melt (White et al., 2007), chloritoid, cordierite, epidote, staurolite and talc (Holland and Powell, 1998), clino- and orthoamphibole (Diener et al., 2007), clinopyroxene (Green et al., 2007), orthopyroxene (White et al., 2002), chlorite

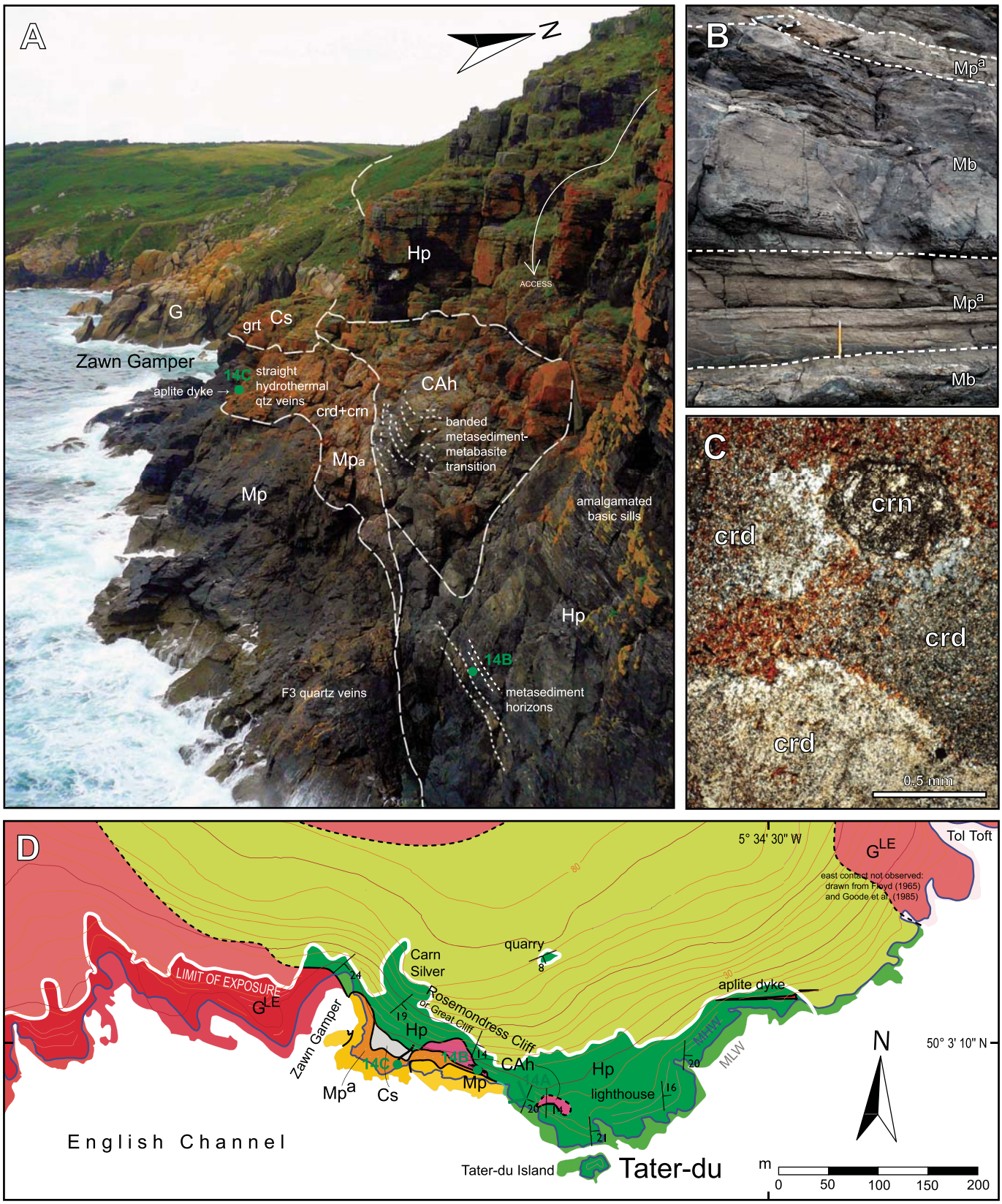

Figure 14. Tater-du, south Land's End Granite. (A) Photograph of Rosemondress Cliff overlain with geological boundaries. Locations of other photos are indicated in green. (B) Metapelite horizons (Mp^a) within metabasalts (Mb). Pencil for scale. (C) Thin-section (XPL) of altered metapelite bearing sapphire (corundum; crn) and cordierite (crd) poikiloblasts. (D) Geological map of Tater-du taken from Plate 1. See Fig. 6 for key to lithologies. MHW and MLW indicate the mean high and low water marks, respectively, and the intertidal zone is shaded in a paler color. The limit of exposure is indicated with the white line.

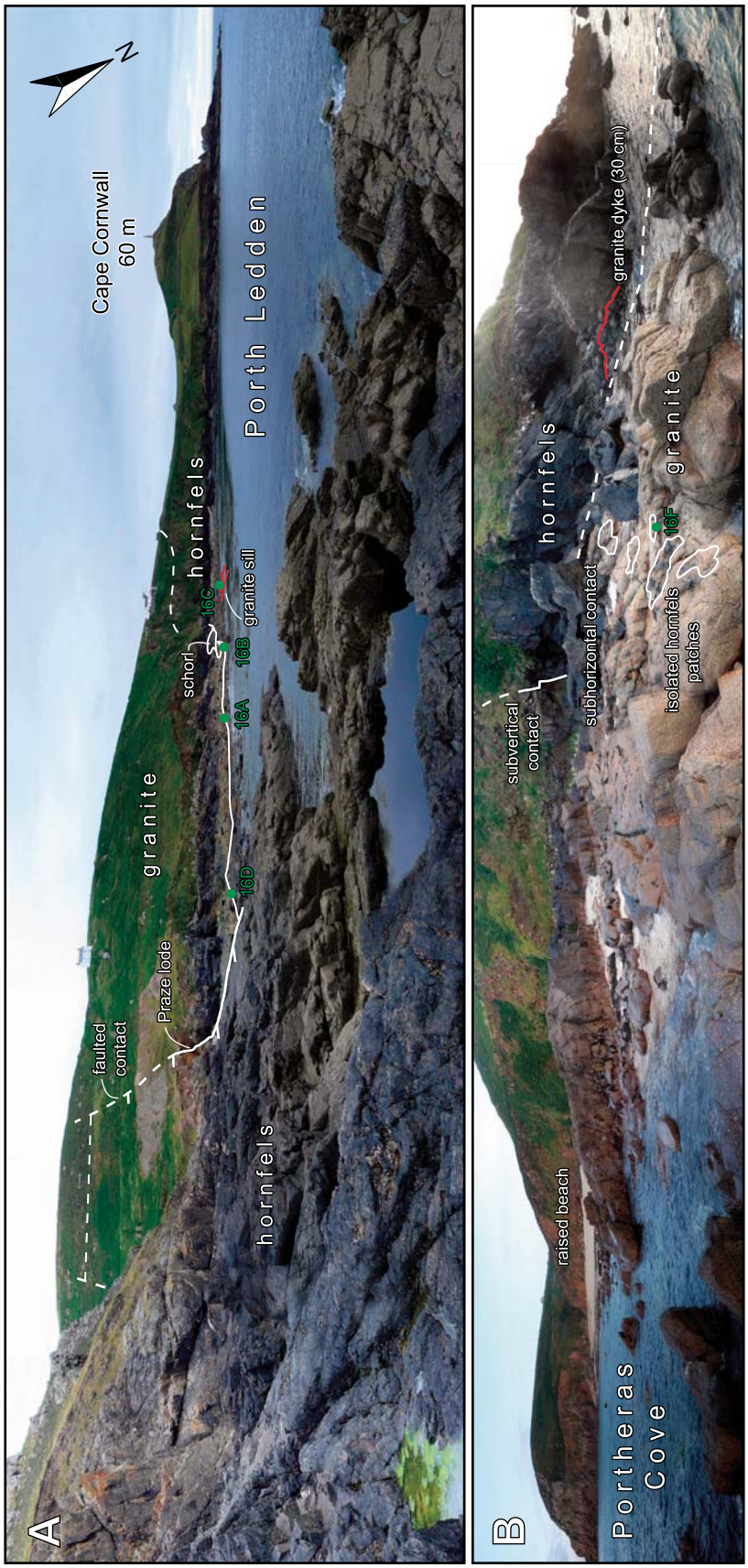

Figure 15. Panoramic photographs of the Land's End granite–aureole contact of the St. Just aureole at (A) Porth Ledden, and (B) Portheras Cove. Locations of photographs shown in Figure 16 are indicated in green.

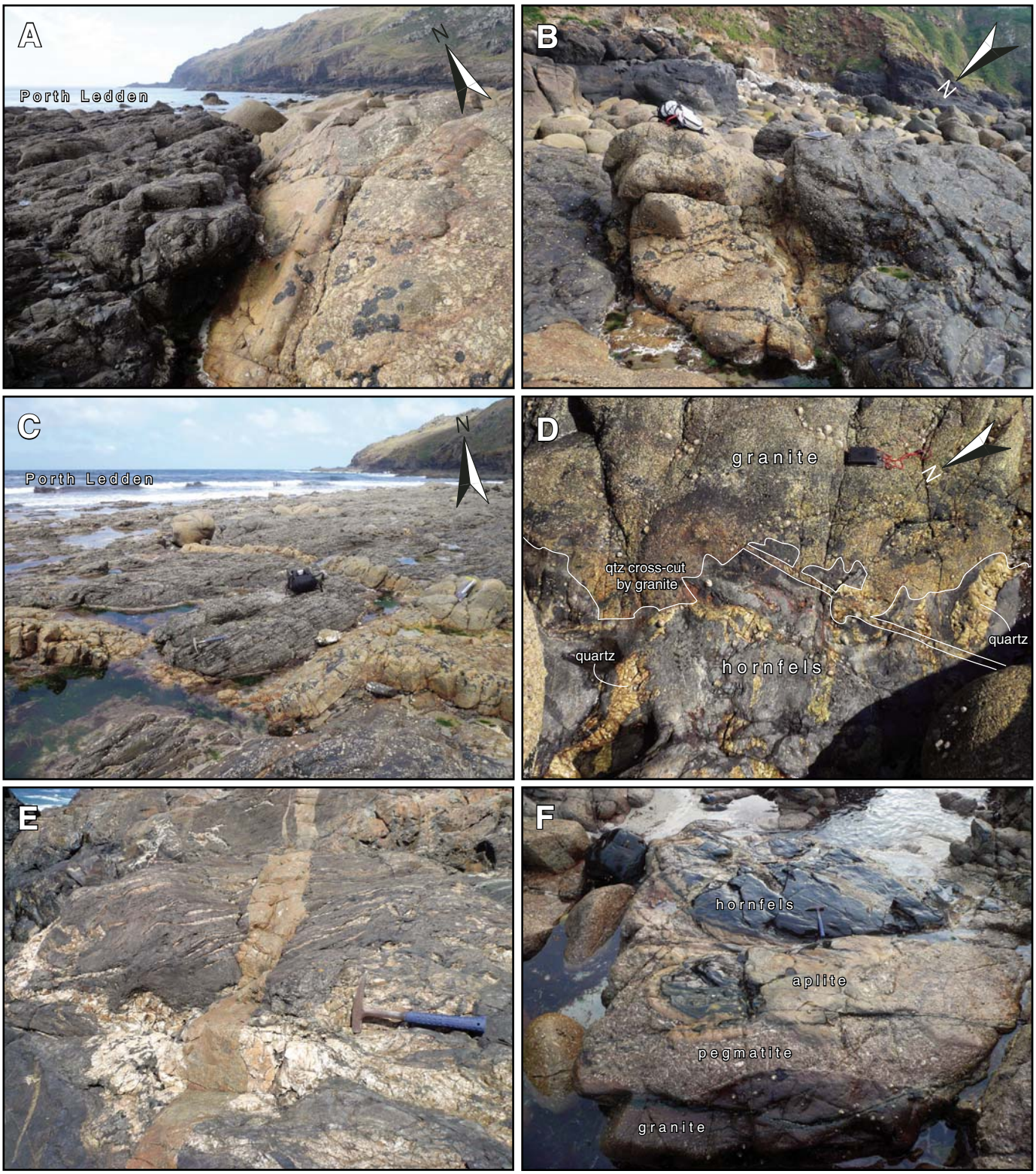

Figure 16. Land's End granite–aureole contact relations, St. Just aureole. See Figs. 7 and 15 for locations. (A) Contact at Porth Ledden between coarse megacrystic granite and spotted hornfels. (B) Wide, vertical granite dyke intruding hornfels alongside contact at Porth Ledden. (C) Granite sill intruding Porth Ledden foreshore near contact. (D) Close-up of contact at Porth Ledden. (E) Granite dyke crosscutting deformed quartz veins in hornfels, east of Wheal Edward Zawn. (F) Small isolated hornfels body sharing subhorizontal contact with aplite and pegmatite sheets at Portheras Cove.

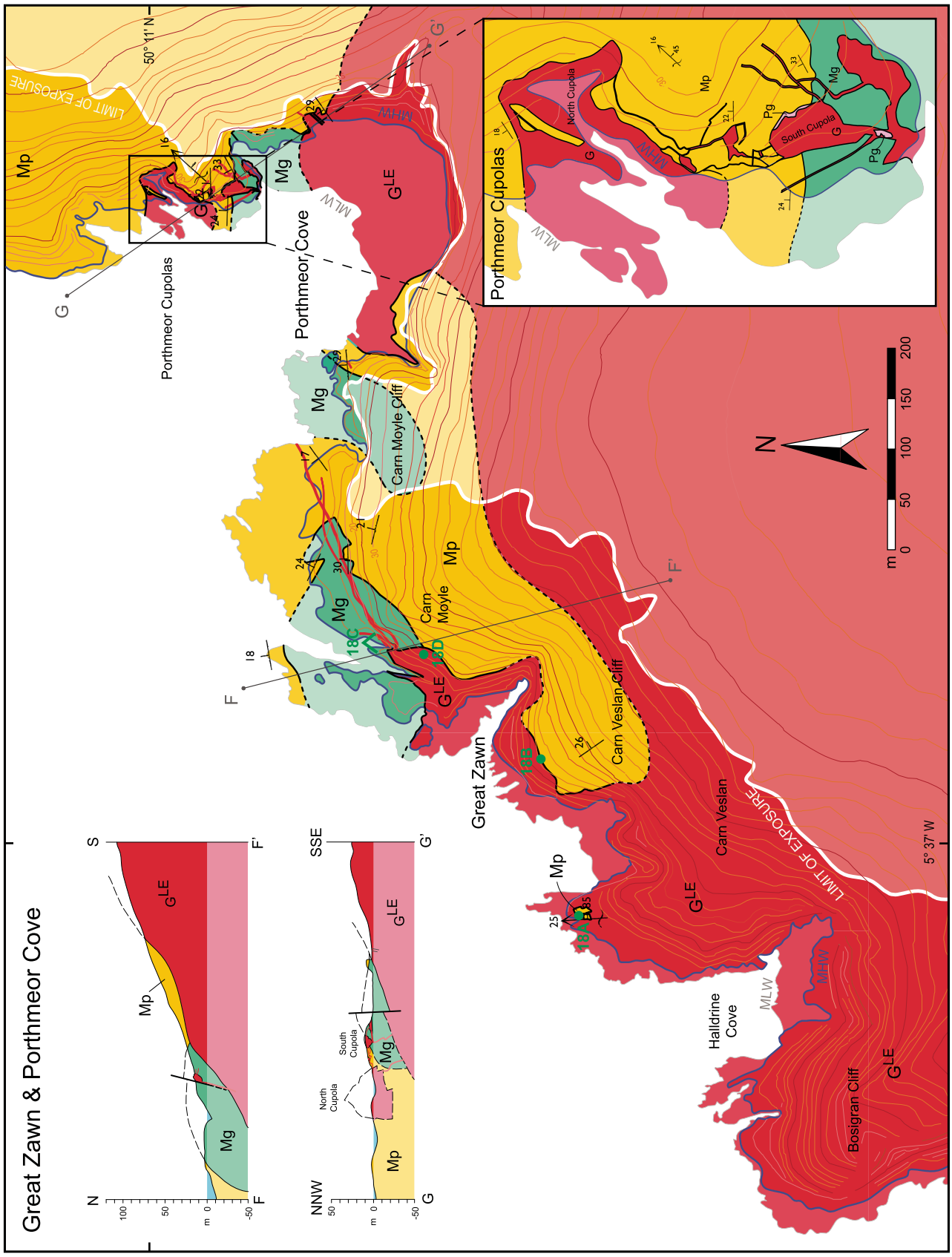

Figure 17. Geological map of Great Zawn and Porthmeor Cove taken from Plate 1. The Porthmeor Cupolas are enlarged at the bottom right. The positions of cross-sections F–F′ and G–G′ (top left) are indicated. See Fig. 6 for key to lithologies. Locations of photographs in other figures are indicated in green. MHW and MLW indicate the mean high and low water marks, respectively, and the intertidal zone is shaded in a paler color. The limit of exposure is indicated with the white line.

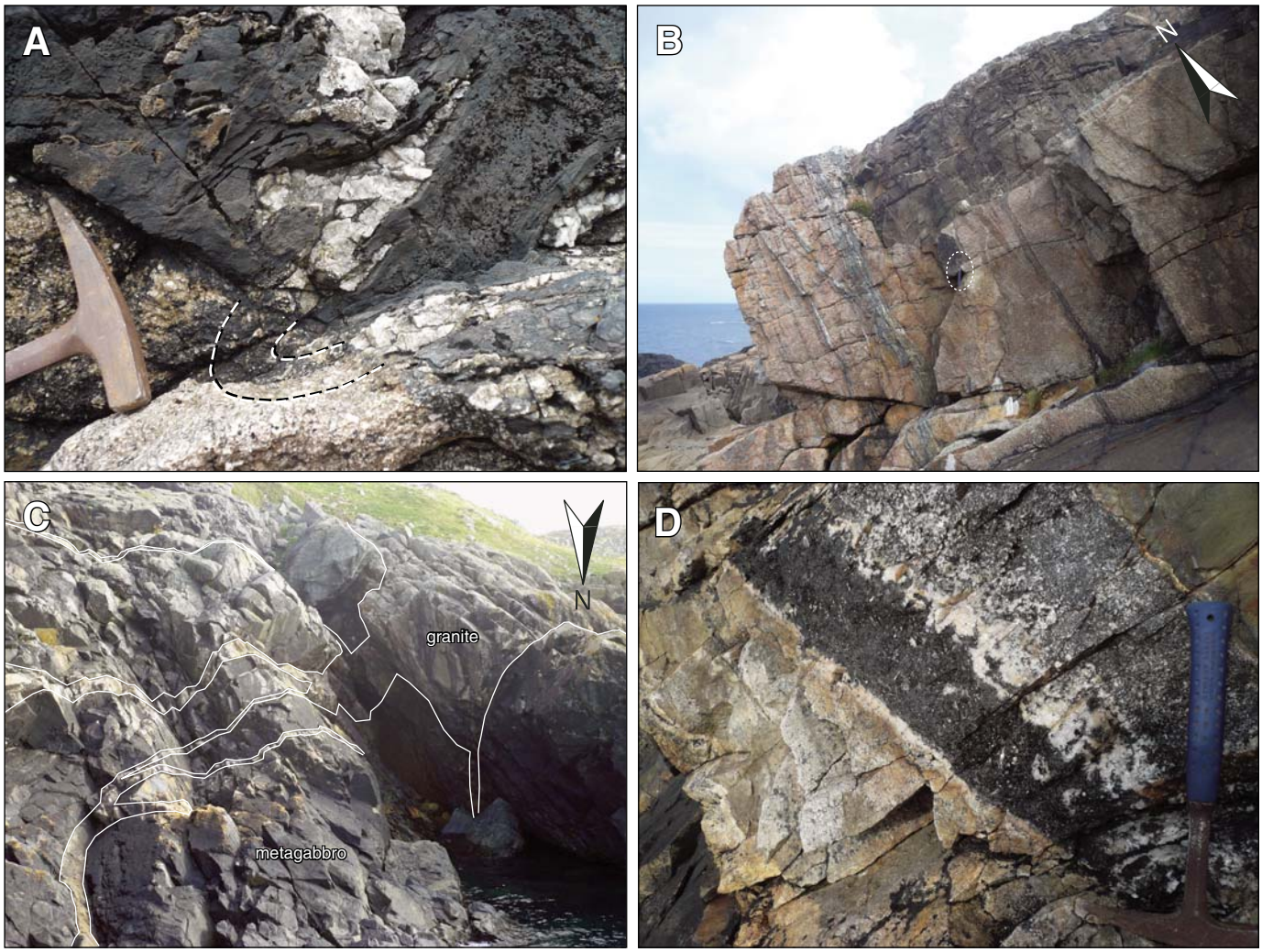

Figure 18. Field relations at Great Zawn. (A) F_3 folded quartz veins cleanly and sharply crosscut by granite contact, suggesting D_3 predated emplacement. (B) Stepped granite-hornfels roof contact, tilted to the northwest, displaying partially mineralized vertical and horizontal jointing, Carn Veslan. Hammer for scale (circled). (C) End profile of granite body and radiating dyke swarm within metagabbros, Great Zawn. (D) Heavily tourmalinized blocky xenolith within granite, Great Zawn. See figure 17 for locations of photographs.

(Holland et al., 1998), muscovite–paragonite (Coggon and Holland, 2002), plagioclase–K-feldspar (Holland and Powell, 2003), spinel–magnetite (White et al., 2002), and ilmenite–hematite (White et al., 2000). Pseudosections were plotted using Drawpd 1.15 (dr115.exe, www.metamorph.geo.uni-mainz.de/thermocalc/documentation/drawpd/index.html). Bulk compositions in terms of NCKFMASHTO oxides, as input to THERMOCALC, are presented in Table 3.

The observed mineral assemblage (Anth+Crd+Bt+Pl+Ilm+Qtz) occupies a large field on each of the three calculated P-T pseudosections, spanning ~0–3 kbar and 500–720 °C. In order to more precisely pinpoint the modeled rocks in this large P-T space, orthoamphibole compositional isopleths were calculated and plotted.

Fe^{3+}

The effect of Fe^{3+} on phase equilibria and pseudosection construction has become a much-discussed topic now that large systems incorporating ferric Fe, such as NCKFMASHTO, have been devised (Diener et al., 2008; Powell and Holland, 2008; Diener and Powell, 2010). $Fe^{2+}O$ and $Fe^{3+}{}_2O_3$ cannot be distinguished by SEM-microprobe and so the percentage of Fe as Fe^{3+} must be estimated. In the analyzed samples, the oxide mineral assemblage can be used to indicate the likely oxidation ratio. Ilmenite is the only Fe-bearing oxide, and in all analyses of fresh material, its Fe+Mn+Mg content is within error of its Ti content, suggesting a negligible content of Fe^{3+}. For the model calculations, therefore, the additional O content of the bulk composition was set at the arbitrarily low value of 0.01.

Natural and Model Amphibole Compositions

Our strategy in comparing the natural to the calculated amphibole compositions is outlined in Appendix 2.

Thermodynamic Basis for Pressure Sensitivity of Orthoamphibole Composition

The tschermak substitution governing anthophyllite–gedrite relations (the *y(anth)* parameter) in a cordierite-orthoamphibole

Figure 19. Field relations at Porthmeor Cove. (A) The Porthmeor Cupolas and associated dykes, as viewed across Porthmeor Cove. The location of photograph 20B is labeled in green. (B) The south cupola, with domed roof contact underlain by pegmatite sheets (red arrows). Note the angular profile and the granite dyke, extending from the SE corner, which has crosscut and offset an older leucogranite dyke—evidence of fault-controlled host-rock uplift. The metapelite–metagabbro (Mp–Mg) contact is indicated.

rock can be expressed as 3Anth + 7Crd = 7Ged + 17Qtz. This equilibrium is associated with a large volume change of about –10% as estimated from Mg end-member data (Holland and Powell, 1998), assuming water is approximately conserved, and so the equilibrium should have promise as a geobarometer. Anthophyllite–sodicanthophyllite relations are controlled by the edenite substitution (as monitored by the *a(anth)* parameter), such as in the equilibrium Anth + Ab = Na-Anth + 4Qtz, a principle that forms the basis for the Holland and Blundy (1994) hornblende-plagioclase geothermometer. Combination of both substitutions leads to sodicgedrite, equivalent to the Ca-amphibole pargasite. Linear trends in natural orthoamphibole compositions when these two substitutions are plotted against each other (Schumacher, 2007) suggest they are partially coupled. In the calculated diagrams (Fig. 27), both sets of isopleths have shallow P-T slopes.

The end-member data that underpin thermodynamic modeling in this system are constrained to differing extents. Anthophyllite properties are well constrained, but the fundamental thermodynamic properties of gedrite (entropy, volume, and specific heat capacity) that are included in the Holland and Powell (1998) DS5 data set are described as "estimated." The Na-amphibole end-members have been developed by analogy with Ca-amphibole end-members (Diener et al., 2007), and constructed by summations from anthophyllite, assuming similar mixing behavior to that in Ca-amphiboles and then by fitting Darken's Quadratic Formalism (DQF) adjustments where necessary to reproduce certain natural compositions (Powell, 1987; Will and Powell, 1992).

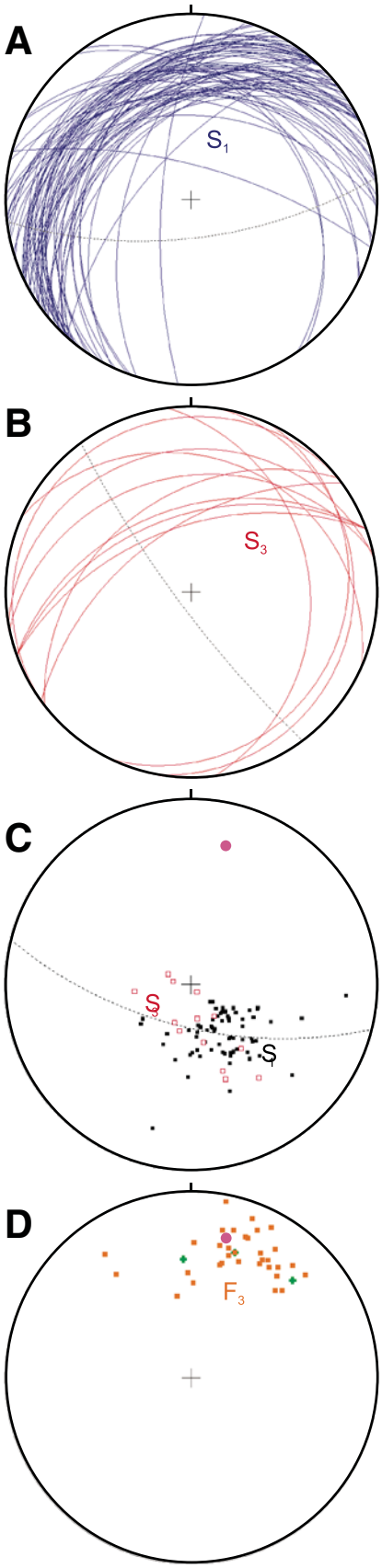

Mixing parameters for the amphibole solid-solution model were refined by Diener et al. (2007) and by Diener and Powell (2012) mainly from natural occurrences of coexisting amphibole species with similar *a(anth)* and *y(anth)* values to the Land's End anthophyllites (Stout, 1972; Clark, 1978; Spear, 1980, 1982; Miyake, 1984; Schneiderman and Tracy, 1991; Frimmel, 1996), and successfully reproduce the relevant miscibility gaps. This mixing model affects the distribution of compositional isopleths, especially in the neighborhood of miscibility gaps, but should have only a second-order effect on the overall sensitivity to pressure, which rests on the molar volumes of amphibole end-members. It is known from earlier studies that cell parameters and molar volumes are smaller for gedrites and sodicgedrites than for members of the anthophyllite-ferroanthophyllite series (Deer et al., 1997). Therefore, a sensitivity to pressure may be predicted using this calibration. Moreover, an assemblage in which orthoamphibole coexists with cordierite, quartz, and sodic plagioclase should, on the basis of the equilibria given above, saturate the orthoamphibole in both gedrite and sodicgedrite components.

Model Predictions

Application of the updated Holland and Powell data set (DS5.5) together with the orthoamphibole solution model of Diener et al. (2007, 2008) and Diener and Powell (2012) shows encouraging trends. Firstly, the calculated changes in modal proportions with pressure along an isotherm approximate to Crd + Pl = Oam + Qtz (actually 1Crd + 0.59Pl = 0.51Oam + 4.45Qtz between 1 and 5 kbar at 620 °C), with the amphibole evidently increasing in Na and Al. Secondly, the calculated amphibole compositions quite closely follow the trend of natural anthophyllite-gedrite amphiboles in the compilation by Schumacher (2007), although the anthophyllites of this study lie a little to the high-Na, low-Al side of this array.

Figure 20. Stereonets (equal-area lower-hemisphere projections) of (A) S_1 cleavage planes, St. Just aureole; (B) S_3 cleavage planes, St. Just aureole; (C) Poles to S_1 (black squares) and S_3 (red squares) with π-girdle (dotted great circle) and pole to π-girdle (pink dot) describing regional fold-axis orientation; (D) F_3 fold axes of the St. Just aureole (orange squares) and Great Zawn (green crosses), oriented parallel to the π-girdle pole (pink dot; 19° plunge, 014°N azimuth), the average S_1–S_3 cleavage-intersection lineation.

Nevertheless, in the absence of precisely measured thermodynamic properties for gedrite and one or more of the sodic end-members, it does not yet appear possible to provide an absolute calibration for a geobarometer based on Al- and Na-saturated orthoamphibole compositions. We therefore rely on the existing Holland and Powell (1998) end member data and the refined activity models of Diener and Powell (2012) to constrain pressure in the aureole.

P-T Estimates for the Land's End aureole

The Na and Al contents of the Kenidjack anthophyllite compositions offer a number of criteria for comparison with the P-dependent model isopleths in Figure 27. As outlined in Appendix 2, the total Na (ed = Na) and tschermak Al (tsch = ½(Al-Na)) provide maximum limits for the calculated parameters *a(anth)* and *y(anth)*, and so should place maximum limits on pressure (see Table 4). Alternatively, one can match the observed and calculated values of total Na, total Al, and tsch (see Appendix 2). These values are not so readily contoured from the output of model calculations, but are listed for the 615 °C isotherm in Table 4, and indicated on the summary diagram Fig. 27E. In practice, because of the relatively high Na, low Al character of Kenidjack anthophyllites, the limits imposed by Al content fall at lower pressure than those from Na, and in some cases lie at negative pressure. It is nevertheless clear that the Land's End assemblages equilibrated at very low pressure, and that the mean of the Na- and Al-based indicators is in the region of 1.5 kbar. The uncertainty on the pressure of calculated isopleths, derived from the uncertainties of the end member thermodynamic data, is around 1 kbar in the temperature range of interest.

We therefore propose that the most likely depth of emplacement for the granite adjacent to the modeled cordierite-anthophyllite rocks is between 5 and 6 km, corresponding to a pressure of 1.5 kbar at a likely density of < 2800 kg m^{-3} for the upper crust, although this depth carries a rather large uncertainty. This is the first P-T estimate of a Cornubian granite aureole to employ modern thermobarometry in a "geologically realistic chemical system" (Diener et al., 2007, p. 644).

PETROGENESIS OF THE KENIDJACK CORDIERITE-ANTHOPHYLLITE ROCKS

The mechanisms behind cordierite-orthoamphibole mineral assemblage development, which notably may arise from a number

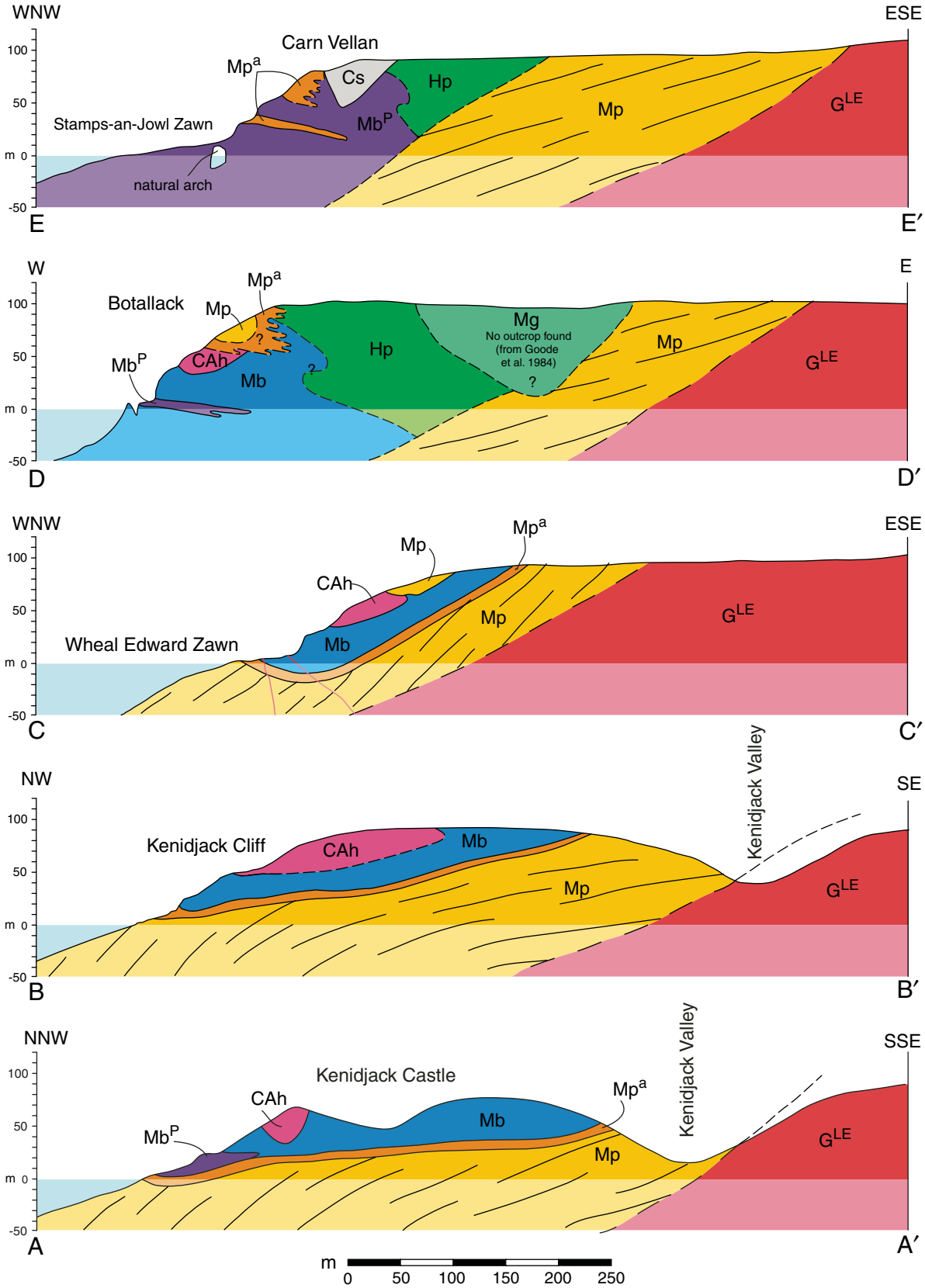

Figure 21. Cross-sections of the St. Just aureole drawn roughly perpendicular to the granite contact, from south (A–A′) to north (E–E′). Dotted lines indicate contacts are inferred. See Plate 1 for locations; see Fig. 6 for key to lithologies. The sea is shown in pale blue.

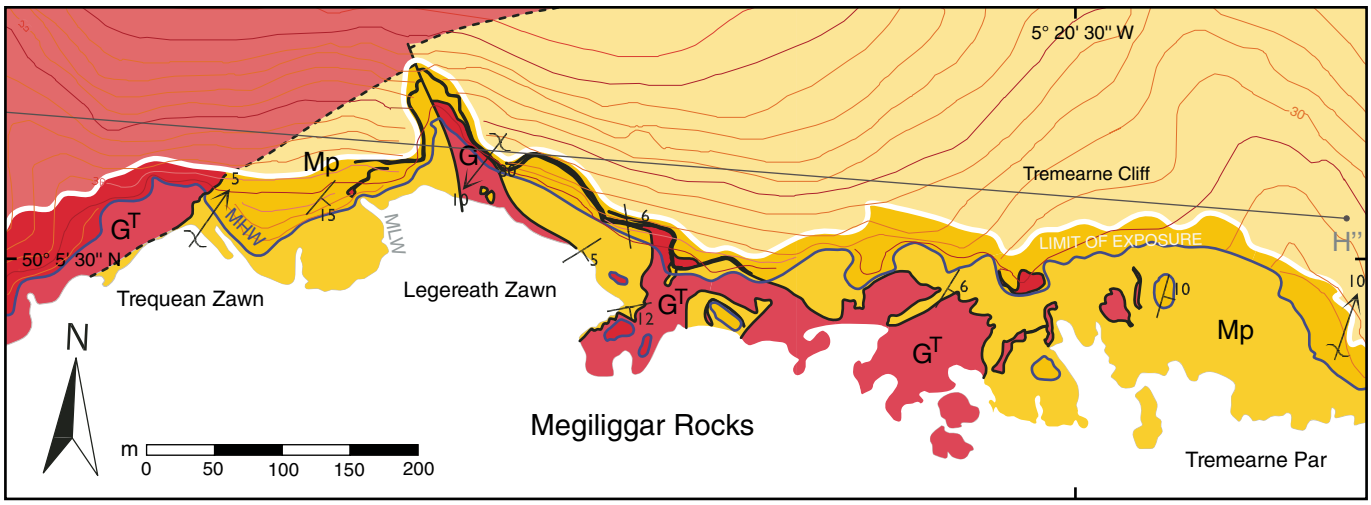

Figure 22. Geological map of Megiliggar Rocks taken from Plate 1. See Fig. 6 for key to lithologies; see Fig. 23 for cross-section H–H′–H″. MHW and MLW indicate the mean high and low water marks, respectively, and the intertidal zone is shaded in a paler color. The limit of exposure is indicated with the white line.

of different protoliths, are contentious (e.g., Robinson et al., 1982; Schumacher, 2007; Diener et al., 2008). There have been three main proposed formation methods to account for the low Ca+Na, high Mg+Al+Fe+K bulk composition: (1) Mg and Fe enrichment of volcanics by metasomatism (Eskola, 1914; Tilley, 1935); (2) Ca and Na depletion of metasediments and metavolcanics by extraction of granitic melt (Grant, 1968); and (3) either pre-metamorphic enrichment in Mg and Al by diagenesis of sediments or evaporites (e.g., Reinhardt, 1987), alteration of basalts (e.g., Vallance, 1967; Chinner and Fox, 1974; Moore and Waters, 1990; Peck and Smith, 2005), or hydrothermal alteration in the presence of sulphides (e.g., Roberts et al., 2003).

The cordierite-anthophyllite hornfelses at Kenidjack occur exclusively within the (meta-) basalts with which they share gradational contacts and grade from homogeneous (17E) to banded (12D,12L) to poikiloblastic (10A) textures toward their interior. Formation from basalt thus seems the only plausible origin. Anthophyllites are Al-poor and therefore close to "pure" end-member composition. Parallel S_1-aligned trains of ilmenite occur throughout all samples (Fig. 13B), consistently at ~3 vol% abundance. They are seemingly the first product of metamorphism and occur throughout the cordierite-anthophyllite as well as the hornblende-plagioclase hornfelses. It can therefore be assumed that both assemblages share a common origin, with the hornblende-hornfelses representing (as suggested by Tilley, 1935) the more typical contact facies. An $X(Fe^{3+})$ of <10% is also sufficient to account for possible deprotonation substitutions in the amphibole. The above evidence supports the theory of Vallance (1967) and Chinner and Fox (1974) of formation from previously hydrothermally altered basalt by isochemical thermal metamorphism. We conclude that the Kenidjack cordierite-anthophyllite rocks formed at very low pressure (1.5 ± 1.0 kbar) and moderately high temperature (615 ± 50 °C). This result is similar to that calculated for the cordierite-cummingtonite rocks of the Stillwater gabbroic complex, Montana (~2 kbar, ~600 °C, Labotka and Kath, 2001), and not too dissimilar from the cordierite-cummingtonite rocks of the Gold Brick District, Colorado (~3 kbar, 550 ± 70 °C, Earley and Stout, 1991), the cordierite-anthophyllite-cummingtonite rocks of the Lar Deposit, Manitoba (3–4 kbar, 550–700 °C, Elliott-Meadows et al., 2000), and the classic COGs of Orijärvi, Finland (~3 kbar, 550–600 °C, Schneiderman and Tracy, 1991), all calculated using conventional thermobarometry. Notably, however, the Al content of anthophyllite coexisting with cordierite in these last two studies is greater than at Kenidjack, lending further support to the low calculated pressure in the Land's End aureole.

DISCUSSION

The deformation and metamorphism of the Land's End and Tregonning aureoles and field relations along the granite-aureole contacts (see Fig. 28) demonstrate that: (1) the plutons are not associated with any observable small-scale wall-rock deformation, with F_3 folds cleanly truncated by sharp, planar granite contacts suggesting that granite intrusion has exploited brittle fractures in the host-rock; (2) sheetlike granite geometries can be inferred from stepped granite-hornfels contact relations and sills extending from the pluton's leading edge; (3) no evidence exists to suggest D_3 deformation represents a cylindrical diapir-induced shear-zone as F_3 fold vergence in the host rocks is typically to the SE throughout the region rather than being directed radially outwards from the pluton; and lastly (4) aureole thermobarometry indicates the Land's End Granite was emplaced at a shallow crustal level (5–6 km depth).

These insights tie in with many of the arguments that have questioned the viability of granite diapirs, namely: (1) the inherent "space problem" of forcefully intruding large volumes of melt into the solid crust (e.g., Pitcher, 1979); (2) dubious or nonexistent field evidence for expected wall-rock features, such as a cylindrical shear zone, pluton-up kinematic indicators, rim-synclines, and evidence for diapir "tails" (Clemens, 1998; Cruden, 1998; Petford et al., 2000); and (3) the tabular shape of many granitoid bodies that have been shown to comprise sill-like structures (McCaffrey and Petford, 1997; Cruden, 1998), both identified in the field (e.g., Michel et al., 2008; Horsman et al., 2009; Rocchi et al., 2010) and by newer geophysical interpretations (e.g., Vigneresse 1990; Evans et al., 1993; Taylor, 2007).

Furthermore, several additional arguments against granitic diapirs are also supported by features of the Land's End granite, albeit in a less direct way. Firstly, the shallow emplacement of the granite demonstrated here would have occurred well into the brittle regime. It

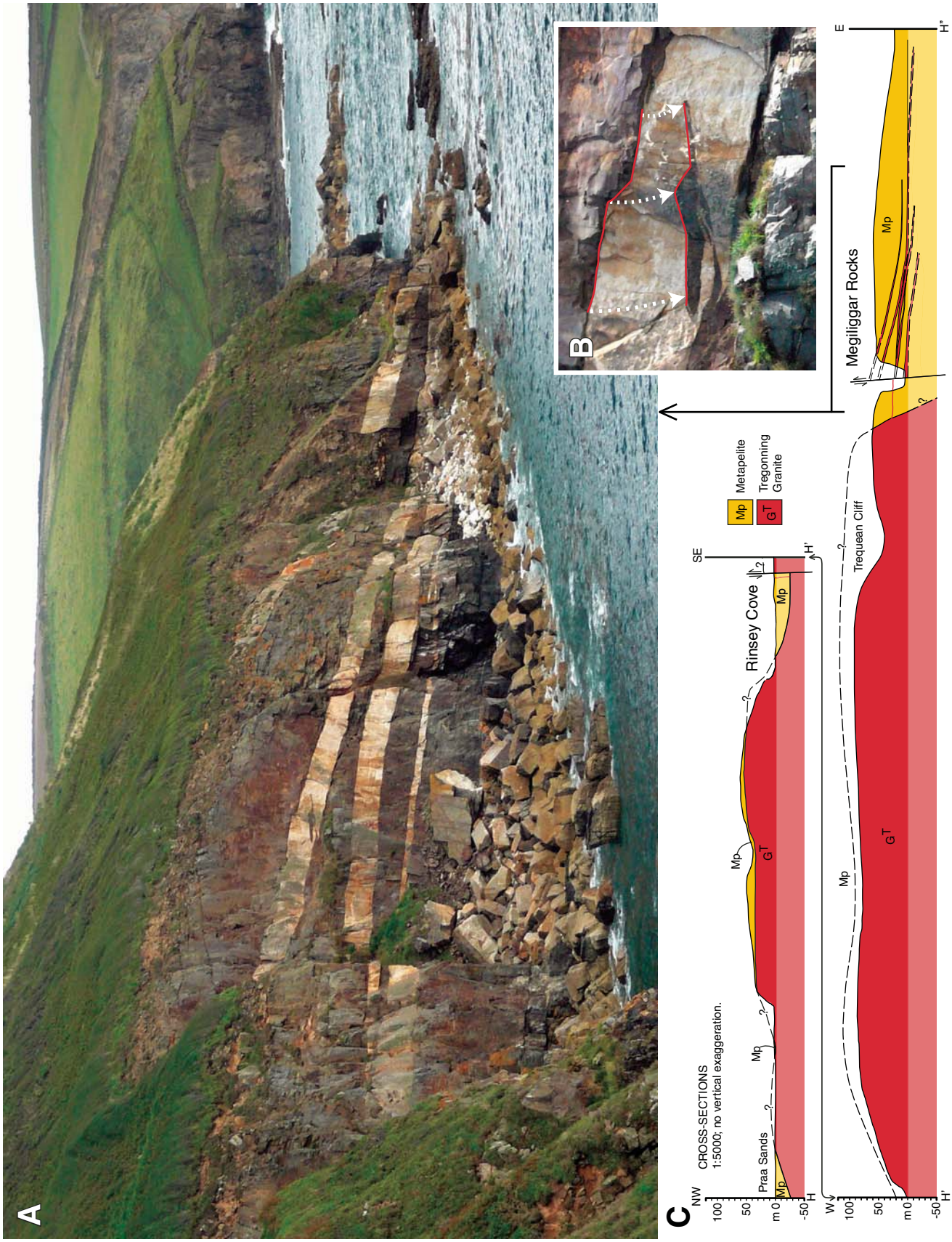

Figure 23. (A) Photograph of Megiliggar Rocks at high tide displaying the spectacular granite sheets—the leading edge of the laccolith—dipping away from the center of the pluton. (B) Close-up view of the uppermost granite sheet displaying small-scale intra-sheet stoping. (C) Cross-section of the Tregonning Granite. See Plate 1 for line of section.

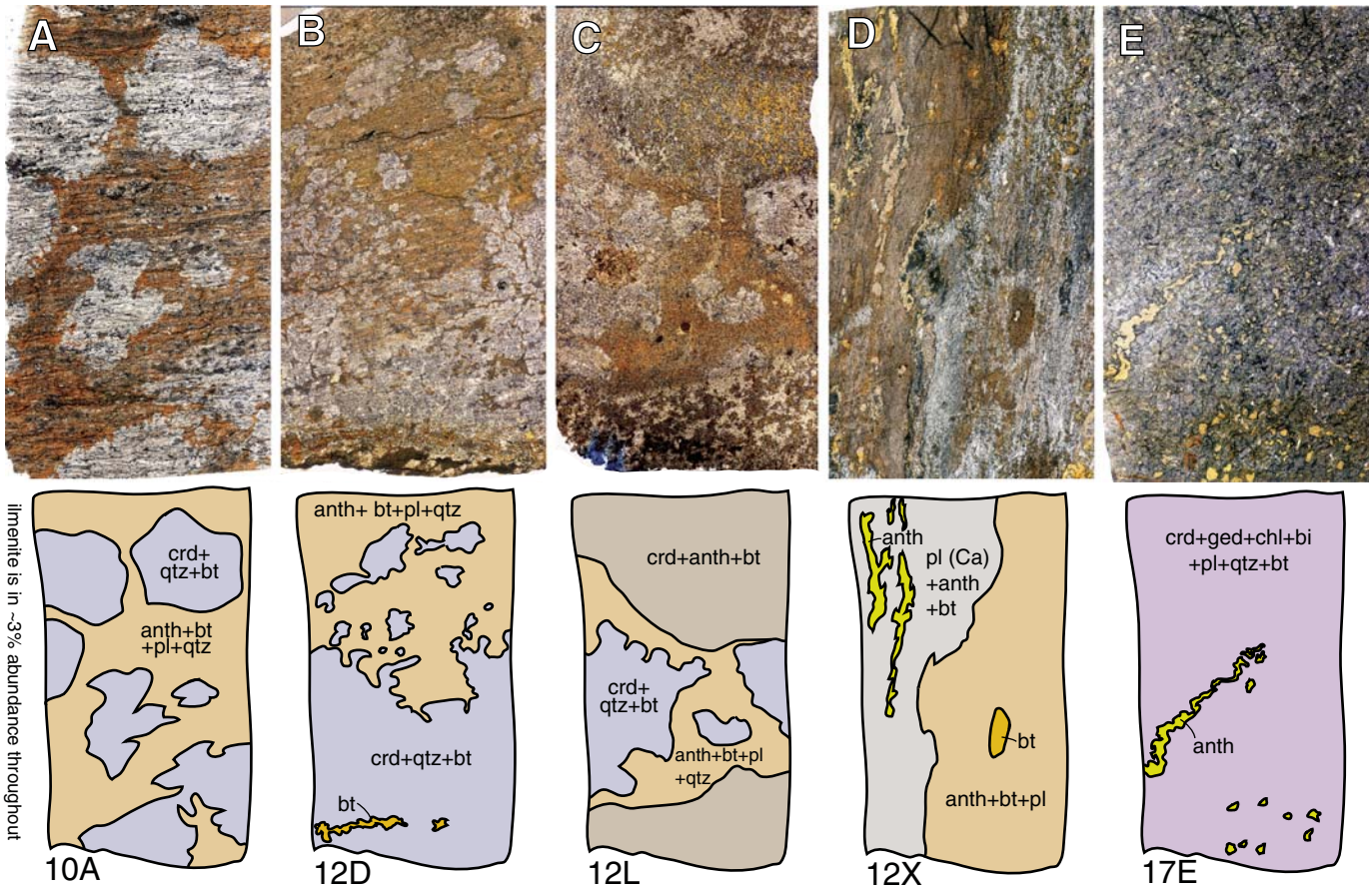

Figure 24. Whole-slide photomicrographs (PPL) of the orthoamphibole-bearing hornfelses accompanied by sketches (below) outlining generalized mineral domains. (A) 10A: Poikiloblastic cordierites developed around pronounced ilmenite trains; (B) 12D: Section through two cordierite- and anthophyllite- rich bands. (C) 12L: Development of large anthophyllite bursts within cordierite. (D) 12X: Section through part of huge calcic plagioclase porphyroblast (left) and matrix (right). No cordierite is present. (E) 17E: Gedrite is present throughout the section, cut by a late anthophyllite vein. Each section is reproduced at the same scale (~40 mm high).

has been argued that heat output required of an ascending diapir to soften and deform the wall rocks would be too great to allow ascent to such high structural levels, and that any diapir would have suffered thermal death in the earlier stages of ascent (e.g., Mahon et al., 1988). Also, it may be argued that the textural and chemical heterogeneity of the Cornubian granites, as demonstrated by the close associations of fine-grained- and (megacrystic) coarse-grained granites as well as chemically different Li-mica and tourmaline granites, would not have been attainable after the degree of convective overturning necessary to facilitate diapiric ascent (Clemens, 1998).

Plentiful evidence exists for stoping around the margins of the Land's End and Tregonning granites, although its overall contribution to accommodation remains unknown. Some have voiced doubts over stoping as a volumetrically significant pluton accommodation process (Glazner and Bartley, 2006) and the observed examples of stoped blocks may arguably be only late-stage phenomena. Alternatively, stoping may well have been a very significant process and operated throughout pluton assembly, as argued by Žák et al. (2006) in the instance of the Central Bohemian Pluton, Czech Republic.

Although a diapiric emplacement mechanism for the plutons of the Cornubian Batholith would seem unlikely, examples of centimeter-scale diapiric structures, present within or between granite sheets, have been identified in Cornwall (e.g., Treen Cliff, south Land's End granite; Powell et al., 1999) although they appear to be secondary processes that do not contribute widely to pluton growth or host-rock deformation. Some authors have defended the role of such small-scale diapirs that operate in the visco-elastic regime (e.g., Miller and Paterson, 1999).

As an alternative to a diapiric mechanism, there is clear evidence to suggest that networks of dykes facilitated the vertical transport and emplacement of the Land's End and Tregonning granites. The clearest example is at Megiliggar Rocks where several major subhorizontal granite sheets extend from the pluton margin and intrude the host-rock (Fig. 22, 23), demonstrating the processes of sill intrusion and amalgamation, as well as host-rock stoping and uplift. Furthermore, the granite cupolas at Porthmeor Cove (Fig. 19) demonstrate that dyking is intrinsically related to their emplacement.

The majority of authors now consider dykes to be the most viable mechanism for vertical transport of felsic magmas in the mid to upper crust (Lister and Kerr, 1991; Clemens and Mawer, 1992; Petford et al., 1993; Petford, 1996), with granite emplacement occurring by transition to horizontal flow and subsequent injection, amalgamation and inflation of sills. Dykes are thought to propagate by elastic fracturing of the country rock, but with a critical width that must be surpassed in order for the dyke to avert freezing and be self-propagating (Clemens and Mawer, 1992). This critical

TABLE 2. SEM-MICROPROBE ANALYSES OF 3 CORDIERITE-ANTHOPHYLLITE HORNFELSES FROM KENIDJACK, LAND'S END AUREOLE

	10A					12D					12L				
Wt%	crd	anth	bt	pl	ilm	qtz	crd	anth	bt	pl	ilm	qtz	crd	anth	bt	pl	ilm	chl	qtz
SiO_2	49.72	55.54	38.55	60.19	0.86	100	48.96	54.73	38.66	62.46	0.89	100	49.86	56.48	39.73	58.86	0.78	29.53	100
TiO_2	0.05	0.10	1.64	0.02	53.10		0.04	0.12	1.46	0.05	54.08		0.06	0.13	1.43	0.05	54.55	0.15	
Al_2O_3	34.63	1.20	16.57	25.84	0.49		33.91	1.86	15.60	24.78	0.64		34.66	1.54	16.08	27.06	0.58	21.79	
FeO	0.02	0.19	0.04	7.36	0.02		0.03	0.24	0.09	5.52	0.15		0.03	0.32	0.10	8.08	0.09	0.07	
MnO	0.02	0.07	0.00	0.00	0.17		0.04	0.17	0.00	0.01	0.73		0.07	0.34	0.04	0.00	0.61	0.08	
MgO	10.44	18.62	15.74	0.34	0.40		10.62	19.43	16.76	0.41	0.29		11.03	20.54	18.34	0.44	0.46	24.32	
CaO	0.02	0.19	0.04	7.36	0.02		0.03	0.24	0.09	5.52	0.15		0.03	0.32	0.10	8.08	0.09	0.07	
Na_2O	0.50	0.33	0.41	6.86	0.00		0.49	0.41	0.31	7.77	0.12		0.68	0.43	0.53	6.87	0.00	0.44	
K_2O	0.01	0.02	7.93	0.05	0.06		0.00	0.02	8.49	0.05	0.08		0.01	0.00	8.27	0.03	0.03	0.02	
Cations	10A						12D						12L						
p.f.u.*	crd	anth	bt	pl	ilm	qtz	crd	anth	bt	pl	ilm	qtz	crd	anth	bt	pl	ilm	chl	qtz
Si	4.918	7.935	5.630	2.655	0.021	1.00	4.928	7.842	5.709	2.728	0.022	1.00	4.923	7.879	5.695	2.588	0.017	2.800	1.00
Ti	0.004	0.010	0.180	0.001	0.985		0.003	0.013	0.162	0.002	0.992		0.004	0.014	0.154	0.002	0.891	0.011	
Al	4.037	0.202	2.853	1.342	0.014		4.023	0.314	2.717	1.276	0.018		4.033	0.254	2.712	1.402	0.014	2.436	
Fe	0.510	2.750	1.838	0.012	0.947		0.456	2.552	1.632	0.012	0.911		0.399	2.417	1.465	0.014	0.809	1.230	
Mn	0.002	0.008	0.000	0.000	0.003		0.003	0.021	0.000	0.000	0.015		0.006	0.040	0.005	0.000	0.011	0.007	
Mg	1.538	3.965	3.434	0.023	0.015		1.594	4.150	3.693	0.027	0.010		1.623	4.271	3.920	0.029	0.015	3.438	
Ca	0.002	0.029	0.006	0.347	0.001		0.003	0.036	0.015	0.258	0.004		0.004	0.048	0.016	0.380	0.002	0.007	
Na	0.097	0.091	0.115	0.586	0.000		0.095	0.114	0.089	0.658	0.006		0.130	0.117	0.149	0.586	0.000	0.081	
K	0.002	0.005	1.478	0.003	0.002		0.000	0.004	1.597	0.003	0.003		0.002	0.000	1.509	0.002	0.001	0.003	
(O)	18	23	22	8	3	2	18	23	22	8	3	2	18	23	22	8	3	14	2
Abundance																			
(vol%†)	24.1	14.0	21.5	17.1	3.2	19.4	31.0	16.4	18.2	18.9	2.9	12.5	24.2	21.8	18.6	14.0	3.1	1.7	16.0

Note: Only phases considered by and input to THERMOCALC are listed (minor accessory phases are ignored); quartz has not been analysed. Analyses performed by a JEOL JSM-840A SEM with Link ISIS EDS system at the University of Oxford, UK.
*p.f.u. = per formula unit, based on the number of oxygen anions given in brackets.
†volume% abundances are careful estimates.

width, as it increases with magma viscosity, has been suggested to vary from 2 to 7 m for granites of the American Cordillera, to ~20 m for the more silicic Himalayan leucogranites (Petford et al., 1993), a feature that explains the rarity of felsic dyke swarms in comparison to their (ultra-)mafic equivalents. Also, it is thought that only a limited number of felsic dykes can be sustained by a typical magma flux, and therefore may co-exist with other melt ascent mechanisms (Weinberg, 1999). During melt formation by crustal anatexis in thickened mountain belts, for example, transport is likely exclusively by pervasive flow within migmatites, as dyking is not possible in hot, ductile crust (Collins and Sawyer, 1996; Brown and Solar, 1999; Weinberg, 1999). Pervasive flow may also continue to operate at higher crustal levels by buoyant percolation through planes of weaknesses such as faults, fractures and shear zones, with flow aided by ongoing tectonic deformation (Brown, 1994) until dyking becomes prevalent. In sufficiently ductile crust, pervasive flow has been interpreted to emplace entire plutons (e.g., Pangong Injection Complex, Indian Karakoram; Weinberg and Searle, 1998). However, the exposed portions of the Land's End and Tregonning granites were emplaced at shallow levels of the crust (5–6 km depth), well into the brittle regime, such that emplacement aided by pervasive flow seems unlikely; however, pervasive flow may have operated at depth during vertical transport of melt from the lower-crustal/uppermantle source region.

Shallow Laccolithic Emplacement of the Land's End and Tregonning Granites

The evidence presented above indicates that the Land's End and Tregonning granites were likely assembled incrementally by intrusion of crosscutting sills and dykes into the host rock that fed granite sheets. This conclusion is in agreement with several recent studies on Cornubian granite emplacement (Salmon and Powell, 1998; Powell et al., 1999; Kratinová et al., 2003, 2010; Bouchez et al., 2006; Taylor, 2007; Hughes et al., 2009). Emplacement by this method would account for the isolation and stoping of blocky hornfels xenoliths located close to the granite margins and would facilitate entire granite sheets to be successively emplaced nondiapirically at pluton scale. Such a process is best illustrated at Megiliggar Rocks, where the emplacement is effectively frozen in action. However, this simple model is insufficient to explain (1) the regional-scale doming of the St. Just aureole identified by compilation of structural data (Fig. 20), and (2) the tilting of originally horizontal S_1 structures to the NW.

TABLE 3. CORDIERITE-ANTHOPHYLLITE HORNFELS BULK COMPOSITIONS (MOL% ABUNDANCE OF OXIDES CONSIDERED IN NCKFMASHTO SYSTEM)

mol%	10A	12D	12L
SiO_2	59.918	58.024	57.755
Al_2O_3	9.709	10.771	9.063
CaO	1.368	1.199	1.320
MgO	13.769	15.487	17.387
FeO	9.687	9.182	9.660
K_2O	1.634	1.385	1.383
Na_2O	1.316	1.637	1.035
TiO_2	2.587	2.302	2.387
O	0.011	0.011	0.011

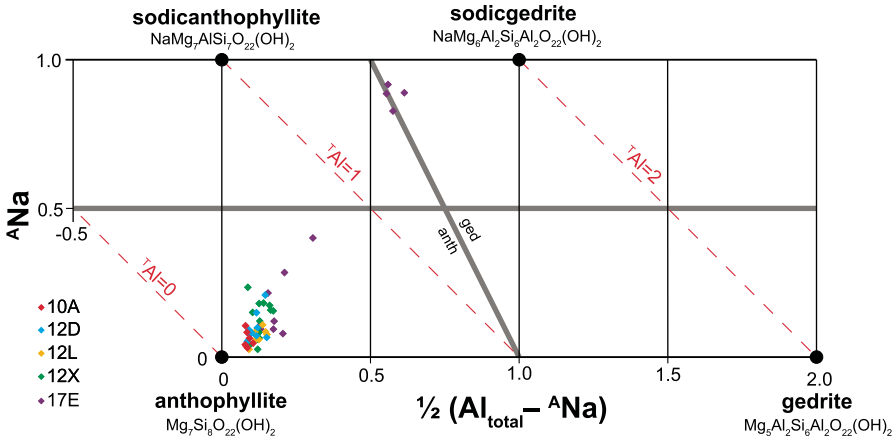

Figure 25. Amphibole compositions plotted in edenite-tschermakite space (projected along the glaucophane vector, gl = Na + Li; diagram modified from Schumacher, 2007). Blue lines divide the space into compositional fields for the four endmembers based on nomenclature of Leake et al. (1997). Dashed lines show aluminum isopleths (^{T}Al). The analyses plot very close to the "pure" anthophyllite endmember due to low Al content. Amphiboles in 17E are split between anthophyllites contained in late veins and gedrites in the main bulk of the rock. Many of these gedrite analyses plot outside of the theoretical composition space and may therefore be altered. Anthophyllites of 12X are partly altered to actinolite+talc and so plot further toward the gedrite endmember.

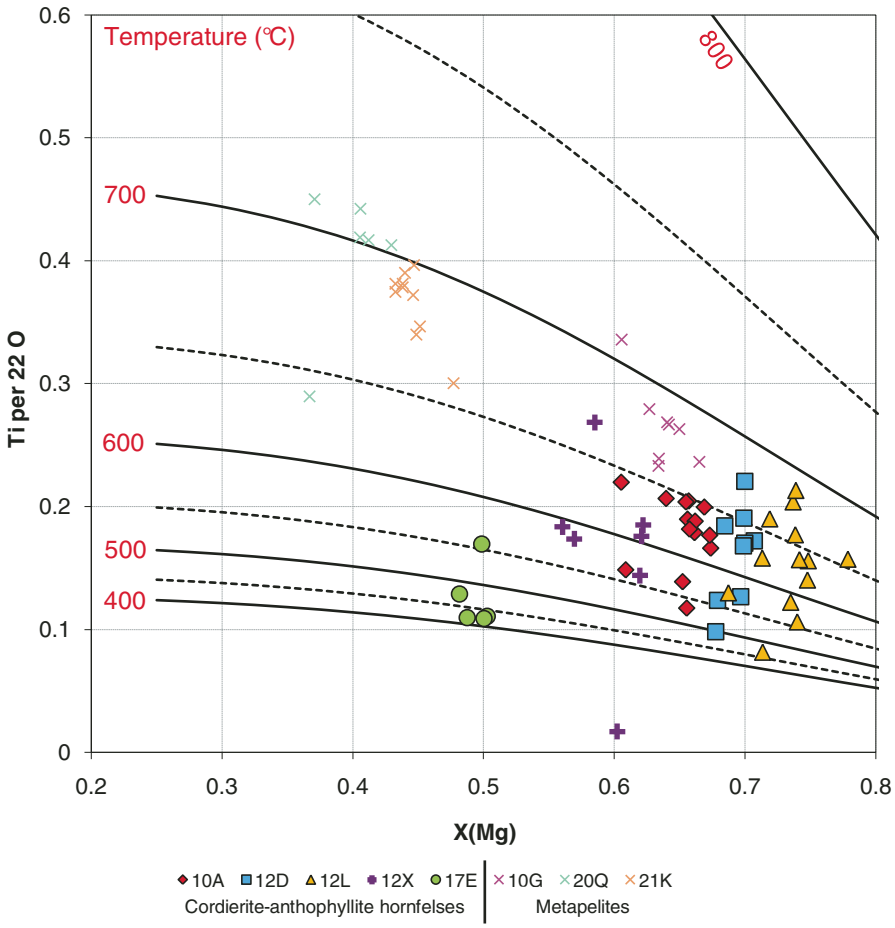

Figure 26. Temperature estimates of the cordierite-anthophyllite hornfelses and three metapelites (for comparison) using the Ti-in-biotite geothermometer of Henry et al. (2005). X(Mg) = Mg/(Mg+Fe). Average temperature estimates for the cordierite-anthophyllite hornfelses are as follows: 10A—615 °C; 12D—613 °C; 12L—616 °C; 12X—601 °C; 17E—460 °C. Error is estimated at ± ~50 °C. Metapelites 10G, 20Q, and 21K are from Kenidjack Cliff, Portheras Cove, and Wheal Edward Zawn, respectively.

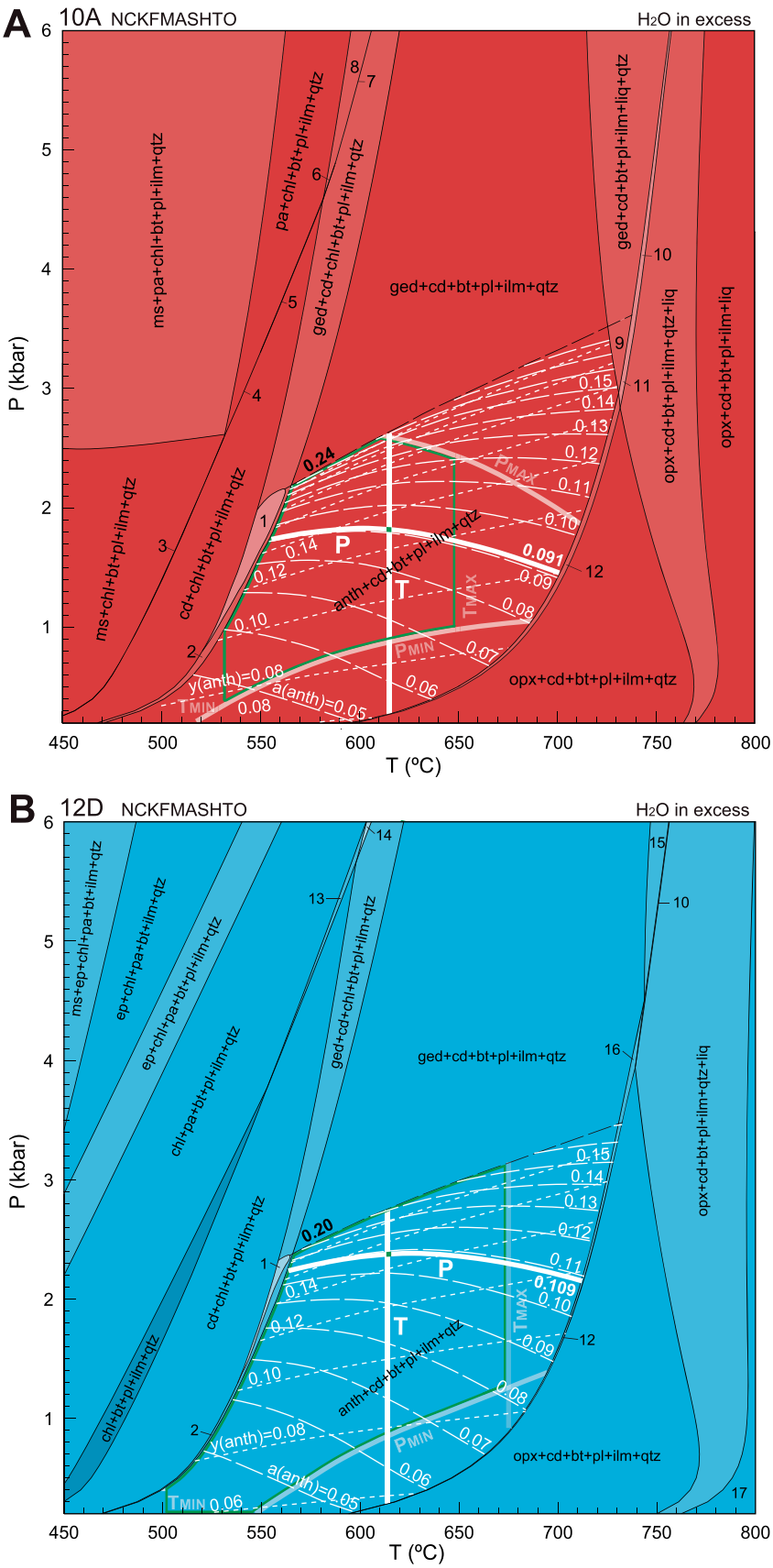

Figure 27 (*Continued on following page*). THERMOCALC P-T pseudosections for (A) 10A, (B) 12D, and (C) 12L in NCKFMASHTO. Darker shades indicate higher variances. Key for all small numbered fields is given in (D). The target field (anth+cd+bt+pl+ilm+qtz) is contoured with *a(anth)* isopleths (dashed white lines) and *y(anth)* isopleths (dotted white lines). The *y(anth)* isopleths representing the suprasolvus extension of the anthophyllite-gedrite transition is marked by a black dashed line. The *a(anth)* isopleths relating to the measured value of the rock is indicated as a thick solid white line, labeled "P," and marks the pressure estimate (offset by P_{MAX} and P_{MIN} error bounds at a distance of 1σ). The thick vertical solid white line labeled "T" marks the temperature estimate calculated by the Henry et al. (2005) Ti-in-biotite geothermometer (offset by T_{MAX} and T_{MIN} error bounds). The P-T estimate for each rock is therefore indicated by the P and T lines intercept (green dot) with the error bounds shown by the green boundary line. (E) Comparison of valid P-T windows for 10A, 12D, and 12L. The region within the green border is common to all, and therefore represents the final P-T estimate based on utilization of *a(anth)* as a geobarometer. Note that lower pressures are indicated by all other approaches used (summarized in Table 4) and therefore this result represents a *maximum* estimate for pressure of contact metamorphism and granite emplacement depth.

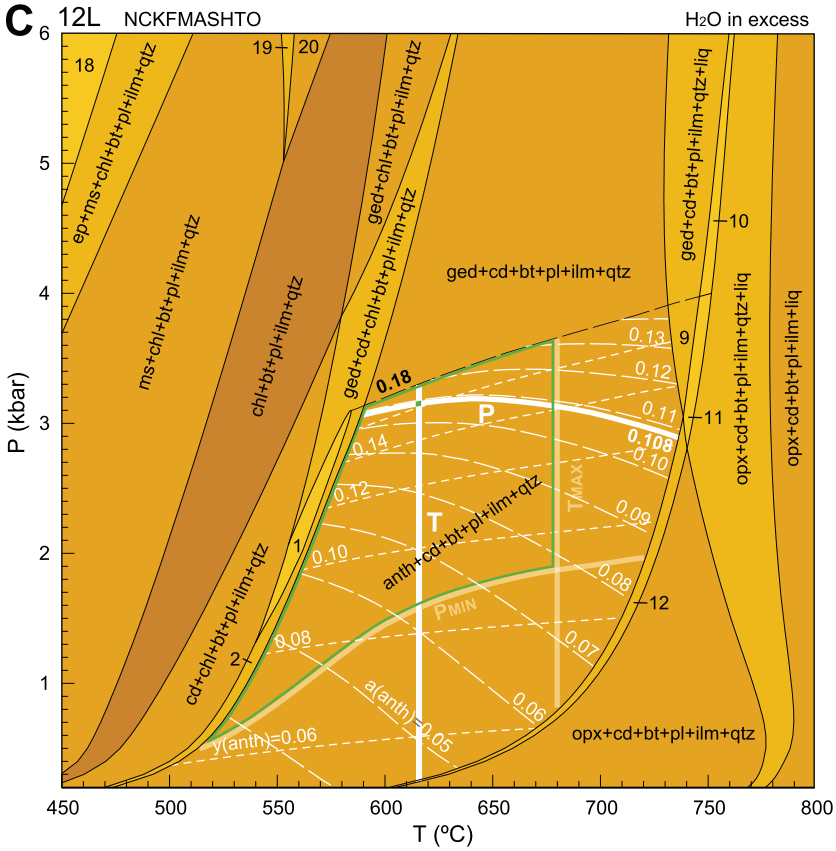

Figure 27 (*Continued*).

D

1) anth+ged+cd+chl+bt+pl+ilm+qtz
2) anth+cd+chl+bt+pl+ilm+qtz
3) ms+cd+chl+bt+pl+ilm+qtz
4) chl+bt+pl+ilm+qtz
5) pa+cd+chl+bt+pl+ilm+qtz
6) ged+pa+cd+chl+bt+pl+ilm+qtz
7) ged+chl+bt+pl+ilm+qtz
8) ged+pa+chl+bt+pl+ilm+qtz
9) anth +cd+bt+pl+ilm+qtz+liq
10) ged +cd+opx+bt+pl+ilm+qtz+liq
11) anth+cd+opx+bt+pl+ilm+qtz+liq
12) anth+cd+opx+bt+pl+ilm+qtz
13) cd+pa+chl+bt+pl+ilm+qtz
14) ged+cd+pa+chl+bt+pl+ilm+qtz
15) ged+cd+bt+pl+ilm+qtz+liq
16) ged+cd+opx+bt+pl+ilm+qtz
17) opx+cd+bt+pl+ilm+liq
18) ab+ep+ms+chl+bt+pl+ilm+qtz
19) pa+ms+chl+bt+pl+ilm+qtz
20) pa+chl+bt+pl+ilm+qtz

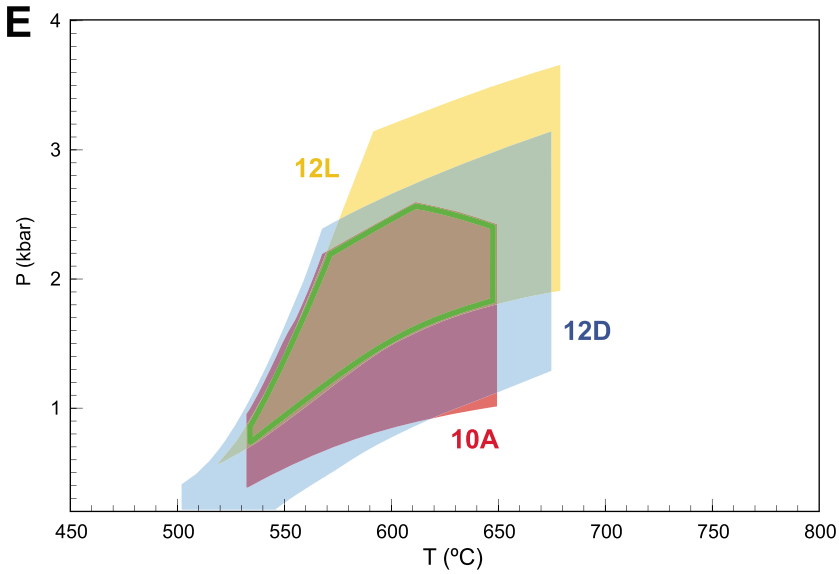

TABLE 4. P-T ESTIMATES FOR 3 CORDIERITE-ANTHOPHYLLITE HORNFELSES FROM KENIDJACK, LAND'S END AUREOLE

Rock	Pressure estimates by various geobarometers* (kbar)					Ti-in-Bt Temperature† (°C)		
	a(anth)§	Na_{total} (= ed)	*y(anth)*	Al_{total}	½(Al–Na) (= tsch)	average	max.	min.
10A	1.8	1.1	0.2	<0.2	<0.2	615	650	530
12D	2.4	1.9	1.5	0.6	0.4	613	675	500
12L	3.2	2.7	1.0	0.4	0.2	616	680	470

*calculated for the 615°C isotherm (average Ti-in-Bt geothermometry result).
†using the Henry et al. (2005) geothermometer.
§utilised on P-T pseudosections of Figure 27.

Both features are likely attributed to country-rock uplift and doming by granite emplacement. It must be concluded that there is a regional scale inflative emplacement dynamic in addition to emplacement by sill propagation as observed at local scale.

It is therefore proposed that the Land's End and Tregonning granites are laccolithic, with inflation of sheets manifested as a broad doming of the aureole. Successive intrusion and coalescence of dyke-fed granite sheets seems to have formed a tabular intrusion (as shown by Taylor, 2007), typically with a large width:height ratio, to produce a laccolith geometry with a flat base and domed roof (cf. Pollard and Johnson, 1973; Jackson and Pollard, 1988). Melt would have ascended from its source, via feeder dykes or by pervasive flow, until the drop-off in overburden pressure favored the lateral intrusion of sills rather than the vertical intrusion of dykes (cf. Hutton, 1997). Further intrusion and amalgamation of the sheets, and migration of the pluton by stoping of country rock, would have then occurred until country-rock uplift (due to sill inflation) became the preferential accommodation mechanism (see Fig. 29).

Emplacement postdated faults, folds, and cleavages generated during both Variscan convergence and subsequent latest Carboniferous–Early Permian end-Variscan extension (D_1–D_3). Emplacement of the granites during continued extension would partially answer the "space problem" of granite accommodation, and indeed there is evidence to suggest that extensional structures exerted a strong control on granite emplacement (Shail and Wilkinson, 1994).

Further support for the feasibility of shallow tabular laccoliths is lent by post-1980s geophysical interpretations. For example, Evans et al. (1993), after conducting a high-resolution seismic survey of the Lake District Batholith, northern England, interpreted sub-horizontal reflectors as country-rock slivers or basalts interspersed throughout a sheeted complex with a "cedar tree" profile. Importantly for this study, Taylor (2007) has recently re-interpreted several plutons of the Cornubian Batholith as shallow tabular bodies with geometries in accordance with the Cruden and McCaffrey (2001) power-law relationship for laccolithic plutons. Furthermore, rapid melt ascent through dykes of up to 10 cm s^{-1} (10^4 to 10^8 times faster than calculated for diapiric ascent; Clemens, 1998) has been shown to allow laccolith assembly by rapid emplacement of discrete magma pulses

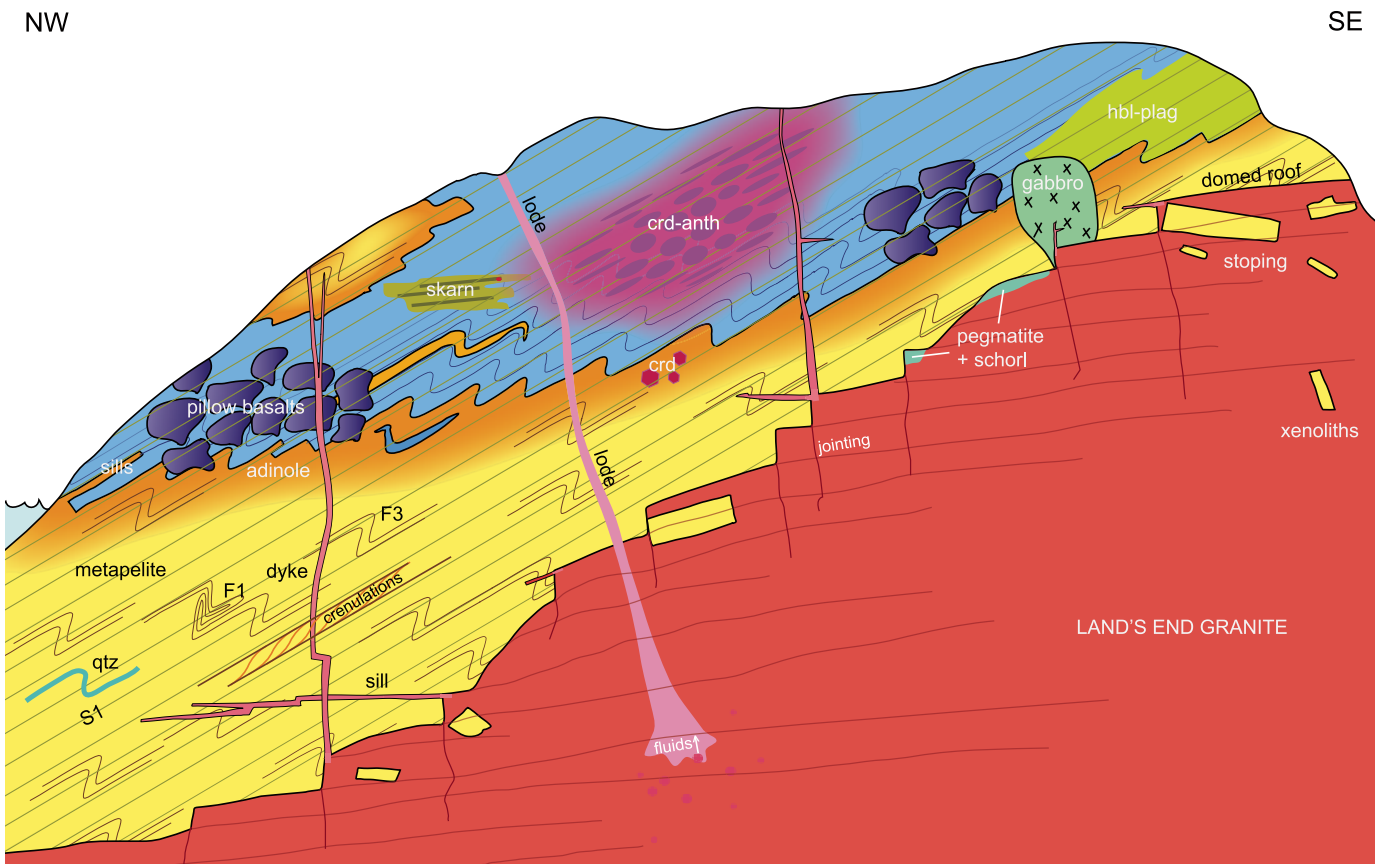

Figure 28. A schematic cross-section summarizing all observed field relations along the St. Just aureole of the Land's End granite.

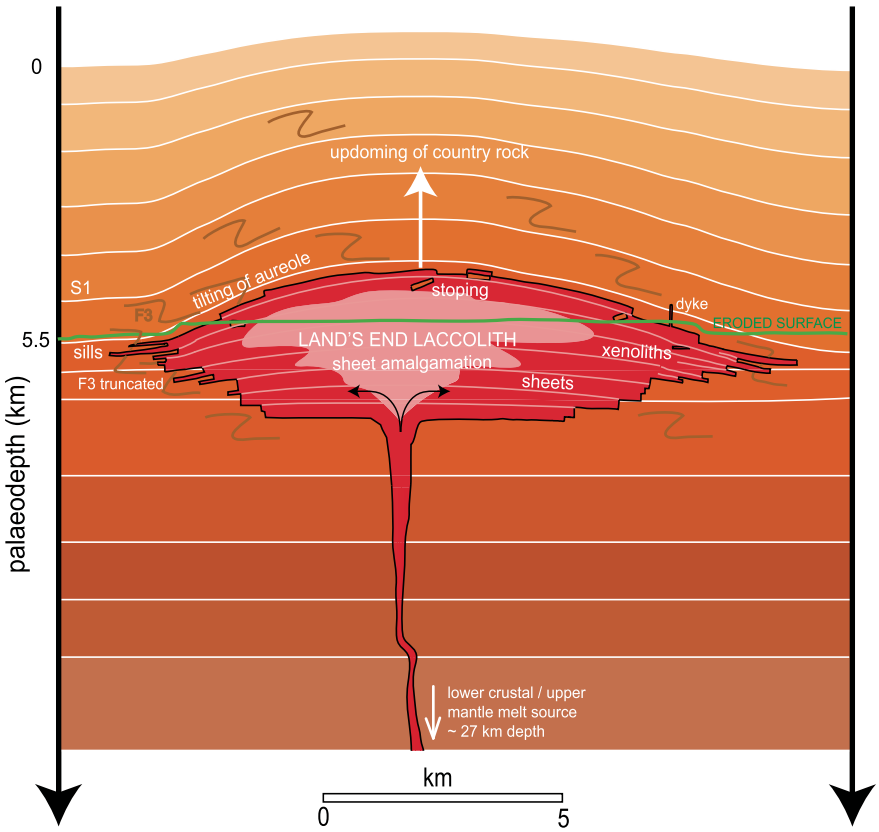

Figure 29. The Land's End laccolith: a semi-schematic cross-section. Granite at the present-day exposure level (green line) is drawn at 5.5 km palaeodepth as calculated by THERMOCALC thermobarometry (mean value) of adjacent aureole rocks. Dips of uppermost granite sheets are inferred from observed tilt of aureole S_1 fabrics. The laccolith has been drawn so its thickness (3 km) is consistent with other Cornubian granites calculated by Taylor (2007), and so that its aspect-ratio is in agreement with the Cruden and McCaffrey (2001) estimate for typical laccolith geometries. The depth of the lowermost crust (27 km) was suggested by Bott et al. (1970). This proposed emplacement mechanism accounts for granite accommodates by regional-scale roof uplift and by localized stoping; however, no ductile deformation is required at outcrop scale, thus D_3 aureole structures (which predated granite emplacement) are cleanly truncated.

(cf. Glazner et al., 2004), as elucidated by recent geochronological studies (e.g., Coleman et al., 2004; Michel et al., 2008; Cottam et al., 2010; Howard et al., 2011), and by work on the plumbing of magma chambers within volcanic systems (Lipman, 2007; Annen, 2009, 2011). U-Pb dating of the Land's End granite shows that granite magmatism was indeed a protracted event and caused the emplacement of at least three distinct bodies of Exley et al. (1983) Type-B granite—the 277 ± 2 Ma Zennor lobe and the 274.5 ± 2 Ma St. Buryan lobe (Chen et al., 1993; Clark et al., 1993, 1994), joined by the poorly megacrystic "St. Just wedge" (Salmon and Shail, 1999). Geochronology of the wider Cornubian Batholith confirms this feature is typical of all the plutons, with chemically and texturally distinct intrusions incrementally emplaced over a ~20 m.y. period (Chen et al., 1993; Chesley et al., 1993).

Elvan dykes (quartz porphyry) and an exposed rhyolite at Kingsand Beach (Plymouth) provide limited evidence for associated acid volcanism (e.g., Darbyshire and Shepherd, 1985; Floyd et al., 1993).

CONCLUSIONS

Field relations observed during mapping of the aureole rocks of the Land's End and Tregonning granites (shown schematically in Fig. 28) have supported the findings of recent studies (Salmon and Powell, 1998; Powell et al., 1999; Kratinová et al., 2003, 2010; Bouchez et al., 2006; Taylor, 2007; Hughes et al., 2009) that a diapiric emplacement mechanism for the granites is unlikely, and instead there is evidence for shallow laccolithic emplacement of the plutons.

The aureole protolith comprised pillow-basalts emplaced upon argillaceous ocean-floor sediments that have both undergone partial alteration by a seafloor hydrothermal system prior to contact metamorphism by the Land's End granite. During contact metamorphism, some basalts are inferred to have formed cordierite-anthophyllite and hornblende-plagioclase assemblages. In contrast, calc-silicate hornfelses formed through granite-associated metasomatism. Field relations show D_3 deformation occurred prior to granite emplacement during end-Variscan NNW–SSE extension. On a small scale, granite emplacement has caused no discernible wall-rock deformation, with pre-existing aureole fabrics (D_1–D_3) undeformed and cleanly truncated. However, on a regional scale, granite emplacement has caused a broad uplift and doming of the host-rocks. We propose that the Land's End and Tregonning granites are laccolith-type bodies emplaced, at least at the current exposure level, by intrusion of dyke-fed sills, which caused at least partial stoping of country-rock blocks. Accommodation of the granite was partly achieved by slight roof uplift driven by laccolith inflation. The "space problem" of granite accommodation is also partially solved by the granites' likely emplacement during continued end-Variscan extension.

THERMOCALC P-T pseudosections suggest the cordierite-anthophyllite hornfelses of Kenidjack reached peak contact metamorphism at 1.5 ± 1.0 kbar and 615 ± 50 °C, indicating a likely emplacement depth of 5–6 km for adjacent granites exposed near present-day sea-level. Furthermore, the roof of the granites, now eroded, would have been emplaced at even shallower depth.

The Land's End biotite granites are likely dyke-fed by a common lower-crustal/upper-mantle melt source, and the Tregonning lithium-mica granites were later generated by metasomatism of the crustal residuum (or of more basic granitoids) by volatiles exsolved from the same region (Stone, 1992). It would seem likely that other plutons of the Cornubian Batholith were similarly emplaced as dyke-fed shallow-crustal laccoliths, with differing fractionation paths of segregated melts during magma ascent accounting for the chemical disparity observed between biotite granites of different plutons.

This shallow emplacement depth is consistent with the typical S-type granite, as is the peraluminous composition; however, certain aspects, such as the batholithic dimensions of

the Cornubian granite system and the mantle melt-contribution, have more of an affinity with I-type granites. We further suggest that while representing useful first-order petrogenetic concepts, the two end-member I- and S-type granite facies cannot be applied in this instance, and that Cornish granites are a hybrid between typical I-type and typical S-type. The proposed shallow-crustal tabular intrusions concur with the most recent geophysical interpretations by Taylor (2007), and we hope our P-T estimates can further quantify this proposal.

APPENDIX 1: AREA-BY-AREA FIELD OBSERVATIONS FOR THE LAND'S END AND TREGONNING GRANITE AUREOLES

In addition to the key field observations described in the main text, here is a more thorough area-by-area account of the aureole rocks of the Land's End and Tregonning granites.

The Land's End Granite Aureole

Starting at Priest's Cove to the South of Cape Cornwall and working clockwise around the mapped sections of the Land's End granite aureole…

Priest's Cove

A mineralized subvertical faulted contact along Saveall's Lode, Priest's Cove, marks the southernmost extent of the St. Just aureole hornfelses. Granite is finer-grained than at localities further north and locally hosts abundant quartz, tourmaline, and hematite veins. It is thought to be part of the St. Just Wedge (Salmon and Shail, 1999) and has been termed the Carn Gloose Granite (Salmon and Shail, 1999; Müller et al., 2006). The fabric of the hornfelsed metapelites adjoining the fault is cleanly truncated with no evidence to suggest it postdates faulting. The metapelites are intruded by thin planar aplite dykes that crosscut F_3 folds.

The metapelites are heavily deformed and display tight F_3 chevron folds (Fig. 8C). Growth of metamorphic minerals, and resultant hornfelsing of the sediment (a possible grain-size inversion; Hughes et al., 2009) appears to have been preferential along certain beds. A dominant primary cleavage (S_1) is usually bedding-parallel as a consequence of isoclinal F_1 folding; it is often intersected by a strong secondary cleavage (S_3), axial-planar to the F_3 folds. Cordierite growth is aligned to S_3. Cleavage relationships are fairly consistent around Cape Cornwall (S_1 ~210/30°NW; S_3 ~010/20°E), and the line of intersection between these two cleavages is approximately parallel to the fold axes of associated F_3 folds.

Porth Ledden

At Porth Ledden (Figs. 7 and 15), the contact between the roof of the granite and the overlying hornfels, typically dipping at 30–40°, is well exposed (Fig. 16A). Along the granite margin, there are a number of small hornfels xenoliths, as well as a large (15 × 8 m) dyke-bound hornfels block. Such inclusions of intact country rock, at one time isolated by sill- and dyke-intrusions that exploited brittle host-rock fractures, demonstrate that stoping at least in part accounted for granite accommodation in such regions. A number of large sills, which could be considered precursors for pluton growth, intrude hornfelses in the Porth Ledden foreshore and truncate quartz veins (Figs. 16C, 16D). Porth Ledden exhibits several different granite facies, including quartz-tourmaline (schorl) rock, interpreted by Müller et al. (2006) as being emplaced as a succession of sheets subparallel to the roof.

Isoclinal folds observed north of Porth Ledden may belong to the F_1 group. The spotted hornfelses, especially on the Porth Ledden side, are characterized by thick S_1-aligned D_3-deformed quartz veins that make the F_3 folds visually prominent (Fig. 8A). Larger quartz vugs are also fairly common.

Kenidjack

In the vicinity of Kenidjack Castle are exposures of cordierite- and orthoamphibole-bearing hornfelses associated with metabasalts and dolerites (see map in Figs. 11 and 12). A more comprehensive description is given in the main body of text. Also, we observed, contrary to Goode et al. (1984), that the metapelite-metabasite contact extends, above low-tide mark, along the very base of Kenidjack Cliff and to the east end of Wheal Edward Zawn (Fig. 10).

Pendeen Watch

Pendeen Watch, ~1 km from the Land's End granite margin, comprises metapelites of lower grade than at Cape Cornwall. Cordierite spots are noticeably smaller, however, the rock is still, in some places, well hornfelsed—the degree of hornfelsing varies, and therefore seems to be controlled largely by lithological variation. Large-scale asymmetrical F_3 folds are well exhibited; S_3 cleavage is often well developed and is axial-planar (Fig. 8D), with crenulation relations with S_1 displayed.

Botallack

At Botallack (Fig. 12), there is an isolated metapelite lens within metabasalts (300 × 100 m). Its outer margin is altered, but it grades inwards to a spotted hornfels similar to that mapped elsewhere in the region. Mapping by Goode et al. (1984) (British Geological Survey 1:50,000 geological map, Penzance sheet) and Goode and Merriman (1987) show both this feature in addition to a second smaller body to its south, but no field evidence could be found for this second feature; in its claimed location are large outcrops of hornblende-plagioclase hornfels. The metapelites within this feature are, in general, even more fine-grained than elsewhere, and contain smaller cordierite spots. Features originating from original bedding are often better preserved, and later-developed cleavages (often which crenulate S_1) are better displayed. Fold geometries and cleavage orientations are consistent with the rest of the coast. Clear examples of minor dolerite sills are seen to the east of Wheal Edward Zawn at the contact with underlying metapelites (Fig. 9B).

Levant

At Carn Vellan, Levant, another isolated metapelite body is present, although it is too small to contain typical spotted hornfelses in its interior; all of the metapelite has been subject to some degree of contact alteration with the enveloping basalts.

The metabasic rocks are predominately extrusive to the north, in the Levant region, and many of the best-displayed pillow lavas can be found here. Many basalts mapped as extrusive further south, such as those forming the natural arch at Stamps-an-Jowl Zawn, display only the characteristic weathering pattern emanating from crisscrossing hydrothermal veins (Fig. 9A).

Portheras Cove

At Portheras Cove, the granite-hornfels contact is unfaulted and forms a stepped profile in the cliff, revealing sheetlike granite geometries. Along the foreshore, the contact is orientated roughly horizontal, and several small remnant patches of hornfels overlying the sheet are exposed at low tide (Fig. 16F). Hornfels just west of the contact is intruded by three ~0.5 m wide granite dykes, which possibly would have preceded the emplacement of further sheeted granites had emplacement continued.

Great Zawn

At Carn Veslan (Fig. 17), granite-truncated F_3 folds within a 10 × 8 m relict patch of hornfels provides convincing evidence that D_3 preceded granite emplacement (Fig. 18A). Further east, above Great Zawn itself, the stepped contact between the granite sheets and overlying metapelite is well exposed, in this instance displaying a northwestern dip (Fig. 19B). Granites display both horizontal jointing, which is aligned with the S_1 fabric of the adjoining hornfelses, and vertical jointing, which runs parallel to the steps in the contact, suggesting the granite was in part accommodated by the stoping of roughly cuboid blocks of country rock that broke off along and perpendicular to the S_1 plane of weakness. Wide, heavily tourmalinized quartz veins have developed along vertical joints in the granite, which may have arisen through late-stage fluid migration.

East of Great Zawn, the granite is emplaced within an extremely hard, coarse-grained Cpx+Pl+Bt+Ms+Chl ± Ap ± Ilm meta-gabbro. This gabbro dome is encircled by overlying metapelites in map view so that its shape in cross-section can be inferred. No evidence could be found for metagabbro at Carn Veslan Cliff as mapped by Goode et al. (1984).

The most significant feature at Great Zawn, which appears to be undocumented in the literature, is the contact relation between granite and metagabbro: toward the narrow zawn beneath Carn Moyle (Fig. 18C), the small, angular end-profile of the granite is underlain by and surrounded by metagabbro. The straight, extremely clean planar contacts, which differ from the intermingled contacts further west, almost certainly faulted to accommodate the granite intrusion. The structure of this granite intrusion differs from the two "satellite" granite cupolas on the other side of Porthmeor Cove (described below) as it is connected to the main Land's End granite to the west. Nevertheless, it likely shares a very similar joint-controlled passive emplacement mechanism. From this intrusion, several major granite dykes radiate to the northeast, and can be followed for 300 m toward the Porthmeor Cove Cupolas before reaching the sea. The granite in this vicinity is especially tourmaline-rich, and a few small tabular xenoliths (quite possibly stoped blocks of country rock) bear an almost complete tourmaline and quartz replacement (Fig. 18D).

The Porthmeor Cupolas

The Porthmeor Cupolas, described by Stone and Exley (1984) and mentioned by Reid and Flett (1907), Hall and Jackson (1975), Floyd et al. (1993), and Müller et al. (2006), are thought to be the only two examples of "satellite" stocks in Southwest England (see Fig. 19). The dominant granite facies present in both cupolas is the same as the main pluton (coarse-grained biotite granite; Type-B). The north cupola, emplaced exclusively in metapelites, is exposed mainly in cliff-section as a tall granite dome with sharp, angular contacts. A network of fine-grained aplite sills connects it to the smaller but more accessible south cupola,

which is intruded into both metapelites and metagabbro. Both cupolas and associated sills and dykes cleanly crosscut all country-rock structures, demonstrating a non-forceful emplacement mechanism. Dykes extend from the corners of the south cupola, as if they once isolated a large block that has since subsided into the underlying granite (Fig. 19B). The roof complex of the south cupola granite, developed beneath a slightly domed roof contact, comprises a banded leucogranite-pegmatite sequence. The only other significant lithological variations are occasional darker horizons rich in biotite. Dykes emanating from the granite display several crosscutting relations: in one instance, a thick, coarse-grained granite dyke intruded outward from the eastern corner crosscuts a fine grained leucogranite dyke, causing a 1.5 m sinistral offset (Fig. 19B). This is evidence for an earlier dyking stage before emplacement of the cupola. Apart from slight roof doming, there is no evidence to suggest that either cupola was emplaced by forceful diapiric intrusion, and no perceivable country-rock deformation, apart from uplift of blocks along dyke-exploited joints, can be discerned.

Tater-du

Tater-du is a small peninsula of isolated aureole rock on the southern margin of the Land's End granite (previously described by Floyd, 1965). The western end of Tater-du (Rosemondress Cliff; Fig. 14A) bears an intricate relation of calc-silicate and amphibole-bearing lithologies atop a low-lying metapelite body. Around Tater-du lighthouse, banded hornblende-plagioclase hornfels is present, which sharply grades into a ~8 m thick amphibole-bearing sill halfway down Rosemondress Cliff. This rock differs from the cordierite-anthophyllite hornfelses of Kenidjack in that it comprises aligned brown fibrous amphibole, probably cummingtonite, within a homogeneous fine-grained green/white matrix containing no cordierite. This "sill" is not laterally extensive and instead is neighbored to the west by a similarly discordant, banded Grt-Px calc-silicate.

Below both these units, the metasedimentary rock, being close to the overlying basic intrusion, is altered, pink-gray in color, poorly hornfelsed, heavily quartz-veined, and contains corundum as well as cordierite (Fig. 14C). In addition, there is a shallow (~2 m) transition zone where this pink metasedimentary rock is interbanded with thin metadolerite sills (Fig. 14B), demonstrating the nature of basalt emplacement. A single subvertical aplite dyke in the center of Rosemondress Cliff crosscuts all other features, and toward the eastern end, a thick (1.2 m) granite+aplite dyke intrudes the banded hornblende-plagioclase hornfelses.

The Tregonning Granite Aureole

Lesceave Rocks

At Lesceave Rocks, a number of small blocks of spotted hornfels crop out through beach sand, or display angular contacts with granite. Pegmatite and schorl are present immediately beneath the hornfels, forming a layered complex. These small isolated bodies of hornfels could be interpreted as xenoliths but probably represent a stepped roof contact with the Tregonning granite sheets.

Rinsey Cove

Rinsey Cove is an eroded roof pendant of the Tregonning granite, with a fairly low angle (~35°) contact along the western foreshore, and a subvertical faulted contact to the east, paralleled by a wide (1 m) granite dyke. Along the western contact, several small xenoliths are present; further afield, a larger xenolith is underlain by pegmatite: both are evidence for stoping.

Megiliggar Rocks

See main text and Figure 23 for description.

APPENDIX 2: METHODOLOGY FOR DEVISING MODEL AMPHIBOLE FROM NATURAL COMPOSITIONS

Amphiboles are defined by the general formula $A_1M4_2(M1+M3)_3M2_2T_8O_{22}(OH)_2$ where T and M1 to M4 denote tetrahedral and octahedral sites, respectively. A-sites represent sites between the bases of tetrahedral chains that can remain vacant or accept large cations. Two equilibria concerned with the Kenidjack orthoamphiboles are: (1) Edenite substitution, $\_Si \leftrightarrow NaAl$ (where "_" denotes a site vacancy), which relates anthophyllite, $Mg_7Si_8O_{22}(OH)_2$, to sodicanthophyllite, $NaMg_7AlSi_7O_{22}(OH)_2$; and (2) Tschermak substitution, $MgSi \leftrightarrow AlAl$, which relates anthophyllite to gedrite, $Mg_5Al_2Si_6Al_2O_{22}(OH)_2$. Anthophyllite (and gedrite) compositions can therefore be described in terms of their edenite (ed) and tschermakite (tsch) coupled-substitution vectors, defined by Schumacher (2007) as $tsch = {}^{T}Al - {}^{A}Na - {}^{A}K - 2{}^{A}Ca$, and $ed = {}^{A}Na + {}^{A}K + {}^{A}Ca$, where superscripts "T" and "A" denote tetrahedral- and A-sites, respectively, and the element symbols represent cations per formula unit. The equivalent composition parameters in the Diener et al. (2007) and related models, for use with THERMOCALC in the simplified system NCFMASHO, are $y(anth) = \frac{1}{2}{}^{M2}Al$, and $a(anth) = {}^{A}Na$. Note that the calculated system does not include K or Ti, but that at low contents of K, Ti and Fe^{3+}, $y(anth) \approx \frac{1}{2}$tsch and $a(anth) \approx$ed. Therefore, by deducing ^{A}Na and the amount of Al involved in tschermak substitution, ^{T,M2}Al, orthoamphibole compositions can be modeled.

Comparison between natural and model amphibole compositions is not straightforward, as both Na and Al occur in multiple sites, with Na divided between A and M4 sites, and Al between M2 and tetrahedral sites. Uncertainties in determining X(^{A}Na) and tschermak Al arise from analytical uncertainty or bias (systematic error, for example, in microprobe calibration), and from uncertainty in substitution mechanisms and site allocation strategies. Added to this is the generally unknown oxidation state of Fe. From a calculation of cations per formula unit from a microprobe analysis on the basis of 23 oxygens, tetrahedral Al is most simply derived by subtracting Si cations from 8. However, the uncertainty on ^{T}Al derived in this way depends on the precision of the Si analysis and will be large at low Al contents. Na (+ K) in the A-site is most simply derived by taking the excess over 15 cations per formula unit, but the uncertainty on ^{A}Na then depends on the precision of the entire analysis and will be large at low Na contents.

These sources of uncertainty and bias need to be considered for the Kenidjack amphibole compositions in which the Na and Al contents are very low, even in relation to the calculated amphiboles at low pressure. Cation totals on the basis of 23 oxygens are lower than required to force all Na onto A sites, and imply a finite amount of glaucophane substitution, which for almost all analyses is within error of 0.1 atoms of Na p.f.u. in M4 sites. However, under low-pressure conditions, Na is expected to reside in the A site, and the calculated amphibole compositions have <0.02 Na in M4. Allocating some Fe as Fe^{3+}, while keeping the oxygen total at 23, lowers the cation totals further, increasing the proportion of Na assigned to M4 sites. However, low cation totals cannot be attributed to systematic underestimation of Si, since Si contents are close to 8 cations p.f.u. and in many analyses give barely sufficient tetrahedral Al to account for an edenite substitution for Na if this is assumed to be dominantly in the A site. In contrast, factors that would cause an overall increase in the cation total, such as the presence of a deprotonation (oxy-) substitution coupled to Fe^{3+} or Ti (cf. in hornblende: Deer et al., 1997, p. 276; Dyar et al., 1993), further decrease the estimated tetrahedral Al content of the natural amphiboles. The possibility exists, therefore, of a systematic analytical bias affecting the relative proportions of the major cations Mg, Fe, and Si.

In consequence, our strategy in comparing the natural to the calculated amphibole compositions is to use the Na and Al contents directly, without an explicit formula recalculation, and to maximize the estimated proportion of edenite by assuming all Na resides on the A site (i.e., ed = *Na*), and that of tschermakite by assuming that all Al not accounted for by Na-edenite is accommodated by the tschermakite substitution (i.e., tsch = $\frac{1}{2}(Al - Na)$. Because both parameters increase with pressure in the model calculations, this should place a maximum pressure constraint on the crustal level of equilibration in the aureole.

ACKNOWLEDGMENTS

The authors are grateful for the helpful comments by Mike Williams and two anonymous reviewers that greatly improved the structure and clarity of the text. We also thank Norman Charnley for assistance with SEM and EDS analysis, Jeremy Hyde and Owen Green for preparation of thin sections, and Jenny Colls for all library-related matters. Many useful discussions were had with Alex Thomas, Ros Rickaby, Richard Palin, Al White, Ryan Langdon, and Hannah Hughes. Analytical costs were defrayed by the Department of Earth Sciences, University of Oxford, as part of a MEarthSci project undertaken by JMP.

REFERENCES CITED

Alderton, D.H.M., and Jackson, N.J., 1978, Discordant calc-silicate bodies from the St. Just aureole, Cornwall: Mineralogical Magazine, v. 42, p. 427–434, doi:10.1180/minmag.1978.042.324.03.

Alexander, A.C., and Shail, R.K., 1995, Late Variscan structures on the coast between Perranporth and St. Ives, Cornwall: Proceedings of the Ussher Society, no. 8, p. 398–404.

Alexander, A.C., and Shail, R.K., 1996, Late- to post-Variscan structures on the coast between Penzance and Pentewan, South Cornwall: Proceedings of the Ussher Society, v. 9, p. 72–78.

Allport, S., 1876, On the metamorphic rocks surrounding the Land's-End mass of granite: Quarterly Journal of the Geological Society of London, v. 32, p. 407–427, doi:10.1144/GSL.JGS.1876.032.01-04.46.

Annen, C., 2009, From plutons to magma chambers: Thermal constraints on the accumulation of eruptible silicic magma in the upper crust: Earth and Planetary Science Letters, v. 284, p. 409–416, doi:10.1016/j.epsl.2009.05.006.

Annen, C., 2011, Implications of incremental emplacement of magma bodies for magma differentiation, thermal aureole dimensions and plutonism–volcanism relationships: Tectonophysics, v. 500, p. 3–10, doi:10.1016/j.tecto.2009.04.010.

Bateman, R.J., 1984, On the role of diapirism in the segregation, ascent and final emplacement of granitoid magmas: Tectonophysics, v. 110, p. 211–231, doi:10.1016/0040-1951(84)90262-2.

Blundy, J.D., and Holland, T.J.B., 1990, Calcic amphibole equilibria and a new amphibole-plagioclase

geothermometer: Contributions to Mineralogy and Petrology, v. 104, p. 208–224, doi:10.1007/BF00306444.

Booth, B., 1966, Petrogenesis of the Land's End granites [Ph.D. thesis]: Newcastle-under-Lyme, UK, University of Keele.

Bott, M.H.P., Day, A.A., and Masson-Smith, D.J., 1958, The geological interpretation of gravity and magnetic surveys in Devon and Cornwall: Philosophical Transactions of the Royal Society, London, Series A, v. 251, p. 161–191.

Bott, M.H.P., Holder, A.P., Long, R.E., and Lucas, A.L., 1970, Crustal structure beneath the granites of South West England, *in* Rast, N., and Newman, T. C., eds., Mechanisms of Igneous Intrusion: Journal of Geology Special Issue, p. 93–102.

Bouchez, J.L., Mintsa Mi Nguema, T., Esteban, L., Siqueira, R., and Scrivener, R., 2006, The tourmaline-bearing granite pluton of Bodmin (Cornwall, UK): Magnetic fabric study and regional inference: Geological Society [London] Journal, v. 163, p. 607–616, doi:10.1144/0016-764905-104.

Bradshaw, P.M.D., and Stoyel, A.J., 1968, Exploration for blind orebodies in southwest England by the use of geochemistry and fluid inclusions: Institute of Mineralogy and Metallurgy Transcripts, v. 77, no. B, p. 144–152.

Brooks, M., Doody, J.J., and Al-Rawi, F.R.J., 1984, Major crustal reflectors beneath SW England: Geological Society [London] Journal, v. 141, p. 97–103, doi:10.1144/gsjgs.141.1.0097.

Brown, M., 1994, The generation, segregation, ascent and emplacement of granite magma: The migmatite-to-crustally-derived granite connection in thickened orogens: Earth-Science Reviews, v. 36, p. 83–130, doi:10.1016/0012-8252(94)90009-4.

Brown, M., and Solar, G.S., 1999, The mechanism of ascent and emplacement of granite magma during transpression: A syntectionic granite paradigm: Tectonophysics, v. 312, p. 1–33, doi:10.1016/S0040-1951(99)00169-9.

Chappell, B.W., and Hine, R., 2006, The Cornubian Batholith: An example of magmatic fractionation on a crustal scale: Resource Geology, v. 56, p. 203–244, doi:10.1111/j.1751-3928.2006.tb00281.x.

Chappell, B.W., and White, A.J.R., 1974, Two contrasting granite types: Pacific Geology, v. 8, p. 173–174.

Chappell, B.W., and White, A.J.R., 2001, Two contrasting granite types: 25 years later: Australian Journal of Earth Sciences, v. 48, no. 4, p. 489–499, doi:10.1046/j.1440-0952.2001.00882.x.

Chen, Y., Clark, A.H., Farrar, E., Wasteneys, H.A.H.P., Hodgson, M.J., and Bromley, A.V., 1993, Diachronous and independent histories of plutonism and mineralization in the Cornubian Batholith, southwest England: Geological Society [London] Journal, v. 150, no. 6, p. 1183–1191, doi:10.1144/gsjgs.150.6.1183.

Chesley, J.T., Halliday, A.N., Snee, L.W., Mezger, K., Shepherd, T.J., and Scrivener, R.C., 1993, Thermochronology of the Cornubian batholith in southwest England: Implications for pluton emplacement and protracted hydrothermal mineralization: Geochimica et Cosmochimica Acta, v. 57, p. 1817–1835, doi:10.1016/0016-7037(93)90115-D.

Chinner, G.A., and Fox, J.S., 1974, The origin of cordierite-anthophyllite rocks in the Land's End aureole: Geological Magazine, no. 5, p. 397–408, doi:10.1017/S0016756800039959.

Ciavarella, V., and Wyld, S.J., 2008, Wall rocks as recorders of multiple emplacement mechanisms—Examples from Cretaceous intrusions of northwest Nevada, *in* Wright, J. E., and Shervais, J. W., eds., Ophiolites, Arcs, and Batholiths: Geological Society of America Special Paper 438, p. 517–550, doi: 10.1130/2008.2438(19).

Clark, A., Chen, Y., Farrar, E., and Northcote, B., 1994, Refinement of the time/space relationships of intrusion and hydrothermal activity in the Cornubian Batholith: Proceedings of the Ussher Society, v. 8, p. 245.

Clark, A., Chen, Y., Farrar, E., Wasteneys, H.A.H.P., Stimac, J., Hodgson, M.J., Willis-Richards, J., and Bromley, A., 1993, The Cornubian Sn-Cu(-As,W) Metallogenetic Province: Produce of a 30 m.y. history of discrete and concomitant anatectic, intrusive and hydrothermal events: Proceedings of the Ussher Society, v. 8, p. 112–116.

Clark, M.D., 1978, Amphibolitic rocks from the Precambrian of Grand Canyon: Mineral chemistry and phase petrology: Mineralogical Magazine, v. 42, p. 199–207, doi:10.1180/minmag.1978.042.322.06.

Clemens, J.D., 1998, Observations on the origins and ascent mechanisms of granitic magmas: Geological Society [London] Journal, v. 155, no. 5, p. 843–851, doi:10.1144/gsjgs.155.5.0843.

Clemens, J.D., and Mawer, C.K., 1992, Granite magma transport by fracture propagation: Tectonophysics, v. 204, p. 339–360, doi:10.1016/0040-1951(92)90316-X.

Clemens, J.D., and Benn, K., 2010, Anatomy, emplacement and evolution of a shallow-level, post-tectonic laccolith: The Mt Disappointment pluton, SE Australia: Geological Society [London] Journal, v. 167, p. 915–941, doi:10.1144/0016-76492009-120.

Coggon, R., and Holland, T.J.B., 2002, Mixing properties of phengitic micas and revised garnet-phengite thermobarometers: Journal of Metamorphic Geology, v. 20, p. 683–696, doi:10.1046/j.1525-1314.2002.00395.x.

Coleman, D.S., Gray, W., and Glazner, A.F., 2004, Rethinking the emplacement and evolution of zoned plutons: Geochronologic evidence for incremental assembly of the Tuolumne Intrusive Suite, California: Geology, v. 32, p. 433–436, doi:10.1130/G20220.1.

Collins, W.J., and Sawyer, E.W., 1996, Pervasive granitoid magma transport through the lower-middle crust during non-coaxial compressional deformation: Journal of Metamorphic Geology, v. 14, p. 565–579, doi:10.1046/j.1525-1314.1996.00442.x.

Cottam, M., Hall, R., Sperber, C., and Armstrong, R., 2010, Pulsed emplacement of the Mount Kinabalu granite, northern Borneo: Geological Society [London] Journal, v. 167, p. 49–60, doi:10.1144/0016-76492009-028.

Coward, M.P., and McClay, K.R., 1983, Thrust tectonics of South Devon: Geological Society [London] Journal, v. 140, p. 215–228, doi:10.1144/gsjgs.140.2.0215.

Cruden, A.R., 1998, On the emplacement of tabular granites: Geological Society [London] Journal, v. 155, no. 5, p. 853–862, doi:10.1144/gsjgs.155.5.0853.

Cruden, A.R., and McCaffrey, K.J.W., 2001, Growth of plutons by floor subsidence: Implications for rates of emplacement, intrusion spacing and melt-extraction mechanisms: Physics and Chemistry of the Earth. Part A: Solid Earth and Geodesy, v. 26, no. 4–5, p. 303–315, doi:10.1016/S1464-1895(01)00060-6.

Dale, J., Powell, R., White, R.W., Elmer, F.L., and Holland, T.J.B., 2005, A thermodynamic model for Ca-Na clinoamphiboles in Na_2O-CaO-FeO-MgO-Al_2O_3-SiO_2-H_2O-O for petrological calculations: Journal of Metamorphic Geology, v. 23, no. 8, p. 771–791, doi:10.1111/j.1525-1314.2005.00609.x.

Darbyshire, D.P.F., and Shepherd, T.J., 1985, Chronology of granite magmatism and associated mineralization, SW England: Geological Society [London] Journal, v. 142, p. 1159–1177, doi: 10.1144/gsjgs.142.6.1159.

Darbyshire, D.P.F., and Shepherd, T.J., 1994, Nd and Sr isotope constraints on the origin of the Cornubian batholith, SW England: Journal of the Geological Society, v. 151, no. 5, p. 795–802, doi:10.1144/gsjgs.151.5.0795.

Deer, W.A., Howie, R.A., and Zussman, J., 1997, Rock-forming minerals. Volume 2B. Double-chain silicates, 2nd ed: London, Bath, Geological Society [London], 764 p.

de la Beche, H.T., 1839, Report on the geology of Cornwall, Devon and west Somerset, Memoirs of the Geological Survey of England and Wales.: London, H.M. Stationary Office, Longman, Orme, Brown, Green, and Longmans.

de Saint-Blanquat, M., Law, R.D., Bouchez, J.L., and Morgan, S., 2001, Internal structure and emplacement of the Papoose Flat pluton: An integrated structural, petrographic and magnetic susceptibility study: Geological Society of America Bulletin, v. 113, no. 8, p. 976–995, doi:10.1130/0016-7606(2001)113<0976:ISAEOT>2.0.CO;2.

Diener, J.F.A., and Powell, R., 2010, Influence of ferric iron on the stability of mineral assemblages: Journal of Metamorphic Geology, v. 28, no. 6, p. 599–613, doi:10.1111/j.1525-1314.2010.00880.x.

Diener, J.F.A., and Powell, R., 2012, Revised activity–composition models for clinopyroxene and amphibole: Journal of Metamorphic Geology, v. 30, p. 131–142, doi:10.1111/j.1525-1314.2011.00959.x.

Diener, J.F.A., Powell, R., and White, R.W., 2008, Quantitative phase petrology of cordierite-orthoamphibole gneisses and related rocks: Journal of Metamorphic Geology, v. 26, no. 8, p. 795–814, doi:10.1111/j.1525-1314.2008.00791.x.

Diener, J.F.A., Powell, R., White, R.W., and Holland, T.J.B., 2007, A new thermodynamic model for clino- and orthoamphiboles in the system Na_2O-CaO-FeO-MgO-Al_2O_3-SiO_2-H_2O-O: Journal of Metamorphic Geology, v. 25, no. 6, p. 631–656, doi:10.1111/j.1525-1314.2007.00720.x.

Dyar, M.D., Mackwell, S.J., McGuire, A.V., Cross, L.R., and Robertson, J.D., 1993, Crystal chemistry of Fe^{3+} and H^+ in mantle kaersutite: Implications for mantle metasomatism: The American Mineralogist, v. 78, p. 968–979.

Earley, D., and Stout, J.H., 1991, Cordierite-cummingtonite facies rocks from the Gold Brick District, Colorado: Journal of Petrology, v. 32, no. 6, p. 1169–1201.

Elliott-Meadows, S.R., Froese, E., and Appleyard, E.C., 2000, Cordierite-anthophyllite-cummingtonite rocks from the Lar Deposit, Laurie Lake, Manitoba: Canadian Mineralogist, v. 38, p. 545–550, doi:10.2113/gscanmin.38.2.545.

England, R.W., 1990, The identification of granitic diapirs: Geological Society [London] Journal, v. 147, p. 931–933, doi:10.1144/gsjgs.147.6.0931.

Eskola, P., 1914, On the petrology of the Orijärvi region in southwestern Finland: Bulletin de la Commission Géologique de Finlande, v. 40, p. 274.

Evans, D.J., Rowley, W.J., Chadwick, R.A., and Millward, D., 1993, Seismic reflection data from within the Lake District batholith, Cumbria, northern England: Geological Society [London] Journal, v. 150, p. 1043–1046, doi:10.1144/gsjgs.150.6.1043.

Exley, C.S., Stone, M., and Floyd, P.A., 1983, Composition and petrogenesis of the Cornubian batholith and post-orogenic rocks in SW England, *in* Hancock, P., ed., The Variscan Fold Belt in the British Isles: Bristol, Adam Hilger Ltd., p. 153–177.

Farina, F., Dini, A., Innocenti, F., Rocchi, S., and Westerman, D.S., 2010, Rapid incremental assembly of the Monte Capanne pluton (Elba Island, Tuscany) by downward stacking of magma sheets: Geological Society of America Bulletin, v. 122, no. 9–10, p. 1463–1479, doi:10.1130/B30112.1.

Flett, J.S., 1903, Petrography of West Cornwall: Great British Geological Survey Summary of Progress, p. 150–162.

Floyd, P.A., 1965, Metasomatic Hornfelses of the Land's End Aureole at Tater-du, Cornwall: Journal of Petrology, v. 6, p. 223–245.

Floyd, P.A., 1968, Distribution of Cu in the basic hornfelses of the Land's End aureole, Cornwall, and other chemically similar rocks: Geochimica et Cosmochimica Acta, v. 32, p. 879–896, doi:10.1016/0016-7037(68)90101-4.

Floyd, P.A., 1971, Temperature distribution in the Land's End granite aureole, Cornwall: Proceedings of the Ussher Society, v. 2, no. 4, p. 335–351.

Floyd, P. A., 1975, Exotic hornfelses from the Land's End aureole: Geological Magazine, v. 112, no. 1975, p. 315–319.

Floyd, P.A., Exley, C.S., and Styles, M.T., 1993, Igneous Rocks of South-West England: Geological Conservation Review Series, Joint Nature Conservation Committee London, Chapman & Hall.

Franke, W., 1989, Variscan plate tectonics in Central Europe-current ideas and open questions: Tectonophysics, v. 169, no. 4, p. 221–228, doi:10.1016/0040-1951(89)90088-7.

Frimmel, H.E., 1996, Witwatersrand iron-formations and their significance for gold genesis and the composition limits of orthoamphibole: Mineralogy and Petrology, v. 56, p. 273–295, doi:10.1007/BF01162607.

Glazner, A.F., and Bartley, J.M., 2006, Is stoping a volumetrically significant pluton emplacement process?: Geological Society of America Bulletin, v. 118, no. 9–10, p. 1185–1195, doi:10.1130/B25738.1.

Glazner, A.F., Bartley, J.M., Coleman, D.S., Gray, W., and Taylor, R.Z., 2004, Are plutons assembled over

millions of years by amalgamation from small magma chambers?: GSA Today, v. 14, no. 4–5, p. 4–11, doi:10.1130/1052-5173(2004)014<0004:APAOMO>2.0.CO;2.

Goode, A.J.J., and Merriman, R.J., 1987, Evidence of crystalline basement west of the Land's End granite, Cornwall: Proceedings of the Geologists' Association, v. 98, no. 1, p. 39–43.

Goode, A.J.J., and Taylor, R.T., 1988, Geology of the country around Penzance: Memoir for 1:50,000 geological sheets 351 and 358 (England and Wales): British Geological Survey, 52 p.

Goode, A.J.J., Taylor, R.T., and Wilson, A.C., 1984, Penzance Sheet 351/358: Solid and Drift Geology Map: British Geological Survey, scale 1:50,000.

Grant, J.A., 1968, Partial melting of common rocks as a possible source of cordierite-anthophyllite bearing assemblages: American Journal of Science, v. 266, p. 908–931, doi:10.2475/ajs.266.10.908.

Green, E.C.R., Holland, T.J.B., and Powell, R., 2007, An order-disorder model for omphacitic pyroxenes in the system jadeite-diopside-hedenbergite-acmite, with applications to eclogite rocks: The American Mineralogist, v. 92, p. 1181–1189, doi:10.2138/am.2007.2401.

Hall, A., and Jackson, N.J., 1975, Summer Field Meeting in west Cornwall: 15–20 September 1974: Proceedings of the Geologists' Association, v. 86, no. 1, p. 95–102.

Harris, N., Ayres, M., and Massey, J., 1995, Geochemistry of granitic melts produced during the incongruent melting of muscovite: Implications for the extraction of Himalayan leucogranite magmas: Journal of Geophysical Research, v. 100, no. B8, p. 15767–15777, doi:10.1029/94JB02623.

Harris, N., and Massey, J., 1994, Decompression and anatexis of Himalayan metapelites: Tectonics, v. 13, no. 6, p. 1537–1546, doi:10.1029/94TC01611.

Henry, D.J., Guidotti, C.V., and Thomson, J.A., 2005, The Ti-saturation surface for low-to-medium pressure metapelitic biotites: Implications for geothermometry and Ti-substitution mechanisms: The American Mineralogist, v. 90, no. 2–3, p. 316–328, doi:10.2138/am.2005.1498.

Holland, T.J.B., and Blundy, J.D., 1994, Non-ideal interactions in calcic amphiboles and their bearing on amphibole-plagioclase thermometry: Contributions to Mineralogy and Petrology, v. 116, p. 433–447, doi:10.1007/BF00310910.

Holland, T.J.B., and Powell, R., 1998, An internally consistent thermodynamic data set for phases of petrological interest: Journal of Metamorphic Geology, v. 16, no. 3, p. 309–343, doi:10.1111/j.1525-1314.1998.00140.x.

Holland, T.J.B., and Powell, R., 2003, Activity-composition relations for phases in petrological calculations: an asymemetric multicomponent formulation: Contributions to Mineralogy, v. 145, p. 492–501, doi:10.1007/s00410-003-0464-z.

Holland, T.J.B., Baker, J., and Powell, R., 1998, Mixing properties and activity-compoisition relationships of chlorites in the system MgO-Fe-Al_2O_3-SiO_2-H_2O: European Journal of Mineralogy, v. 10, p. 395–406.

Horsman, E., Morgan, S., de Saint-Blanquat, M., Habert, G., Nugent, A., Hunter, R.A., and Tikoff, B., 2009, Emplacement and assembly of shallow intrusions from multiple magma pulses, Henry Mountains, Utah: Earth and Environmental Science Transactions of the Royal Society of Edinburgh, v. 100, p. 117–132, doi:10.1017/S1755691009016089.

Howard, K.A., Wooden, J.L., Barnes, C.G., Premo, W.R., Snoke, A.W., and Lee, S.-Y., 2011, Episodic growth of a Late Cretaceous and Paleogene intrusive complex of pegmatitic leucogranite, Ruby Mountains core complex, Nevada, USA: Geosphere, v. 7, no. 5, p. 1220–1248, doi:10.1130/GES00668.1.

Hughes, S.P., Stickland, R.J., Shail, R.K., LeBoutillier, N.G., Alexander, A.C., and Thomas, M., 2009, The chronology and kinematics of late Paleozoic deformation in the NW contact metamorphic aureole of the Land's End Granite: Geoscience in South-West England, v. 12, p. 140–152.

Hutton, D.H.W., 1997, Syntectonic granites and the principle of effective stress: a general solution to the space problem? *in* Bouchez, J. L., Stephens, W. E., and Hutton, D. H. W., eds., Granite: From melt segregation to emplacement fabrics: Dordrecht, The Netherlands, Kluwer, p. 189–197.

Jackson, N.J., and Pollard, D.D., 1988, The laccolith-stock controversy: New results from the southern Henry Mountains, Utah: Geological Society of America Bulletin, v. 100, p. 117–139, doi:10.1130/0016-7606(1988)100<0117:TLSCNR>2.3.CO;2.

Kirby, G.A., 1979, The Lizard complex as an ophiolite: Nature, v. 282, p. 58–61, doi:10.1038/282058a0.

Klein, T., Kiehm, S., Siebel, W., Shang, C.K., Rohrmüller, J., Dörr, W., and Zulauf, G., 2008, Age and emplacement of late-Variscan granites of the western Bohemian Massif with main focus on the Hauzenberg granitoids (European Variscides, Germany): Lithos, v. 102, p. 478–507, doi:10.1016/j.lithos.2007.07.025.

Knox, D.A., and Jackson, N.J., 1990, Composite granite intrusions of SW Dartmoor, Devon: Proceedings of the Ussher Society, v. 7, p. 246–251.

Kossmat, F., 1927, Gliederung des varistischen Gebirgsbaues: Abhandlungen Sächsischen Geologischen Landesamts, v. 1, p. 1–39.

Kratinová, Z., Schulmann, K., Hrouda, F., Shail, R. K., 2003, The role of regional tectonics and magma flow coupling versus magmatic processes in generating contrasting magmatic fabrics within the Land's End Granite, Cornwall: Geoscience in south-west England, v. 10, p. 442–448.

Kratinová, Z., Ježek, J., Schulmann, K., Hrouda, F., Shail, R.K., and Lexa, O., 2010, Non-coaxial K-feldspar and AMS sub-fabrics in the Land's End Granite, Cornwall: Evidence of magmatic fabric decoupling during late deformation and matrix crystallization: Journal of Geophysical Research, Solid Earth, v. 115, doi:10.1029/2009JB006714.

Labotka, T.C., and Kath, R.L., 2001, Petrogenesis of the contact-metamorphic rocks beneath the Stillwater Complex, Montana: Geological Society of America Bulletin, v. 113, no. 10, p. 1312–1323, doi:10.1130/0016-7606(2001)113<1312:POTCMR>2.0.CO;2.

Leake, B.E., Wooley, A., Arps, C.E.S., Birch, W.D., and Gilbert, M.C., 1997, Nomenclature of amphiboles: Report of the Subcommittee on Amphiboles of the International Mineralogical Association, Commission on New Minerals and Mineral Names: The American Mineralogist, v. 82, p. 1019–1037.

LeBoutillier, N.G., 2003, The tectonics of Variscan magmatism and mineralisation in South West England [Ph.D. thesis]: Exeter, UK, University of Exeter, 712 p.

Leuthold, J., Müntener, O., Baumgartner, L.P., Putlitz, B., Ovtcharova, M., and Schaltegger, U., 2012, Time resolved construction of a bimodal laccolith (Torres del Paine, Patagonia): Earth and Planetary Science Letters, v. 325–326, p. 85–92, doi:10.1016/j.epsl.2012.01.032.

Leveridge, B.E., Holder, M.T., and Day, G.A., 1984, Thrust nappe tectonics in the Devonian of south Cornwall and the western English Channel, *in* Hutton, D. W., and Sanderson, D. J., eds., Variscan Tectonics of the North Atlantic Region, Special Publication of the Geological Society [London], p. 103–112.

Lipman, P.W., 2007, Incremental assembly and prolonged consolidation of Cordilleran magma chambers: Evidence from the Southern Rocky Mountain volcanic field: Geosphere, v. 3, no. 1, p. 42–70, doi:10.1130/GES00061.1.

Lister, C.J., 1978a, Luxullianite *in situ* within St. Austell Granite, Cornwall: Mineralogical Magazine, v. 42, no. 322, p. 295–297, doi:10.1180/minmag.1978.042.322.30.

Lister, C.J., 1978b, Some tourmalinised rocks from Cornwall and Devon: Proceedings of the Ussher Society, v. 4, no. 2, p. 211–214.

Lister, J.R., and Kerr, R.C., 1991, Fluid-mechanical models of crack propagation and their application to magma transport in dikes: Journal of Geophysical Research, v. 96, p. 10049–10077, doi:10.1029/91JB00600.

Mahon, K.I., Harrison, T.M., and Drew, D.A., 1988, Ascent of a granitoid diapir in a temperature varying medium: Journal of Geophysical Research, v. 93, p. 1174–1188, doi:10.1029/JB093iB02p01174.

Manning, D., 1981, The application of experimental studies in determining the origin of topaz-quartz-tourmaline rock and tourmaline-quartz rock: Proceedings of the Ussher Society, v. 5, p. 121–127.

Manning, D., Hill, P., and Howe, J., 1996, Primary lithological variation in the kaolinized St Austell Granite, Cornwall, England: Journal of the Geological Society, v. 153, p. 827–838, doi:10.1144/gsjgs.153.6.0827.

Marsh, B.D., 1982, On the mechanics of igneous diapirism, stoping, and zone melting: American Journal of Science, v. 282, p. 808–855, doi:10.2475/ajs.282.6.808.

Matte, P., 1986, Tectonics and plate tectonics model for the Variscan belt of Europe: Tectonophysics, v. 126, no. 2–4, p. 329–374, doi:10.1016/0040-1951(86)90237-4.

McCaffrey, K.J.W., and Petford, N., 1997, Are granitic intrusions scale invariant?: Geological Society [London] Journal, v. 154, no. 1, p. 1–4, doi:10.1144/gsjgs.154.1.0001.

Michel, J., Baumgartner, L., Putlitz, B., Schaltegger, U., and Ovtcharova, M., 2008, Incremental growth of the Patagonian Torres del Paine laccolith over 90 k.y: y: Geology, v. 36, p. 459–462, doi:10.1130/G24546A.1.

Miller, R.B., and Paterson, S.R., 1999, In defense of magmatic diapirs: Journal of Structural Geology, v. 21, p. 1161–1173, doi:10.1016/S0191-8141(99)00033-4.

Mitropoulos, P., 1984, Rare-earth element distribution in the metabasic rocks of the Land's End granite aureole, SW England: Mineralogical Magazine, v. 48, p. 495–505, doi:10.1180/minmag.1984.048.349.03.

Miyake, A., 1984, Phase equilibria in the hornblende-bearing basic gneisses of the Uvete area, central Kenya: Journal of Metamorphic Geology, v. 2, no. 2, p. 165–177, doi:10.1111/j.1525-1314.1984.tb00294.x.

Moore, J.M., and Waters, D.J., 1990, Geochemistry and origin of cordierite-orthoamphibole/orthopyroxene-phlogopite rocks from Namaqualand, South Africa: Chemical Geology, v. 85, no. 1–2, p. 77–100, doi:10.1016/0009-2541(90)90124-P.

Morgan, S.S., Law, R.D., and Nyman, M.W., 1998, Laccolith-like emplacement models for the Papoose Flat pluton based on porphyroblast-matrix analysis: Geological Society of America Bulletin, v. 110, no. 1, p. 96–110, doi:10.1130/0016-7606(1998)110<0096:LLEMFT>2.3.CO;2.

Müller, A., Seltmann, R., Halls, C., Siebel, W., Dulski, P., Jeffries, T., Spratt, J., and Kronz, A., 2006, The magmatic evolution of the Land's End pluton, Cornwall, and associated pre-enrichment of metals: Ore Geology Reviews, v. 28, no. 3, p. 329–367, doi:10.1016/j.oregeorev.2005.05.002.

Nance, R.D., Gutiérrez-Alonso, G., Keppie, J.D., Linnemann, U., Murphy, J.B., Quesada, C., Strachan, R.A., and Woodcock, N.H., 2010, Evolution of the Rheic Ocean: Gondwana Research, v. 17, no. 2–3, p. 194–222, doi:10.1016/j.gr.2009.08.001.

Paterson, S.R., Vernon, R.H., and Fowler, T.K., 1991, Aureole tectonics: Mineralogical Society of America Reviews in Mineralogy, v. 23, p. 673–722.

Paterson, S.R., and Vernon, R.H., 1995, Bursting the bubble of ballooning plutons, A return to nested diapirs emplaced by multiple processes: Geological Society of America Bulletin, v. 107, p. 1356–1380, doi:10.1130/0016-7606(1995)107<1356:BTBOBP>2.3.CO;2.

Pattison, D.R.M., and Harte, B., 1997, The geology and evolution of the Ballachulish Igneous Complex and Aureole: Scottish Journal of Geology, v. 33, p. 1–29, doi:10.1144/sjg33010001.

Peck, W.H., and Smith, M.S., 2005, Cordierite–gedrite rocks from the Central Metasedimentary Belt boundary thrust zone (Grenville Province, Ontario): Mesoproterozoic metavolcanic rocks with affinities to the Composite Arc Belt: Canadian Journal of Earth Sciences, v. 42, p. 1815–1828, doi:10.1139/e05-071.

Petford, N., 1996, Dykes or diapirs?: Geological Society of America Special Papers 315, p. 105–114.

Petford, N., and Atherton, M., 1996, Na-rich partial melts from newly underplated basaltic crust: The Cordillera Blanca Batholith, Peru: Journal of Petrology, v. 37, no. 6, p. 1491–1521, doi:10.1093/petrology/37.6.1491.

Petford, N., and Clemens, J.D., 2000, Granites are not diapiric!: Geology Today, v. 16, p. 180–184, doi:10.1111/j.1365-2451.2000.00008.x.

Petford, N., Cruden, A.R., McCaffrey, K.J.W., and Vigneresse, J.L., 2000, Granite magma formation, transport and emplacement in the Earth's crust: Nature, v. 408, p. 669–673, doi:10.1038/35047000.

Petford, N., Kerr, R.C., and Lister, J.R., 1993, Dike transport of granitoid magmas: Geology, v. 21, p. 845–848, doi:10.1130/0091-7613(1993)021<0845:DTOGM>2.3.CO;2.

Phillips, J.A., 1876, On the so-called "Greenstones" of Western Cornwall: Quarterly Journal of the Geological Society of London, v. 32, no. 1–4, p. 155–179, doi:10.1144/GSL.JGS.1876.032.01-04.22.

Pitcher, W.S., 1979, The nature, ascent and emplacement of granitic magmas: Geological Society [London] Journal, v. 136, no. 6, p. 627–662, doi:10.1144/gsjgs.136.6.0627.

Pitra, P., Burg, J.P., and Guiraud, M., 1999, Late Variscan strike-slip tectonics between the Tepla-Barrandian and Moldanubian terranes (Czech Bohemian Massif): Petrostructural evidence: Geological Society [London] Journal, v. 156, p. 1003–1020, doi:10.1144/gsjgs.156.5.1003.

Pollard, D.D., and Johnson, A.M., 1973, Mechanics of growth of some laccolithic intrusions in the Henry Mountains, Utah, II: Tectonophysics, v. 18, p. 311–354, doi:10.1016/0040-1951(73)90051-6.

Powell, R., 1987, Darken's quadratic formalism and the thermodynamics of minerals: The American Mineralogist, v. 72, p. 1–11.

Powell, R., and Holland, T.J.B., 1988, An internally consistent dataset with uncertainties and correlations: 3. Applications to geobarometry, worked examples and a computer program: Journal of Metamorphic Geology, v. 6, no. 2, p. 173–204, doi:10.1111/j.1525-1314.1988.tb00415.x.

Powell, R., and Holland, T.J.B., 2008, On thermobarometry: Journal of Metamorphic Geology, v. 26, no. 2, p. 155–179, doi:10.1111/j.1525-1314.2007.00756.x.

Powell, T., Salmon, S., Clark, A.H., and Shail, R.K., 1999, Emplacement styles within the land's end granite, west Cornwall: Geoscience in South-west England, v. 9, no. January, p. 333–339.

Ramberg, H., 1981, Gravity, Deformation and the Earth's Crust: London, Academic Press, 452 p.

Rattey, P.R., 1980, Deformation in south-west Cornwall: Proceedings of the Ussher Society, v. 5, no. 1, p. 39–43.

Rattey, P.R., and Sanderson, D.J., 1984, The structure of SW Cornwall and its bearing on the emplacement of the Lizard Complex: Journal of the Geological Society, v. 141, no. 1, p. 87–95, doi:10.1144/gsjgs.141.1.0087.

Reid, C., and Flett, J.S., 1907, Geology of the Land's End district: Geological Survey of Great Britain Memoir.

Reinhardt, J., 1987, Cordierite-anthophyllite rocks from north-west Queensland, Australia: metamorphosed magnesian pelites: Journal of Metamorphic Geology, v. 5, no. 4, p. 451–472, doi:10.1111/j.1525-1314.1987.tb00396.x.

Roberts, M.D., Oliver, N.H.S., Fairclough, M.C., Hölttä, P.S., and Lahtinen, R., 2003, Geochemical and oxygen isotope signature of seafloor alteration associated with a polydeformed and highly metamorphosed massive sulphide deposit, Ruostesuo, central Finland: Economic Geology and the Bulletin of the Society of Economic Geologists, v. 98, p. 535–556.

Robinson, P., Spear, F.S., and Schumacher, J.C., 1982, Phase relations of metamorphic amphiboles: natural occurrences and theory, *in* Veblen, D. R., and Ribbe, P. H., eds., Amphiboles: Petrology and Experimental Phase Relations: Review in Mineralogy, 9B: Chelsea, Michigan, Book Crafters Inc., p. 228.

Rocchi, S., Westerman, D.S., Dini, A., and Farina, F., 2010, Intrusive sheets and sheeted intrusions at Elba Island, Italy: Geosphere, v. 6, no. 3, p. 225–236, doi:10.1130/GES00551.1.

Salmon, S., 1994, Mingling between coexisting granite magmas within the Land's End Granite. 1: Preliminary observations: Proceedings of the Ussher Society, v. 8, no. January, p. 219–223.

Salmon, S., and Powell, T., 1998, Variation in the fine-grained granites of the Land's End pluton: Geoscience in South-west England, v. 9, p. 157–164.

Salmon, S., and Shail, R.K., 1999, Field Excursion to examine the granites in the area between Cape Cornwall and Porth Nanven, West Penwith, 3rd January 1999: Geoscience in South-West England, v. 10, p. 391–393.

Scheuvens, D., and Zulauf, G., 2000, Exhumation, strain localization, and emplacement of granitoids along the western part of the Central Bohemian shear zone (central European Variscides, Czech Republic): International Journal of Earth Sciences, v. 89, p. 617–630, doi:10.1007/s005310000108.

Schmidt, M.W., 1992, Amphibole composition in tonalite as a function of pressure: an experimental calibration of the Al-in-hornblende barometer: Contributions to Mineralogy and Petrology, v. 110, p. 304–310, doi:10.1007/BF00310745.

Schneiderman, J.S., and Tracy, R.J., 1991, Petrology of orthoamphibole-cordierite gneisses from the Orijärvi area, Southwest Finland: The American Mineralogist, v. 76, no. 5–6, p. 942–955.

Schumacher, J.C., 2007, Metamorphic amphiboles: Composition and coexistence: Reviews in Mineralogy and Geochemistry, v. 67, p. 359–416, doi:10.2138/rmg.2007.67.10.

Searle, M.P., 1999, Emplacement of Himalayan leucogranites by magma injection along giant sill complexes: examples from the Cho Oyu, Gyachung Kang and Everest leucogranites (Nepal Himalaya): Journal of Asian Earth Sciences, v. 17, p. 773–783, doi:10.1016/S1367-9120(99)00020-6.

Searle, M.P., Cottle, J.M., Streule, M.J., and Waters, D.J., 2009, Crustal melt granites and migmatites along the Himalaya: Melt source, segregation, transport and granite emplacement mechanisms: Earth and Environmental Science Transactions of the Royal Society of Edinburgh, v. 100, p. 219–233, doi:10.1017/S175569100901617X.

Searle, M.P., Parrish, R.R., Thow, A.V., Noble, S.R., Phillips, R.J., and Waters, D.J., 2010, Anatomy, age and evolution of a collisional mountain belt: The Baltoro granite batholith and Karakoram Metamorphic Complex, Pakistani Karakoram: Geological Society [London] Journal, v. 167, p. 183–202, doi:10.1144/0016-76492009-043.

Searle, M.P., Whitehouse, M.J., Robb, L.J., Ghani, A.A., Hutchinson, C.S., Sone, M., Ng, S.W.-P., Roselee, M.H., Chung, S.-L., and Oliver, G.J.H., 2012, Tectonic evolution of the Sibumasu-Indochina terrane collision zone in Thailand and Malaysia: Constraints from new U-Pb zircon chronology of SE Asian tin granitoids: Geological Society [London] Journal, v. 169, p. 489–500, doi:10.1144/0016-76492011-107.

Shackleton, R.M., Ries, A.C., and Coward, M.P., 1982, An interpretation of the Variscan structures in SW England: Geological Society [London] Journal, v. 139, no. 4, p. 533–541, doi:10.1144/gsjgs.139.4.0533.

Shail, R.K., and Alexander, A.C., 1997, Late Carboniferous to Triassic reactivation of Variscan basement in the western English Channel: Evidence from onshore exposures in south Cornwall: Geological Society [London] Journal, v. 154, no. 1, p. 163–168, doi:10.1144/gsjgs.154.1.0163.

Shail, R.K., and Leveridge, B.E., 2009, The Rhenohercynian passive margin of SW England: Development, inversion and extensional reactivation: Comptes Rendus Geoscience, v. 341, no. 2–3, p. 140–155, doi:10.1016/j.crte.2008.11.002.

Shail, R. K., Stuart, F. M., Wilkinson, J. J., and Boyce, A. J., 2003, The role of Post-Variscan extensional tectonics and mantle melting in the generation of lower Permian granites and the giant W–As–Sn–Cu–Zn–Pb orefield of SW England: Applied Earth Sciences (Transactions of the Institute of Mining and Metallurgy, Section B), v. 112, p. 127–129, doi:10.1179/037174503225001712

Shail, R.K., and Wilkinson, J.J., 1994, Late- to post- Variscan extensional tectonics in south Cornwall: Proceedings of the Ussher Society, v. 8, p. 262–270.

Smith, M.S., Dymek, R.F., and Schneiderman, J.S., 1992, Implications of Trace Element Geochemistry for the Origin of Cordierite-Orthoamphibole Rocks from Orijärvi, SW Finland: The Journal of Geology, v. 100, p. 545–559, doi:10.1086/629607.

Spear, F.S., 1980, NaSi↔CaAl Exchange Equilibrium Between Plagioclase and Amphibole: An Empirical Model: Contributions to Mineralogy and Petrology, v. 72, no. 1, p. 33–41, doi:10.1007/BF00375566.

Spear, F.S., 1982, Phase equilibria of amphiboles from the Post Pond Volcanics, Mt. Cube quadrangle, Vermont: Journal of Petrology, v. 23, p. 383–426.

Stimac, J.A., Clark, A.H., Chen, Y., and Garcia, S., 1995, Enclaves and their bearing on the origin of the Cornubian batholith, southwest England: Mineralogical Magazine, v. 59, p. 273–296, doi:10.1180/minmag.1995.059.395.12.

Stone, M., 1975, Structure and petrology of the Tregonning-Godolphin granite, Cornwall: Proceedings of the Geologists' Association, v. 86, p. 155–170.

Stone, M., 1984, Textural evolution of lithium mica granites in the Cornubian batholith: Proceedings of the Geologists' Association, v. 95, p. 29–41.

Stone, M., 1992, The Tregonning granite: petrogenesis of Li-mica granites in the Cornubian batholith: Mineralogical Magazine, v. 56, no. 383, p. 141–155, doi:10.1180/minmag.1992.056.383.01.

Stone, M., 1997, A geochemical dichotomy in the Cornubian batholiths: Proceedings of the Ussher Society, v. 9, p. 206–210.

Stone, M., 2000a, The early Cornubian plutons: A geochemical study, comparisons and some implications: Geoscience in south-west England, v. 10, p. 37–41.

Stone, M., 2000b, Petrogenetic implications from biotite compositional variations in the Cornubian granite batholiths: Mineralogical Magazine, v. 64, p. 729–735, doi:10.1180/002646100549580.

Stone, M., and Exley, C.S., 1984, Emplacement of the Porthmeor granite pluton, west Cornwall: Proceedings of the Ussher Society, v. 6, p. 42–45.

Stout, J.H., 1972, Phase petrology and mineral chemistry of coexisting amphiboles from Telemark, Norway: Journal of Petrology, v. 13, no. 1, p. 99–145.

Tartèse, R., and Boulvais, P., 2010, Differentiation of peraluminous leucogranites "en route" to the surface: Lithos, v. 114, no. 3–4, p. 353–368, doi:10.1016/j.lithos.2009.09.011.

Taylor, G.K., 2007, Pluton shapes in the Cornubian Batholith: New perspectives from gravity modelling: Geological Society [London] Journal, v. 164, no. 3, p. 525–528, doi:10.1144/0016-76492006-104.

Tilley, C.E., 1935, Metasomatism associated with the greenstone-hornfelses of Kenidjack and Botallack, Cornwall: Mineralogical Magazine, v. 24, no. 151, p. 181–202, doi:10.1180/minmag.1935.024.151.01.

Tilley, C.E., and Flett, J.S., 1929, Hornfelses from Kenidjack, Cornwall: Summary of Progress of the Geological Survey of Great Britain, v. 2, p. 24–41.

Turner, R.E., Taylor, R.T., Goode, A.J.J., and Owens, B., 1979, Palynological evidence for the age of the Mylor slates, Mount Wellington, Cornwall: Proceedings of the Ussher Society, v. 4, p. 274–283.

Vallance, T.G., 1967, Mafic rock alteration and isochemical development of some cordierite-anthophyllite rocks: Journal of Petrology, v. 8, p. 84–96.

Vernon, R.H., 1986, K-feldspar megacrysts in granites: Phenocrysts, not porphyroblasts: Earth-Science Reviews, v. 23, no. 1, p. 1–63, doi:10.1016/0012-8252(86)90003-6.

Vernon, R.H., and Paterson, S.R., 2008, How late are K-feldspar megacrysts in granites?: Lithos, v. 104, no. 1–4, p. 327–336, doi:10.1016/j.lithos.2008.01.001.

Vigneresse, J.L., 1990, Use and misuse of geophysical data to determine the shape at depth of granitic intrusions: Geological Journal, v. 25, no. 3–4, p. 249–260, doi:10.1002/gj.3350250308.

Vigneresse, J.L., 1999, Intrusion level of granitic massifs along the Hercynian belt: balancing the eroded crust: Tectonophysics, v. 307, no. 3–4, p. 277–295, doi:10.1016/S0040-1951(99)00104-3.

Warr, L.N., 2000, The Variscan Orogeny: the welding of Pangaea, *in* Woodcock, N. H., and Strachan, R. A., eds., Geological History of Britain and Ireland: Oxford, Blackwell Science, p. 271–294.

Warr, L.N., Primmer, T.J., and Robinson, D., 1991, Variscan very low-grade metamorphism in southwest England: a diastathermal and thrust-related origin: Journal of Metamorphic Geology, v. 9, no. 6, p. 751–764, doi:10.1111/j.1525-1314.1991.tb00563.x.

Weinberg, R.F., 1999, Mesoscale pervasive felsic magma migration: alternatives to dyking: Lithos, v. 46, no. 3, p. 393–410, doi:10.1016/S0024-4937(98)00075-9.

Weinberg, R.F., and Podladchikov, Y.Y., 1994, Diapiric ascent of magmas through power law crust and mantle: Journal of Geophysical Research, v. 99, p. 9543–9559, doi:10.1029/93JB03461.

Weinberg, R.F., and Searle, M.P., 1998, The Pangong Injection Complex, Indian Karakoram: A case of pervasive granite flow through hot viscous crust: Geological Society [London] Journal, v. 155, no. 5, p. 883–891, doi:10.1144/gsjgs.155.5.0883.

White, R.W., Powell, R., and Clarke, G.L., 2002, The interpretation of reaction textures in Fe-rich metapelitic granulites of the Musgrave Block, central Australia: Constraints from mineral equilibria calculations in the system K_2O–FeO–MgO–Al_2O_3–SiO_2–H_2O–TiO_2–Fe_2O_3: Journal of Metamorphic Geology, v. 20, no. 1, p. 41–55, doi:10.1046/j.0263-4929.2001.00349.x.

White, R.W., Powell, R., and Holland, T.J.B., 2007, Progress relating to calculation of partial melting equilibria for metapelites: Journal of Metamorphic Geology, v. 25, no. 5, p. 511–527, doi:10.1111/j.1525-1314.2007.00711.x.

White, R.W., Powell, R., Holland, T.J.B., and Worley, B.A., 2000, The effect of TiO_2 and Fe_2O_3 on metapelitic assemblages at greenschist and amphibolite facies conditions: mineral equilibria calculations in the system K_2O-FeO-MgO-Al_2O_3-SiO_2-H_2O-TiO_2-Fe_2O_3: Journal of Metamorphic Geology, v. 18, p. 497–511, doi:10.1046/j.1525-1314.2000.00269.x.

Will, T.M., and Powell, R., 1992, Activity-composition relations in multicomponent amphiboles: An application of Darken's quadratic formalism: The American Mineralogist, v. 77, p. 954–966.

Williamson, B.J., Müller, A., and Shail, R.K., 2010, Source and partitioning of B and Sn in the Cornubian batholiths of southwest England: Ore Geology Reviews, v. 38, p. 1–8, doi:10.1016/j.oregeorev.2010.05.002.

Willis-Richards, J., and Jackson, N.J., 1989, Evolution of the Cornubian Ore Field, Southwest England: Part 1. Batholith modelling and ore distribution: Economic Geology and the Bulletin of the Society of Economic Geologists, v. 84, p. 1078–1100, doi:10.2113/gsecongeo.84.5.1078.

Žák, J., Holub, F.V., and Kachlik, V., 2006, Magmatic stoping as an important emplacement mechanism of Variscan plutons: Evidence from roof pendants in the Central Bohemian plutonic complex (Bohemian Massif): International Journal of Earth Sciences, v. 95, p. 771–789, doi:10.1007/s00531-006-0076-8.

Žák, J., Verner, K., Finger, F., Faryad, S.W., Chlupáčová, M., and Veselovský, F., 2011, The generation of voluminous S-type granites in the Moldanubian unit, Bohemian Massif, by rapid isothermal exhumation of the metapelitic middle crust: Lithos, v. 121, no. 1–4, p. 25–40, doi:10.1016/j.lithos.2010.10.002.